



TECHNISCHE
UNIVERSITÄT
DARMSTADT



Politecnico
di Torino

Faculty of Engineering
Master of Science in Civil Engineering



Erasmus+
Enriching lives, opening minds.

FINAL THESIS

ULTRALIGHT CEMENTITIOUS FOAMS

Academic tutor

Dr.-Ing. CHRISTOPH MANKEL

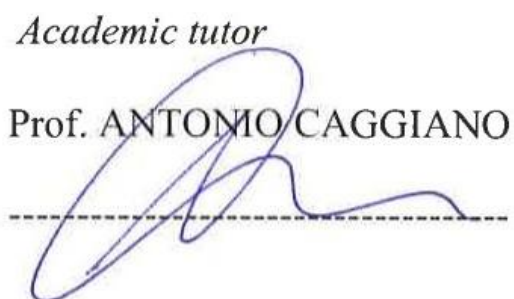
'Thesis Project' coordinator
Prof. Dr.ir. EDDIE KOENDERS



'Thesis Project' coordinator

Prof. ALESSANDRO P. FANTILLI

Academic tutor
Prof. ANTONIO CAGGIANO



The student S249311
TURMATOV AZIZJON



ERASMUS+ THESIS PROJECT
2020/2021

Abstract

Foam concrete is a type of *aerated lightweight concrete*. Foam concrete does not contain any coarse aggregate. It requires no compaction, but it will flow readily from an outlet to fill restricted and irregular cavities.

Foam concrete FC has the potential of being an alternative to ordinary concrete, as it reduces dead loads on the structure and foundation, contributes to energy conservation, and lowers the cost of production and labor cost during the construction and transportation. The paper reports a state-of-the-art review of foam concrete in terms of its components, and material properties like drying shrinkage, compressive strength, stability and pore structure, etc.

Some shortcomings and technical limitations as well as emerging direction for performance enhancement of FC are also discussed.

Meanwhile performed deep research on Fastening concepts for an External Thermal Insulation Composite System made of foamed concrete

Foam concrete with different thicknesses was analyzed with Abaqus software to analyze heat transfer through the wall for two cases with and without anchors.

The current review concludes that the long-term performance and enhancement-associated properties need to be deeply investigated. This study can help modify consumer concerns and further encourage the wider application of FC in civil engineering.

Contents

| | |
|---|----|
| Abstract..... | 1 |
| Introduction | 4 |
| Chapter 1..... | 6 |
| History and Recent Development | 6 |
| Material Components and Preparation | 7 |
| Drying Shrinkage | 9 |
| 28 Days dry Shrinkage of Foam Concrete with Various Densities | 9 |
| Compressive Strength | 11 |
| Compressive strength-density relationship of foamed concrete..... | 12 |
| Durability..... | 13 |
| Thermal Conductivity..... | 15 |
| Pore Structure | 17 |
| Outline of the experimental program..... | 19 |
| Test set-up | 20 |
| Test set-up scheme | 21 |
| 3. Test results | 22 |
| 3.1. Failure load Analysis | 23 |
| 3.2. Deformations..... | 25 |
| 3.3. Other benefits of reinforcement..... | 26 |
| 4. Conclusions..... | 26 |
| Chapter 2..... | 27 |
| Hygrothermal Performance of ETICS on Concrete Wall after Low-Budget Energy Renovation | 27 |
| METHODS..... | 28 |
| Renovation Solution..... | 28 |
| Renovation solution was selected based on the energy and economical calculations: | 28 |
| Measurements | 29 |
| RESULTS | 31 |
| Technical Condition of External Walls..... | 32 |
| Indoor Climate | 32 |
| DISCUSSION..... | 40 |
| Thermal Bridges | 41 |
| Hygrothermal Performance of ETICS on a Concrete Element..... | 42 |
| Chapter 3..... | 46 |
| Thermal design of ETICS made with cementitious foam | 46 |
| Analysis 1 | 51 |
| Analysis 2 | 58 |
| Analysis 3 | 60 |

| | |
|---|----|
| Analysis 4 | 63 |
| Analysis 1 of the wall with Anchors | 67 |
| Analysis 2 of wall with Anchors..... | 70 |
| Analysis 3 of the wall with Anchors | 73 |
| Analysis 4 of the wall with Anchors | 77 |
| Conclusion..... | 82 |
| REFERENCES | 84 |

Introduction



Figure 1. Foam Concrete, is an environmentally friendly building material

FC is a type of cement mortar containing cement, water, and stable and homogeneous foam introduced using a suitable foaming agent, which can be regarded as self-compacting materials. Other academic terms describing this material are lightweight cellular concrete, low-density foam concrete, cellular lightweight concrete, etc.

In practice, it provides satisfactory solutions to address various challenges and problems faced in construction activities. Fewer chemicals contained in this material well meet the sustainable and environmental demands, and sometimes, it can be partially or even entirely substituted for normal concrete.

The textural surface and microstructural cells make it widely used in the fields of thermal insulation, sound absorbance, and fire resistance. A great number of environmentally friendly buildings using FC

as non-structural members have been built in recent years. It is also used for bridge abutment filling to eliminate differential settlement. In addition, the applications for prefabricated components production, building foundation, and airport buffer system are also reported. Foam concrete has been commonly used in construction applications in different countries such as the USA, Germany, Brazil, UK, and Canada.[1]

This material has renewed interest in terms of underground engineering. This is the requirement of underground structure to control the overlying dead load, whereas the controllable density and low self-weight could be effectively used for reducing the dead load. Other properties, such as seismic resistance, ideal coordinated deformation capacity, and easy pumping, also contribute to enhancing the popularity of this material. Nowadays, the FC has been quickly promoted as construction materials for tunnels and underground works. Its excellent self-flowing capacity can be used to fill voids, sinkholes, disused sewage pipes, abandoned subways, and so on. The low and controlled self-weight makes it capable of load reduction or liner elements in tunnel and metro systems.

Though there are limited studies regarding the practical applications of FC in civil engineering, its properties have been deeply studied. The compressive strength of FC increases with density and confining pressure, whereas the modulus of elasticity has a positive correlation only with densities regardless of confining pressure. And no notable correlation was observed between peak strain and density, but peak strain increases with confining pressure.

The depth of absorption was considered a critical predictor in developing freeze-thaw-resistant concrete, which will contribute to promoting effectiveness in terms of using FC as insulation material for tunnels in cold regions. Sun explored the influence of different foaming agents on compressive strength, drying shrinkage, and workability of FC, which will be helpful to determine specification and implementation details. Significant progress in FC application has been made over the past few decades. In Canada, cement-based FC has been widely used for tunnel grouting. [2]

Chapter 1

History and Recent Development

There is confusion existed between FC and similar materials in early literature, aerated concrete, and air-entrained concrete. The closed air-voids system in FC notably reduces its density and weight and at the same time produces efficient insulation and fire resistance capacity.

The first Portland cement-based FC was patented by Axel Eriksson in 1923, and then, small-scale commercial production activities were launched. FC was initially envisaged as a void filling, stabilization, and insulation material. The booming development of this new constituent material in buildings and constructions was enhanced in the late 1970s.[3]

Over the past 30 years, FC are widely used for bulk filling, ditch repair, retaining walls, bridge abutment backfills, slab structure of the concrete floor, housing insulation, etc. (Figure 2).[4] Currently, people are increasingly interested in using it as a non-structure or semi-structure member for underground engineering, such as grouting works for tunnels, damage treatment, and liner structures. [5]

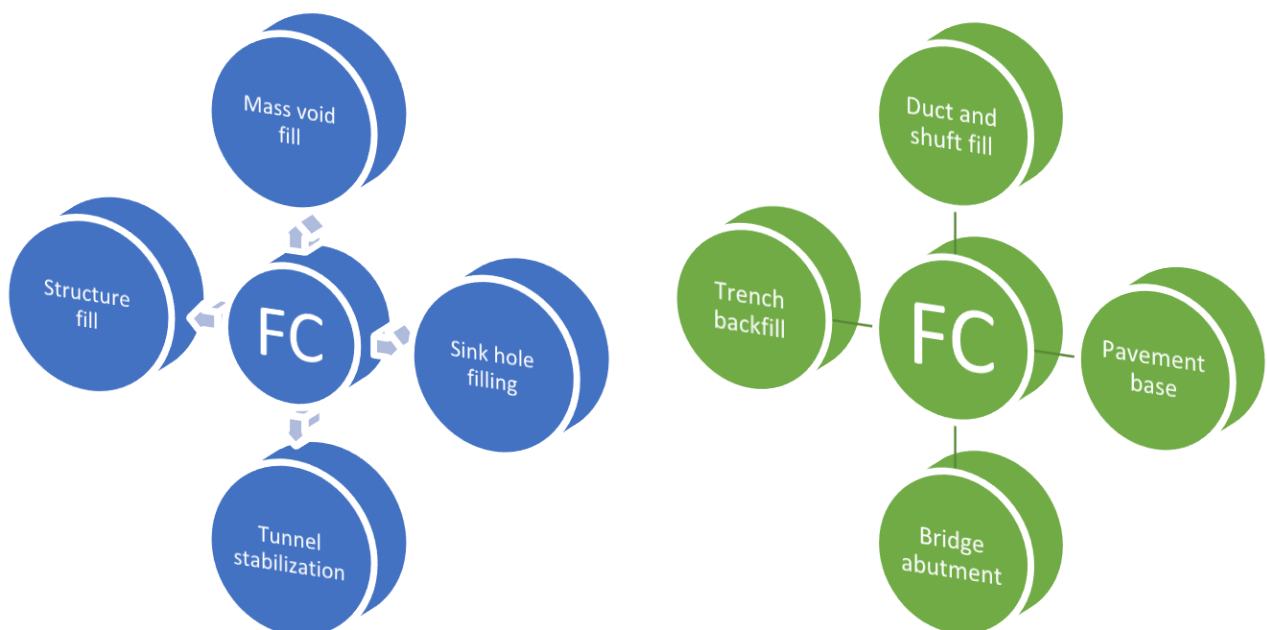


Figure 2. Different applications of FC.

Material Components and Preparation

The basic components of FC consist of water, binder, foaming agent, filler, additive, and fiber. The state-of-the-art research and findings on these components to date are described as follows: The water requirement for constituent material depends on the composition, consistency, and stability of the mortar body. The lower water content leads to a hard mixture, which easily results in bubble bursting. The higher water content causes the mixture too thin to accommodate bubbles, thereby causing bubbles to separate from the mixture. The American Concrete Institute (ACI) recommends that mixed water should be fresh, clean, and drinkable. Sometimes, the mixed water can be replaced by equivalent-performance water received from municipal sectors in case the strength FC could reach 90% within a specified curing time. [6]

Binder: Cement is the most commonly used binder. The ordinary Portland cement, rapid hardening Portland cement, calcium sulphate-aluminate cement, and high-alumina can be used in ranges between 25% and 100% of the binder content.

Foaming agent: The foaming agent determines FC density by controlling the generation rate of the bubbles in cement paste. The resin-based was one of the earliest used foaming agents in FC. So far, synthetic, protein-based, composite, and synthetic surfactants have been derived and developed, while the most frequently used are synthetic and protein-based ones.

Filler: Various fillers such as silica fume, fly ash, limestone powder, granulated blast furnace slag, and fly-ash ceramicist have been widely adopted for the purpose to enrich FC mechanical performances. The addition of these fillers is helpful to improve mix proportion design, and long-term strength, and reduce costs. In addition, some fine aggregates such as fine sand, recycled glass powder, and surface-modified chip are commonly used for the production of high-density FC.

Additive: Commonly used additive includes the water reducer, water-proofing additive, retarder, coagulation accelerator, etc.

Plasticizers are always considered to enhance compatibility. In fact, they are defined as water reducers to improve the performance of fresh concrete by reducing fluidity and plasticity, and there is no notable impact on concrete segregation was observed.

Fiber: A variety of fibers are added into FC to improve strength and reduce shrinkage. They are mainly polypropylene, glass and polypropylene, red ramie, palm oil, steel, coconut, waste paper cellulose,

carbon, and polypropylene, which are usually introduced in ranges between 0.2% and 1.5% of the mixture volume.[7],[8],[9]



Figure 3. Foam concrete at TU Darmstadt [Labaraostry], Germany

FC is commonly prepared by the pre-foaming method or mix-foaming method. The majority of common mixers such as the inclined drum, pan mixer used for concrete, or mortar are applicable to FC production. The mixer type, mix proportion, and mixing order used for FC depend on the adoption of the above-mentioned two methods. The major procedures using these two methods are presented below:[10]

Pre-foaming Method. The foam and base mixture are prepared independently. Totally mix the foam and base mixture.

Mix-Foaming Method. Surfactants or foaming agents are mixed with the base mixture together (especially the cement paste). The foam produces cellular structures in FC.

There are two ways, dry or wet process, used for bubble generation. The dry process produces more stable bubbles with sizes less than 1 mm compared to the wet process, for which the sizes of the generated bubbles are between 2 mm and 5 mm. The stable foam helps to resist mortar pressure until cement solidifies, which is advantageous to generate a reliable pore structure in FC.[11]

Though the mixing process and FC quality in these two methods can be controlled, the performing method is considered superior to the mix-forming method due to the following. Lower requirements for foaming agents. The foaming agent content is closely related to air content in the mixture.

Drying Shrinkage

Lack of coarse aggregates leads to 4–10 times higher shrinkage of the FC than that observed in ordinary concrete. There are many factors affecting the drying shrinkage, such as density, foaming agent, filler, additive, and moisture contents. Table 1 presents different drying shrinkage values observed in some cement-based materials.

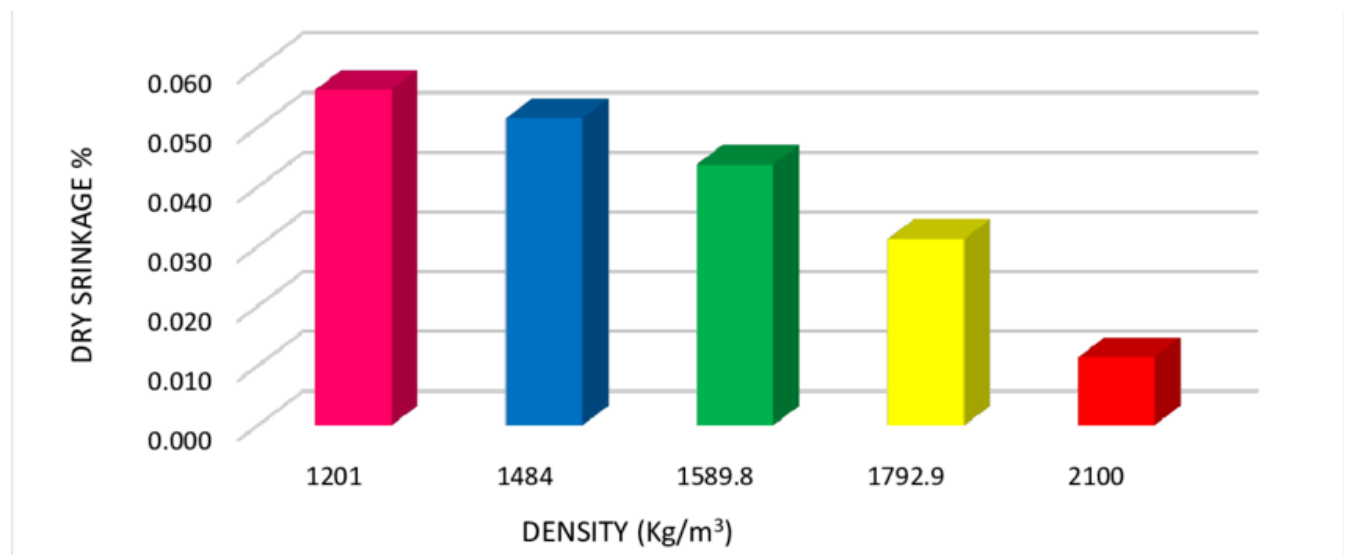


Table 1. Various drying shrinkage values observed in some cement-based materials.

28 Days dry Shrinkage of Foam Concrete with Various Densities

In general, drying shrinkage decreases with density reduction. The shrinkage differences induced by foaming agents are bound up with the pore structure of FC, and the lower pore connectivity helps to reduce the drying shrinkage. The decrease in drying shrinkage when fine sand was used as fillers instead of fly ash, is because the fine sand provides a superior capacity in resisting shrinkage deformation. Many findings demonstrate that fine aggregate such as light ceramicist expanded perlite, vitrified microsphere, and magnesium expansive agent together with a reduction of foam volume can reduce drying shrinkage. Meanwhile, restrictive effects from an increase in water and aggregate also provide support for drying shrinkage reduction.

It is reported that autoclaving technique reduces 12–50% drying shrinkage and brings a strength enhancement; therefore, autoclaving is an ideal option for maintaining FC products within an acceptable strength and shrinkage level. To reduce drying shrinkage, some aspects like water content control, selection of binder and foaming agent as well as mixture modifying with fine aggregate are worthy of further studies. The use of fibbers can significantly enhance resistance capacity on drying shrinkage due to tensile strength improvement of cement base mixture, prevention of further cracks development in cement base mixture, and capacity improvement of resisting deformation. Table 2 summarizes and reviews different results and findings on the drying shrinkage.

| Review of filler, foaming agent, and additive used in FC, and the resulting density ranges and drying shrinkage. | | | | | |
|--|--|-----------|--|------------------------------|----------------------|
| Filler | Foaming agent | w/c ratio | Additive | Density (kg/m ³) | Drying shrinkage (%) |
| Blast-furnace slag + limestone fine | Fatty alcohol-based liquid | 0.29 | Magnesium expansive agent + calcium sulfoaluminate | 1611–1638 | 0.05–0.32 28 d |
| Polymer fiber | Foamin C [®] | 0.3 | Viscosity enhancing agent | 380–830 | 0.1–0.49 |
| N/A | Animal based + synthetic + plant based surfactants | 0.5 | N/A | 600 | 0.25–0.3 90 d |
| Crushed sand + FA | Hydrogen peroxide | 0.3 | Na ₂ SiO ₃ + NaOH | 1889–2106 | 0.09–0.1 180 d |
| FA + natural sand | Protein foaming agent | 0.71–2.22 | N/A | 1000–1400 | 0.09–0.2 365 d |
| N/A | Synthetic polymeric latex | 0.45–0.6 | N/A | 260–800 | 0.18–0.31 |
| N/A | Synthetic based | 0.52–0.75 | N/A | 300–800 | 0.26–0.35 90 d |
| Sand | Hydrolyzed protein | 0.5 | N/A | 900–1100 | 0.7–0.72 28 d |
| Quartz sand | PB-2000 | N/A | Microreinforcing additive | N/A | 0.15–0.3 |
| FA | Organic based | 0.3–0.5 | Na ₂ SO ₄ + Triethanolamine | 400–800 | 0.09–0.18 28 d |

N/A, not available; FA, fly ash.

Table 2. Foam concrete: A state-of-the-Art and State-of-the-Practice

Some adverse factors such as poor early curing, insufficient water conservation measures, or harsh production conditions may cause water evaporation, thereby leading to shrinkage or even crack in FC. Some technical measures improving these situations are illustrated as follows: Suitable cement dosage. Lower water-cement ratio. Strengthen water conservation in the early stage. A Use waterproofing agent. Use crack prevention net.[12]

Compressive Strength

Though FC has been deeply studied, some shortcomings such as low strength still restrict its wider applications. The strength of FC is determined by different cementitious materials, cement dosage, mix proportion, water-cement ratio, foam volume, foaming agent, curing method, additive, etc. [13]

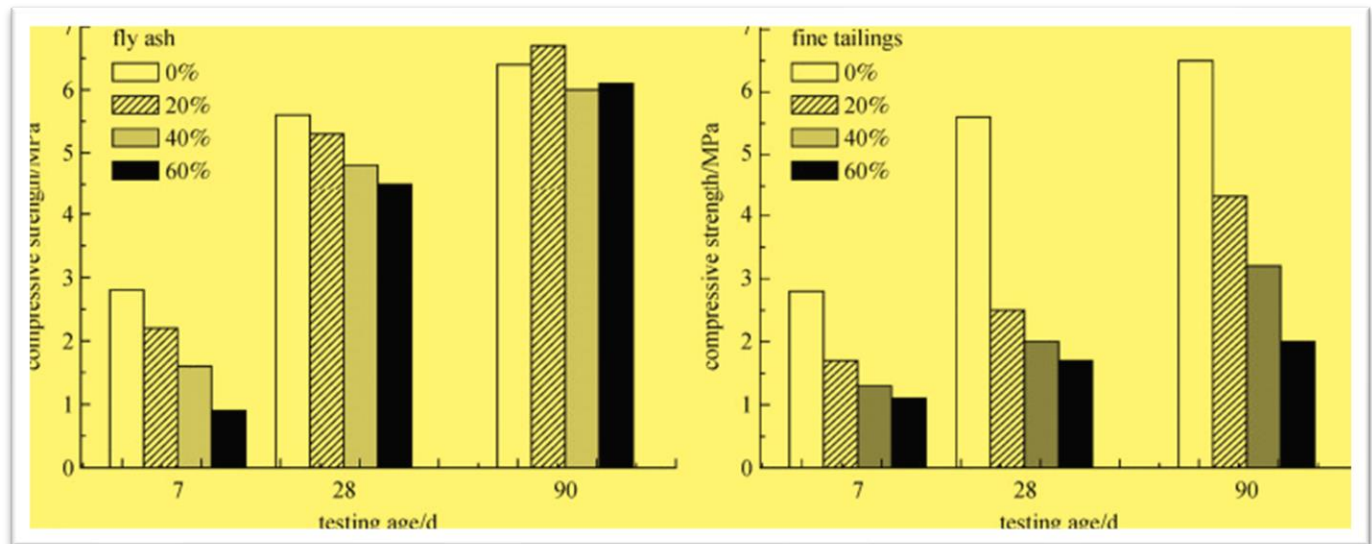


Table 3. Change of compressive strength over the days

To a certain extent, the density controls the strength. Hence, it is always to seek a balance between strength and density, for the purpose to maximize strength while reducing density as much as possible. Sometimes, this can be achieved through optimizing cementitious materials and selecting high-quality foaming agents and ultralight aggregates. The filler types determine the water-solid ratios when FC density is constant, and the reduction of sand particle size will help to improve strength. The foam volume exerts a notable impact on the flow behavior of FC, and a reduction in particle size of filler shows a positive effect on the strength improvement of FC. [14]

Park added carbon fiber into the base mixture so as to produce carbon-fiber-reinforced FC, and they reported that the strength and fracture toughness were obviously improved due to the carbon fiber reinforcement effect. The results confirmed that reasonable water-cement ratios exhibit a notable impact on enhancing strength. The higher water-cement ratio ensures excellent slurry fluidity thereby introducing foam into cement paste with an even distribution, so as to achieve durability growth. On the contrary, the decrease in the water-cement ratio results in poor fluidity, thus reducing the strength.

The dominant factor affecting strength is cement quality added into mortar slurry, whereas the high strength cement is considered an effective way for strength enhancement. However, it should be added appropriately considering the increase in the subsequent cost.[15]

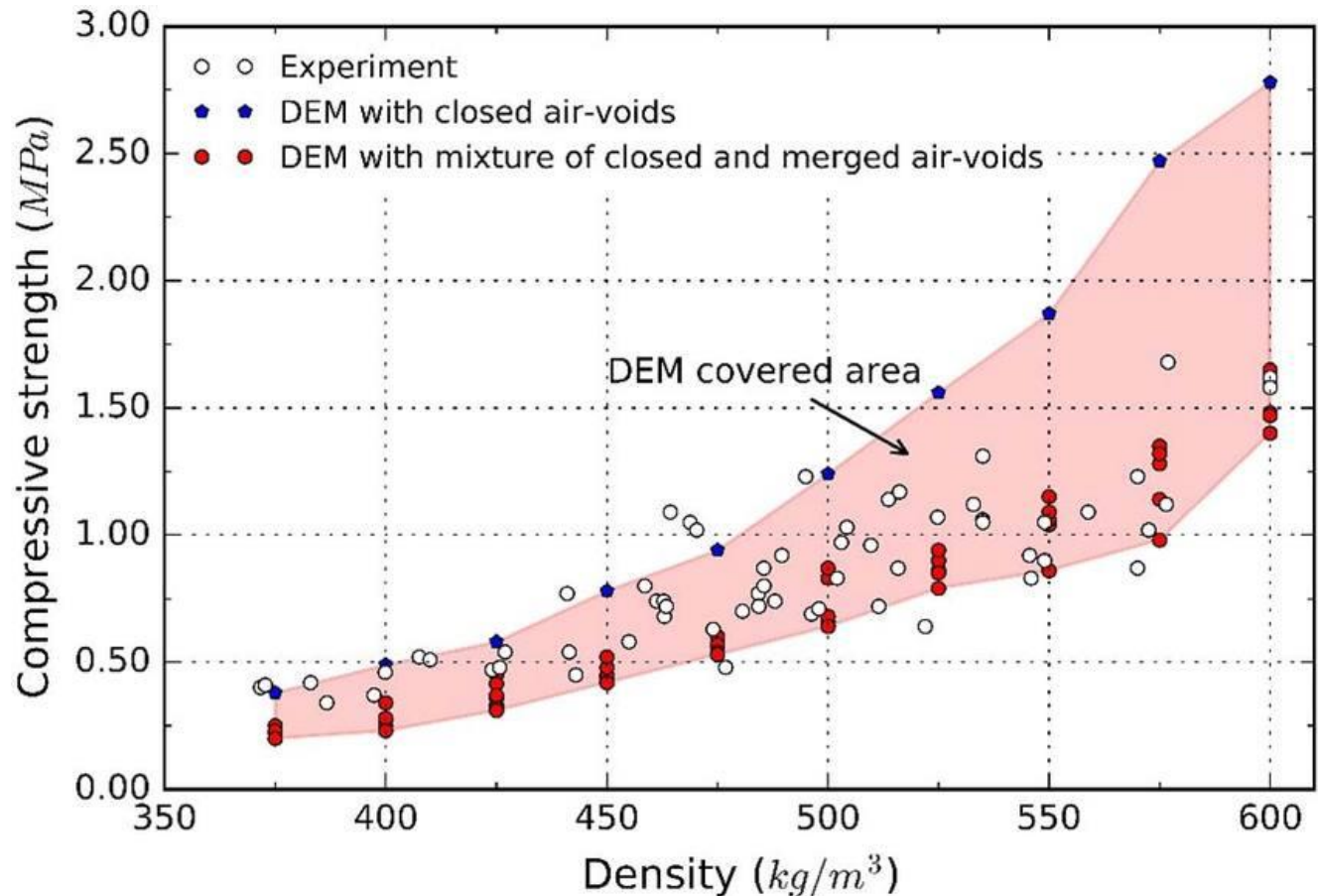


Table 4. Compressive strength distribution for verity of density.

Compressive strength-density relationship of foamed concrete

The investigation indicated that FC strength decreases with the voids increase. The impact of the foaming agents on strength is mainly manifested in aspects of the bubble size, distribution uniformities of bubbles, foam stability, and foaming capacity. Ideally, foaming agents should be characterized by strong foaming capacity, poor water-carrying capacity per unit, and little adverse impacts on FC.

Attempts and investigations can be considered regarding the selection of the high-performance foaming agent so as to prepare the small and uniform bubbles. The experimental results showed that the water-cement ratio and air-ash ratio have crucial impacts on FC strength; it also reported that the addition of fibers is helpful to increase strength. The prediction models on compressive strength were

also investigated by some researchers. These findings are mainly based on the artificial neural network, extreme learning machine, and regression analysis based on empirical models. [16]

Durability

The underground members are usually faced with various adverse conditions such as temperature change, freeze-thaw cycles, and acid-base corrosion. These factors may lead to poor durability of the FC-based structures and members, resulting in structural damages, which seriously affect project safety.

(1) *Permeability*. Water absorption of FC is attributed to the capillary pore infiltration and connected pore infiltration. The water absorption of FC was higher than that observed in other concrete types due to the least 20% foam embedded in plastic mortar. This capacity is generally twice that of the normal concrete with the same water-binder ratio. Permeability of concrete mortar decreases with porosity decrease after the addition of the aggregate. An increase in the aggregate volume in the mixture leads to increased permeability. Meanwhile, the increase of ash/cement quantity in the base mixture proportionally increases the water vapor permeability, especially at low densities. The dry density directly affects the porosity, but slight impacts of fly ash on porosity were observed. In addition, an empirical model for permeability prediction was proposed:[17]

$$k_d = G_d / (A_c t \Delta p)$$

where:

k_d = vapor flow time rate through the unit area

G = weight loss thorough t time in hours

A_c = cross sectional-area perpendicular to flow (m^2)

d = thickness of specimen in m

t = time in an hour

Δp = distance between dry and moist sides of the specimen.



Figure 4. Foam concrete application from Frankfurt.

The critical pore diameter and the pore diameter size (>200 nm) decrease with density increase, which is closely related to the permeability. Therefore, the manufacturer's ability to ensure air is contained in stable, small, and uniform bubbles should be highlighted, which is helpful to reduce the permeability of cement paste due to its integrity and isolation effects.

The adsorption of FC mainly depends on filler types, pore structure, and infiltration mechanism. It was reported that the filling effect from mineral aggregates affects the pore structure and permeability of cement paste. The fly ash-based mix was endowed with higher water absorption than that mixed with sand. The FC adsorption was generally lower than the corresponding basic mixture and decreases with foam volume increase. The water absorption dramatically increases owing to the use of steel and polypropylene fibers in the basic mixture. Each kind of fiber has a different surface morphology that plays an important role in the water absorption rate of lightweight FC. Another study suggested that using pozzolanic admixture and turbulent mixing techniques can produce water-resistant and durable FC.[18]

(2) *Frost Resistance*. The freeze-thaw cycle is one factor that is responsible for deterioration and failure in concrete. The addition of limestone powder reduced frost resistance of FC and limestone cement concretes indicate lower resistance to freezing and thawing compared to the pure cement concrete.

(3) *Carbonization* increases the risks of cracking and durability loss of FC. A higher incidence of carbonization was observed in low-density concrete. Compared with fine sand replaced mixture, replacing fly ash with cement in the mixture notably improved carbonization resistance capacity. In

addition, the foam content increases with the decrease of foam density so as to reduce carbonization in FC.

(4) *Corrosion*. The resistance capacity of FC to an erosive environment depends on its cellular structure. However, this structure does not necessarily reduce resistance capacity for water penetration, whereas voids produced cushioning effect to prevent rapid penetration. Sulfate erosion is identified as a complex process and can be influenced by various factors such as cement type, water-cement ratio, exposure time, mineral admixture, permeability, etc. In addition, the corrosion resistance capacity of studied samples increases with the decrease of FC density.[19]

Thermal Conductivity.

Outstanding thermal insulation properties of FC make it popular in the building insulation. It is widely reported in relevant studies that thermal conductivity is an important parameter influencing thermal insulation performance. FC has excellent thermal insulation properties due to its porous structure; thermal conductivity values are 5–30% of those measured on normal concrete and range from 0.1 to 0.7 W/mK for dry density values of 600–1600 kg/ m³, reducing with decreasing densities, the thermal conductivity of FC is controlled by the filler, density, fibber, mix ratio, temperature, and pore structure. [20]

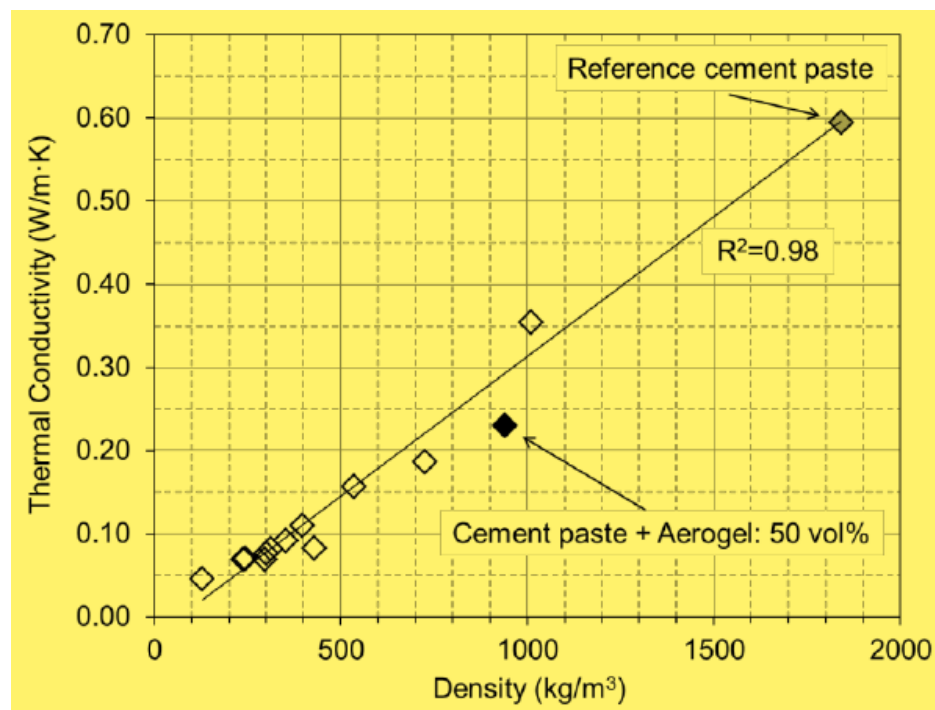


Table 5. Thermal conductivity of foam concrete as a function of the density

(1) Influence of Filler. Different aggregates and mineral admixtures have a significant effect on thermal conductivity. It was observed that the addition of the lightweight aggregate in FC reduces the thermal conductivity. It is specified that the thermal conductivity value for lightweight aggregate FC with a dry density of 1000 kg/m³ is 1/6 of that measured on a typical cement mortar. Artificially introducing pores into the mortar matrix combined with the use of lightweight aggregate with low particle density has been identified to be helpful for reducing thermal conductivity. Low density and hollow particles are advantageous to increase the heat flow paths so as to reduce the thermal conductivity.

(2) Influence of Density. For FC, it was found that the thermal conductivity reacts proportionally with a density. In terms of the application of FC in wall brick masonry, an increase up to 23% in thermal insulation was obtained compared to the normal concrete when the inner leaf of the wall was constructed with the FC at a density of 800 kg/m³.

(3) Influence of fiber. The thermal conductivity of several fibers consisting of AR-glass, polypropylene, steel, kenaf, and oil palm fibers, results showed that the thermal conductivity on samples with steel fiber inclusion is higher than those observed in FC with other fibers inclusion, while polypropylene fiber presented the lowest thermal conductivity. Also, the higher the fiber inclusion, the higher the thermal conductivity.

(4) Influence of Mix Ratio, insulation capacities of FC are proven to be sensitive to the change of mortar-foam ratios. The denser cement paste with a lower water-cement ratio is easier to form pores of larger size than that with a higher water-cement ratio.

(5) Influence of Temperature. It is reported that thermal insulation is improved with the decrease in temperature. FC with a larger size and a wider distribution of bubbles were found to have a lower thermal conductivity at low densities. Also, it was shown that the higher the porosity, the lower the thermal conductivity. However, the increase of the joint strength of pore paths was found to occasionally increase the thermal conductivity, location and relative orientation of the pores have a great influence on the thermal conductivity. More thermal resistance was observed when the pores are arranged at right angles to the heat flow, leading to more heat passing through the pores. On the contrary, if a layer of pores is parallel to the direction of heat flow, a smaller thermal resistance will be produced.

(6) Influence of Pore Structure. FC with larger sizes and a wider distribution of bubbles were found to have a lower thermal conductivity at low densities. Also, it was shown that the higher the porosity, the lower the thermal conductivity. However, the increase of the joint strength of pore paths was found to occasionally increase the thermal conductivity.

The location and relative orientation of the pores have a great influence on the thermal conductivity. More thermal resistance was observed when the pores are arranged at right angles to the heat flow, leading to more heat passing through the pores. On the contrary, if a layer of pores is parallel to the direction of heat flow, a smaller thermal resistance will be produced.[21]

Pore Structure

A critical task in FC production is to control the nature, size, and distribution of pores because the pore characteristic is the key factor to determine the density and strength of FC. Pores can be generated by

- (i) mixing a gas releasing agent such as H₂O₂ or zinc powder in the Pasteur cement mortar
- (ii) introducing a large volume of bubbles in mortar. Often different foaming methods, the composition of the mixture, and the curing process will produce individual bubbles with different sizes and distributions, which further affects the performance of the FC pore characteristic is an important factor that controls the compressive strength, thermal conductivity, and permeability of the FC pores are composed of the interlayer pores/spaces, gel pores, capillary pores, and air void, with pore sizes varying from nanoscale scale to millimeter scale.

Some parameters such as volume, size, size distribution, shape, and spacing of pores can be used to characterize these pores gel and capillary pores are mainly responsible for the microstructure features the use of additives and the variation of water-cement ratio will affect the pore characteristics.



Figure 5. Foam concrete zoom with different densities[22]

For a given density, the addition of additive reduces the pore size and connectivity so as to obtain the higher strength introduction of mineral admixture such as slag or fly ash in FC results in a reduction in the pore size distribution and total porosity. The narrower the pore distribution, the greater the conductivity and the smaller the density addition of superplasticizer in a combination with other additives in foam concrete can further benefit improvement of the pore structure. Researchers found that the pores may be influenced by the water-cement ratio owing to the changes in the rheological properties and the ability to resist collapse from the foams.

It is observed that the pores were small, irregular-shaped, and highly connected at water-cement ratios below 0.8 pores were determined to be rounded, expansive, and with wider pore size distribution for water-cement ratios over 0.8, because of the ability to limit the growth of air bubbles decreased at high water-cement ratios. It is reported that reduction of water-cement ratio or the addition of fillers often brings difficulties in generating an arranged pore area. The lower water content helps FC to capture the smaller pore size as well as the increased mass density and compressive strength.

Pore distribution is one of the important microscopic parameters affecting the strength of foam concrete. In general, foam concrete with narrower bubble distribution will have a higher strength. It is observed that pore sizes in FC produced by mechanical foaming are smaller than those made by chemical foaming connectivity of pores depends on the density of the mixture, not on the foaming method. If the density reaches a level that allows the adhesive to separate individual bubbles, the pores tend to be closed.

Otherwise, the FC will be dominated by the opening pore structures. Scanning electron microscope (SEM) to characterize pore size and shape parameters, and effects of different additives on strength

performance investigation demonstrated that the addition of additives notably enhanced microstructure and pore structure of FC slurry compared with the conventional mixture the additives increase the number of pores, higher strength was obtained due to the reduction of pore size and connectivity, which prevents pores from merging and producing a narrow distribution (see Figure 6). It is confirmed that FC strength not only depends on pore structure

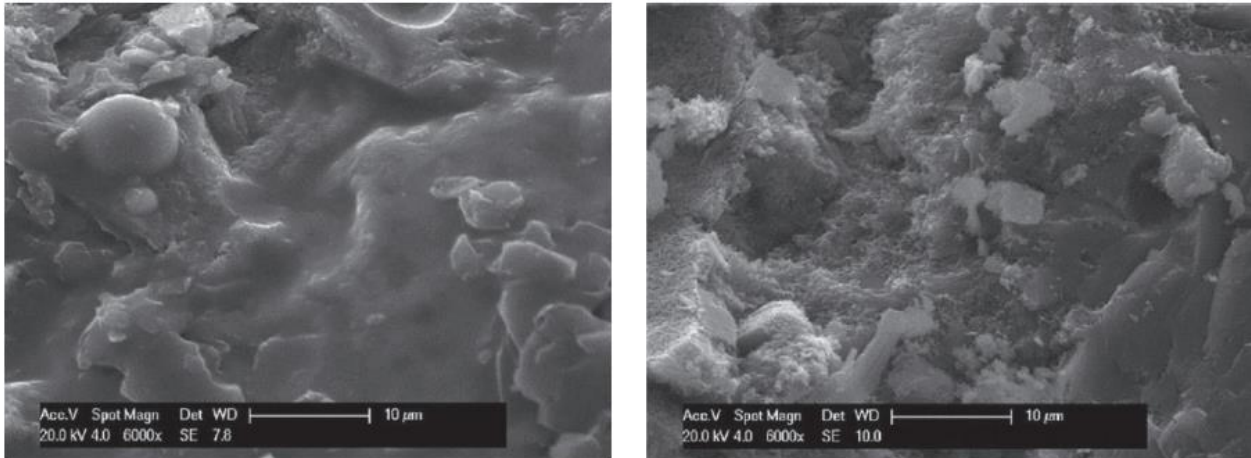


Figure 6: Effect of additives on cement paste microstructure, (a) with additive (more homogeneous) and (b) without additive [23]

enhancement, but also microstructure improvement of the cement pastes many globally sourced literature on FC have been documented, it is worth noting that research concerning performance enhancement from FC micro mechanism should not be neglected, whereas microstructure signifies its various performance behaviors macroscopic aspect such as concrete type, filler, additive, foaming agent, and water-cement ratio have been widely studied. However, there are very limited literature on FC microstructure, so this may be a direction for future efforts to improve FC performance.

Outline of the experimental program

The performed experimental program aimed to determine what effect composite mesh reinforcement has on the bending capacity of the foam concrete structural members. The research program contained 9 slab elements tested in three-point bending, including 3 reference slabs without

any reinforcement, 3 slabs reinforced with a basalt fiber grid, and the last 3 with a carbon fiber grid. Investigations were completed by the necessary tests of material properties.

Test set-up

All tested foam concrete specimens were made of the same concrete mixture. The applied mixture comprises Portland cement, a small amount of gravel, water, technical foam, fiber additive, and superplasticizer. The volume weight of ready concrete was designed at 800kg/m³ and was individually controlled for each tested member. Concrete curing was performed in natural conditions, at a temperature near 10°C.

In the initial phase, members were covered with Styrofoam boards to reduce the loss of temperature and water. Figure 7 shows the scheme of tested specimens. To ensure the proper amount of reinforcement slab-type elements were chosen of section dimensions 120 × 350 mm, a total length of about 700 mm, and a span length of 600 mm. Such configuration provides a span-to-depth ratio equal to 5 which should effectively reduce the impact of the shear on the final results.

As it is difficult to ensure a proper bond of reinforcement due to the brittleness of foamed concrete, specimens were reinforced with a composite grid wherein the perpendicular fibers provide anchorage. Two types of grids were used: one based on relatively cheap basalt fibers and the second one on more expensive, but also stronger carbon fibers. Table 6 shows a comparison of the main properties of the applied meshes.

| | | |
|---|----------------------------|----------------------|
| | BSC220.220.260.100 | C-GRID®C50-2.36×2.36 |
| Type of reinforcing fibers | Basalt continuous filament | Carbon fiber |
| Grid geometry (longitudinal × transverse spacing) | 25 mm × 25 mm | 60 mm × 60 mm |
| Supply form (roll width) | 1.0 m | 1.2 m |
| Break load | >50 kN/m | >54.17 kN/m |
| Elongation at break | 2.5±1% | 0.99% |
| Tensile modulus of elasticity | 86÷94 GPa | 234.5 GPa |

| | | |
|------------------|--|---|
| Other properties | Non-corrosive, lightweight, outstanding mechanical bond with concrete | Resistance to chemically aggressive environment, dielectric, easy to install |
| Applications | Slabs on-grade, overlays, silos and concrete tanks, shotcrete, balconies, precast architectural concrete | The construction industry, reinforcement of mortars and non-load-bearing concrete |

. Table 6 shows a comparison of the main properties of the applied meshes.

The properties of the hardened foam concrete were evaluated by performing uniaxial compression tests at the same age as the main bending tests. Particularly the age was 54 days.

Test set-up scheme

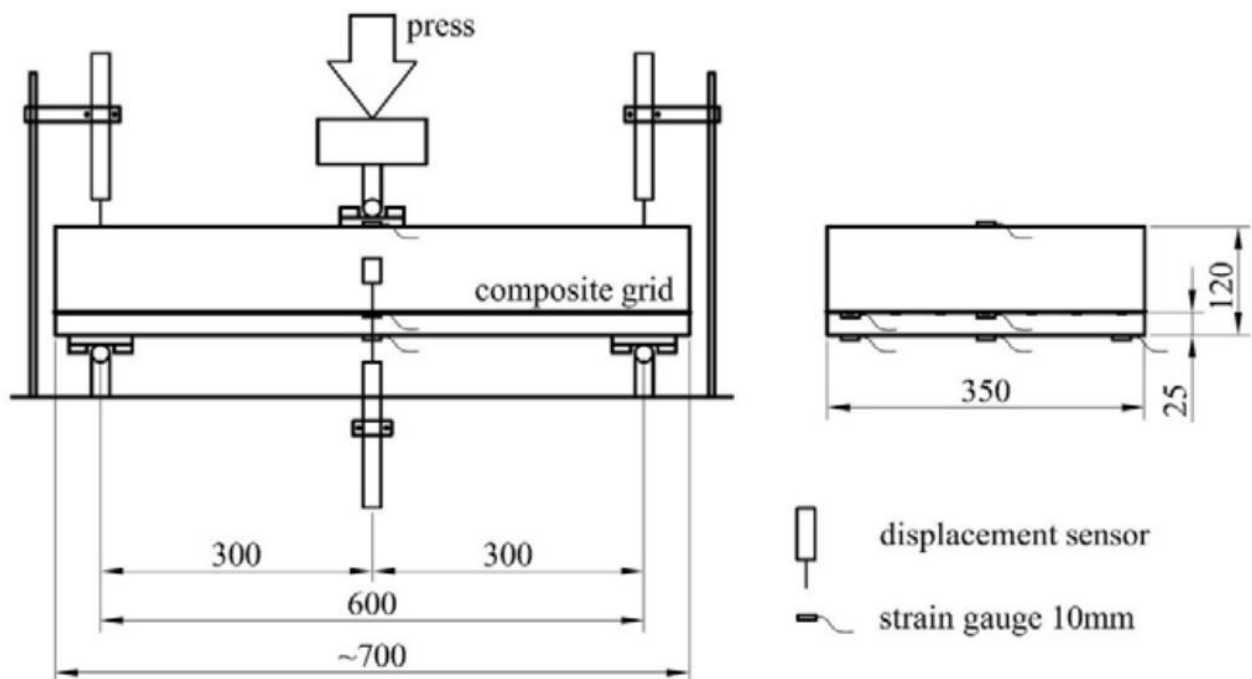


Figure 7 shows the scheme of tested specimens

According to standard PN EN 12390-3:2009, compressive strength, f_c , cube, was evaluated on six single cubes with side dimensions of 120 mm, while compressive cylindrical strength, f_c , and secant modulus of elasticity, E_c , were estimated testing six single cylinders with a diameter of 150 mm and height of 300 mm. The mean results can be found in Table 7

| Age of test | f_c [MPa] | $f_{c,cube}$ [MPa] | E_c [GPa] |
|-------------|-------------|--------------------|-------------|
| 54 | 1.68 | 1,87 | 1.65 |

Table 7. Hardened foam concrete mechanical properties.

Laboratory tests were executed in the three-point bending test shown in Figure 7. All slabs were loaded until failure monotonically with a loading speed of 0.05 kN/s. Force was applied using a hydraulic press with automatic recording of the applied force. To determine deflections, the test stand was equipped with linear displacement transducers at three points along the slab's length (at supports and in the middle of the span). Electrical strain gauges were glued on the reinforcement and on the upper and bottom surface of each tested specimen according to Fig. 7. Due to the homogeneous structure of foam concrete, relatively short gauges were used with a base length of 10 mm. Additionally, the test was recorded using a high-resolution camera to allow an optical analysis of strains and displacements, especially crack propagation and width.

3. Test results

The evaluation of the flexural behavior was made by recording failure load and analysis of deformations during the test. Table 8 shows the summary of the achieved results for all slabs.

| Specimen | reinforcement | Density of foamed concrete [kN/m ³] | Failure force [kN] | Failure moment [kNm] | Deflection at failure [mm] |
|----------|---------------|---|--------------------|----------------------|----------------------------|
| FC_1 | No | 7.78 | 0.953 | 0.157 | 0.98 |
| FC_2 | | 7.93 | 1.196 | 0.193 | 1.13 |
| FC_3 | | 7.78 | 1.269 | 0.204 | 1.39 |
| BC_1 | Basalt mesh | 7.63 | 9.196 | 1.393 | 10.25 |
| BC_2 | | 7.98 | 7.926 | 1.203 | 6.04 |
| BC_3 | | 8.09 | 9.238 | 1.399 | 8.31 |

| | | | | | |
|------|-------------|------|--------|-------|------|
| CC_1 | | 7.67 | 11.792 | 1.783 | 7.46 |
| CC_2 | Carbon grid | 7.74 | 10.746 | 1.626 | 7.91 |
| CC_3 | | 7.44 | 9.957 | 1.508 | 6.57 |

Table 8. Selected test results.

3.1. Failure load Analysis

of failure load shows directly the effectiveness of the applied reinforcement. As it is visible in Table 8, the highest bending capacity was achieved in slabs reinforced with a carbon grid. The mean failure force was equal in this case 10.831 kN. A slightly smaller failure force (mean 8.786 kN) was obtained in specimens reinforced with basalt mesh. Both of these results are impressive in comparison to unreinforced elements for which the failure force did not exceed 1.269 kN. Reinforcing grids did not break during the test.

Differences in bearing capacities of basalt-reinforced (BC) specimens and carbon-reinforced (CC) specimens could be explained by the greater modulus of elasticity of carbon fibers. As a result of the smaller rotation of cross-section, the strain and consequently also the stress in the compressed zone of foamed concrete were smaller. An interesting observation can be made from destruction images of un-reinforced and reinforced slabs shown in Fig. 8. Specimens without reinforcement failed in a conventional manner, after cracking in the cross-section of the largest bending moment (Fig. 8a). Slabs reinforced with basalt and carbon grids also initially cracked in the central zone, but finally, they failed due to inclined shear crack with delamination and slippage along the surface of the reinforcing grid. It is shown in Fig. 9. The transverse fibers provided effective anchorage, but at extreme load, they acted like a knife cutting sample through the plane of the grid (Fig. 9b).

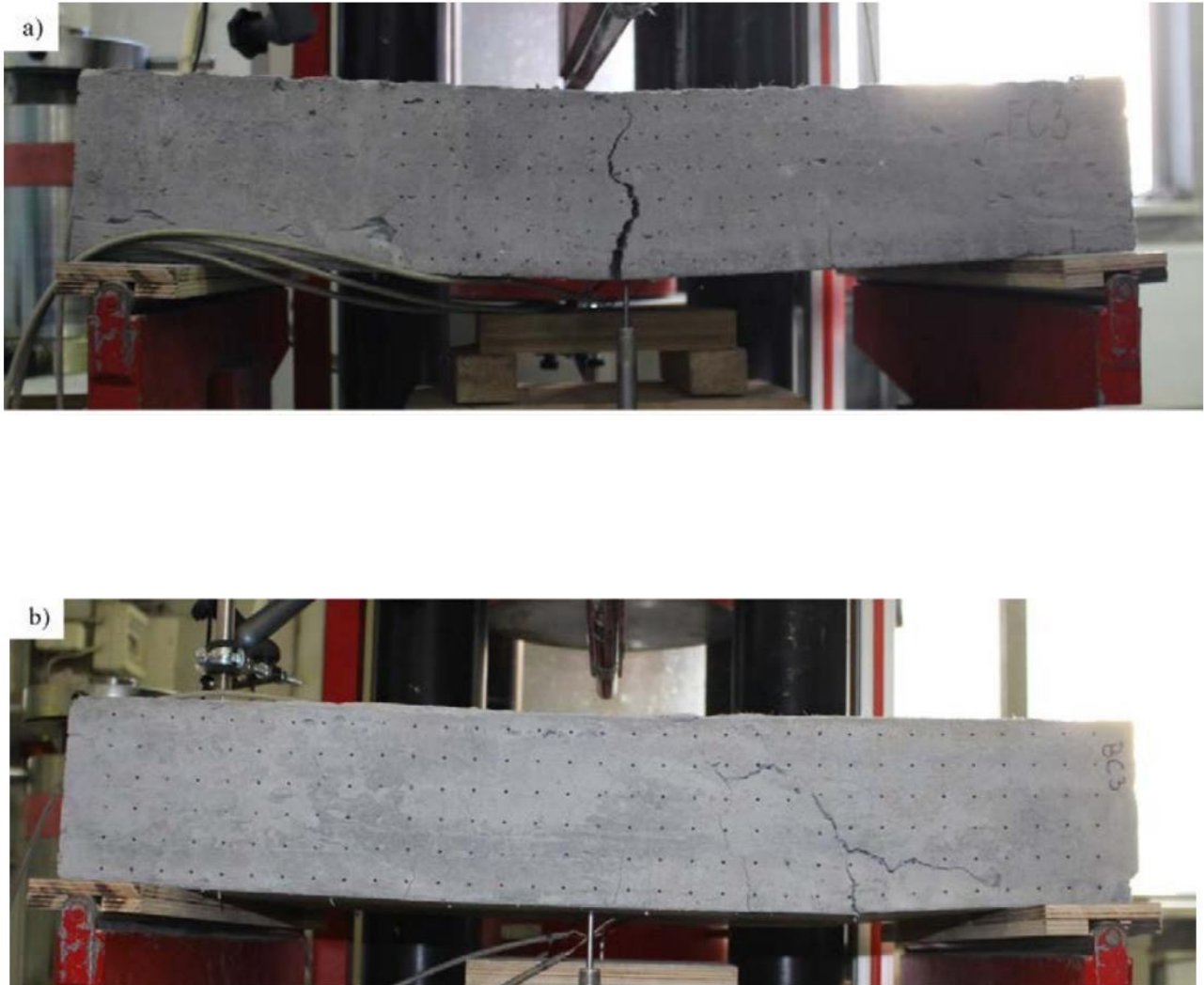


Fig. 8. Typical failure modes of tested specimens: a) no reinforcement (FC3), b) reinforcing mesh (BC3).

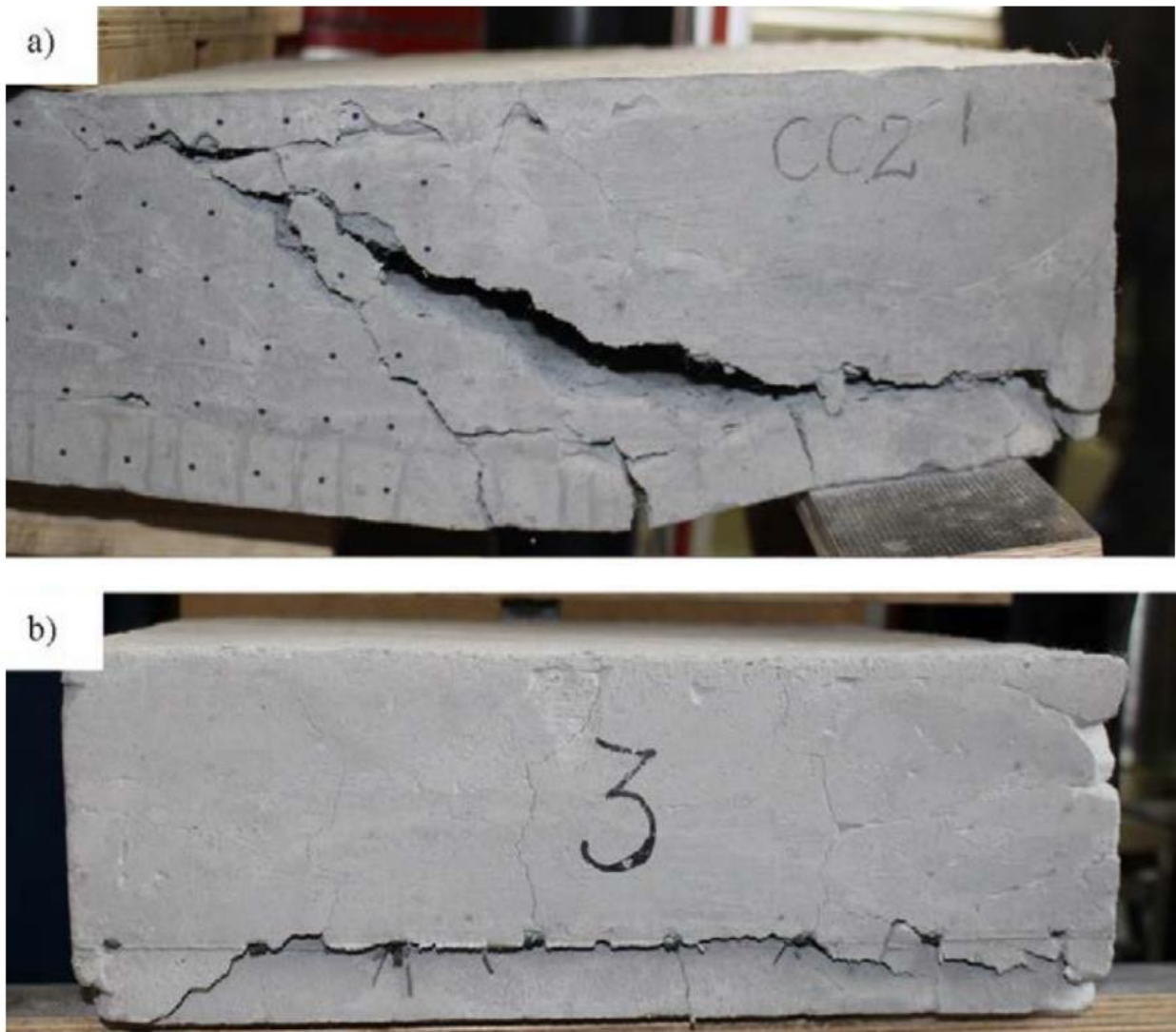


Fig. 9. Delamination and slippage along the surface of reinforcing mesh: a) side; b) front of the specimen.

3.2. Deformations

Figure 10 shows a comparison of mid-span deflection curves for all tested specimens. What is also presented in Table 8, the failure deflection of specimens reinforced with basalt grid was greater than the one in slabs reinforced with carbon grid. This is understandable and is the result of more than twice the higher value of the elastic modulus of carbon fibers. The scale of difference in flexural stiffness is interesting, which for CC models is almost two times greater than for BC models. It shows a much greater impact of the reinforcement parameters on the deformability of specimens made of foam concrete in comparison to those made of ordinary concrete.

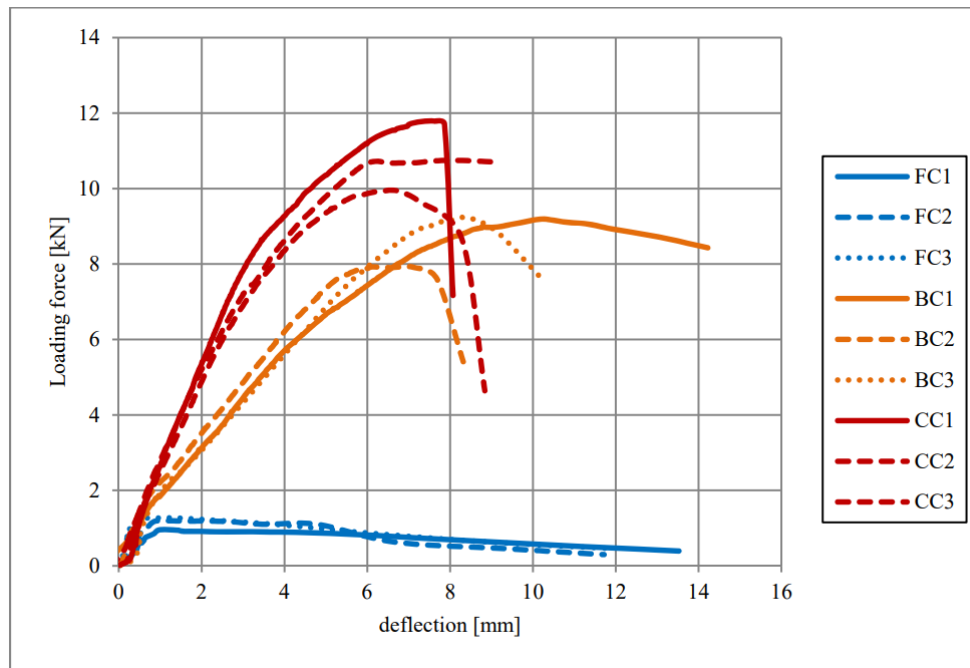


Fig. 10. Comparison of deflections of tested specimens.

3.3. Other benefits of reinforcement

One of the major drawbacks of foam concrete is its large shrinkage. For this reason, the production of elements of large dimensions is associated with a high risk of cracking. The use of composite grid reinforcement effectively, though not completely, reduces the occurrence of shrinkage cracks. The least number of cracks was found on samples reinforced with carbon mesh which could be associated with its lowest deformability. What is important, the use of reinforcing mesh prevents brittle separation of cracked elements and retains the ability to transfer tensile forces.

4. Conclusions

There is no doubt that internal composite reinforcement has a beneficial effect on foam concrete specimens under flexure. The mean failure load of elements reinforced with basalt grid is more than 7 times higher than in elements without composite reinforcement, while for carbon grids that factor reaches almost 9.

Transverse grid fibers create effective anchorage for fibers in the main direction. It is proved by failure which occurs as a result of delamination and slippage in the plane of the reinforcing mesh. The composite grid effectively prevents the growth of flexural cracks. Because of the greater modulus of elasticity, the flexural stiffness of specimens reinforced with a carbon grid is greater than the stiffness of specimens reinforced with a basalt grid.

The composite grid may be a remedy to the greatest disadvantage of foam concrete which is its susceptibility to shrinkage cracking. It not only limits the occurrence of such cracks but also very effectively sews existing ones. The paper shows only preliminary studies of specimens made of a relatively weak type of foam concrete. The study will be continued with the use of higher density foam concrete and other types of reinforcing grids, such as glass and cheap PP geogrids.

Chapter 2

Hygrothermal Performance of ETICS on Concrete Wall after Low-Budget Energy Renovation

Hygrothermal performance of mineral wool and expanded polystyrene external thermal insulation composite system (ETICS/ EIFS) was studied in field conditions and by computer simulations with the Delphin program. Temperature and relative humidity were measured in an additionally insulated large panel concrete element wall from September 2011 to January 2013 in the cold climate of Estonia. Measurements of indoor climate, air leakage, and thermal bridges through building fabric were conducted before and after the low-budget energy renovation pilot project of an apartment building.

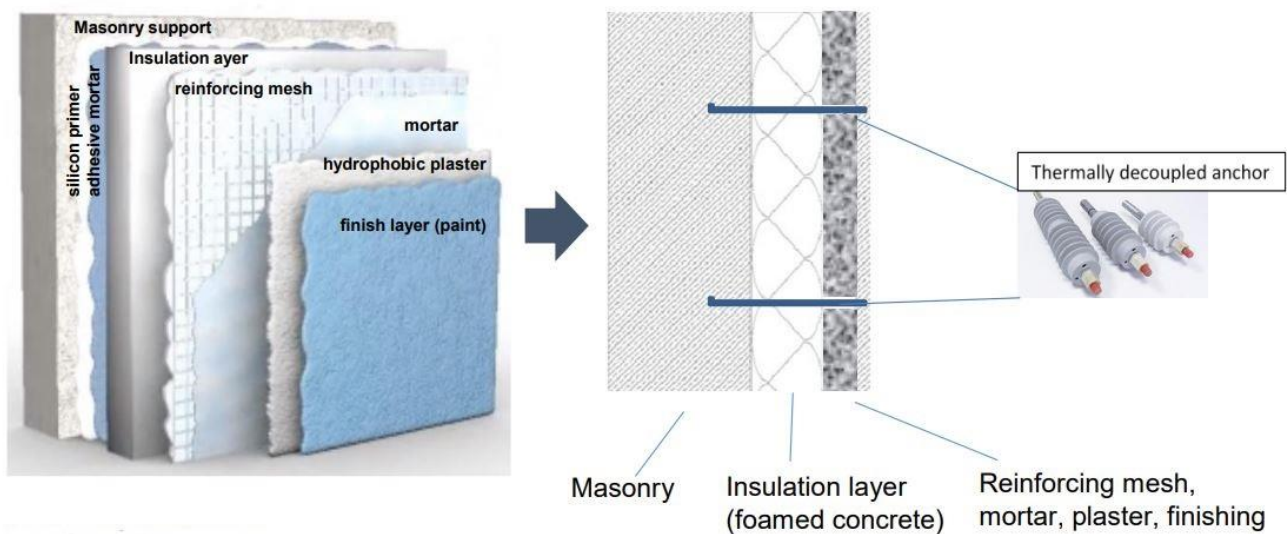
Results showed that indoor climate and thermal comfort were not improved a lot in all aspects and the same was true for airtightness. Unacceptable thermal bridges remained at the external wall/balcony, external wall/foundation wall junction, and also around the windows because they stayed in their original position. Built-in moisture of the whole wall dried out during the first heating season. A better agreement was found between measured results if the convective moisture flow in addition to diffusion was taken into account in simulations. The average measured thermal transmittance during the winter was $U_{\text{wall}} 0.17 \text{ W}/(\text{m}^2 \cdot \text{K})$ in the case of graphite enhanced EPS and

0.19 W/(m² ·K) with mineral wool. The long-term durability of ETICS in a cold climate and under wind-driven rain loads needs further investigation.[24]

METHODS

An energy-renovation pilot project “Healthy and Cost Saving Home” was started in the spring of 2010 in cooperation with two financing institutions together with a ministry, an energy company, a local municipality, and a university. The global purpose was to carry out an example renovation of a typical apartment building to demonstrate energy-saving and improve indoor climate as well to motivate people to renovate their buildings.

The case-study building is a five-story block of flats (Figure 11) constructed in 1966 with prefabricated large panel concrete elements. Approximately half of the apartment buildings in Estonia are composed of prefabricated concrete large panel elements.



Renovation Solution

Renovation solution was selected based on the energy and economical calculations:

- Improvement of the building envelope:

- External walls: +15 cm graphite enhanced expanded polystyrene (EPS) in the external thermal insulation composite system (ETICS): $U_{\text{external walls}} = 0.17 \text{ W}/(\text{m}^2 \cdot \text{K})$;
- Basement walls: +10 cm EPS covered with drained and ventilated cladding: $U_{\text{basement wall}} = 0.36 \text{ W}/(\text{m}^2 \cdot \text{K})$;
- Roof: +30 cm EPS above the roof $U_{\text{roof}} = 0.11 \text{ W}/(\text{m}^2 \cdot \text{K})$;
- Replacing of 33% of the old windows: $U_{\text{old window}} = 1.8 \text{ W}/(\text{m}^2 \cdot \text{K})$, $U_{\text{new window}} = 1.0 \text{ W}/(\text{m}^2 \cdot \text{K})$; because only 1/3 of the windows were replaced with new; all windows were left at their original position: inboard of the exterior concrete core of the external wall;
- Ventilation system: new exhaust ventilation with heat recovery (exhaust air [water to water] heat pump);
- Heating system: new hydronic radiator heating with thermostats.



Figure 11 View of the external wall with measurement areas of ETICS

Measurements

Measurements on the case-study building concentrated on the indoor climate, energy performance, and hygrothermal performance of the building envelope. During the study the following measurements were taken:

- The values of indoor temperature (t) and relative humidity (RH) conditions were measured with small data loggers at 1 h intervals over a 2 years period;

- Surface temperature of thermal bridges was measured by using infrared image camera “FLIR Therma Cam E320” (EN 13187) with minimum indoor and outdoor temperature difference of at least 20 K. Tabulated surface emissivity’s from FLIR Therma Cam E320 user’s manual was used;
- The air leakages of the building fabric of the apartment were measured with the standardized fan pressurization method (EN 13829), using “Minneapolis Blower Door Model 4” equipment; hygrothermal performance of east-facing external wall (see Figure 1 and Figure 2), additionally insulated with ETICS, was studied using temperature and relative humidity sensors and heat flux plates.

Hygrothermal performance of face sealed, non-drainable external thermal insulation composite system (ETICS) (also called exterior insulation and finish systems, EIFS) with two different insulation materials was compared in two test walls: mineral wool (MW) and graphite enhanced expanded polystyrene (EPS).

All the other components (adhesive, base coat, reinforcement [glass fiber mesh], mineral finishing coat, paint coating) of two test walls were the same. Test-walls were located exterior to the same room so that both test-walls experienced the same climatic conditions. Two walls were separated from each other with polyurethane (PU) foam insulation to minimize wall-direction moisture movement. The location of the test walls at the upper corner of the wall was selected based on it having the highest driving rain intensity.[25]

Simulations The temperature and humidity measurement results from test-walls were compared with a hygrothermal simulation model Delphin 5.7

- to validate the simulation model for future simulations with different initial and climatic conditions as well as with different dimensions of the building envelope;
- to understand better the performance of the external thermal insulation composite system.

Modified material properties were used from the Dolphin’s database. Table 9 shows the properties of materials used as compared to measured and simulated results when the best correlation was obtained. The dependency of hygrothermal mal properties on the environmental conditions was taken into account: water vapor permeability, liquid water conductivity, and thermal conductivity depending on the water content of the material (an example of concrete is shown in Figure 12 [left]).

A cross-section of the simulated wall is presented in Figure 12 (right). Thermal bridges before and after the renovation were evaluated by using a thermal camera and two-dimensional heat-transfer simulation software THERM 6.3 according to standard EN ISO 10211. Thermal bridges were assessed using the temperature factor (EVS-EN ISO 13788). The limit value for temperature factor in a dwelling with high or unknown humidity loads is considered to be ≥ 0.8 [26]

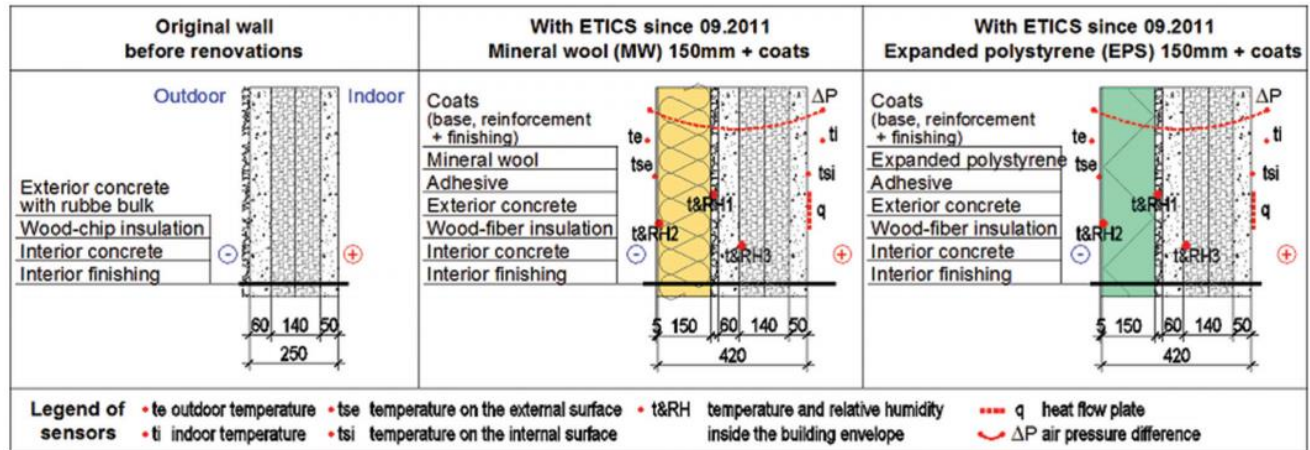


Figure 12 View of the simulated wall

| | Concrete | Wood-Cement Chip Board | Adhesive Mortar | EPS | MW | Exterior Coating |
|---|---------------------|------------------------|---------------------|-------------------|-------------------|----------------------|
| Bulk density ρ , kg/m ³ | 2320 | 500 | 700 | 35 | 75 | 1270 |
| Porosity f , m ³ /m ³ | 0.14 | 0.93 | 0.73 | 0.94 | 0.92 | 0.50 |
| Specific heat capacity c , J/(kg·K) | 850 | 1470 | 945 | 1500 | 840 | 960 |
| Thermal conductivity* λ , W/(m·K) | 1.5 | 0.12 | 0.19 | 0.035 | 0.038 | 1.0 |
| Water vapour diffusion resistance factor* μ , — | 19 | 3.8 | 15 | 15 | 2 | 10 |
| Liquid water conductivity* k , kg/(m·s·Pa) | $44 \cdot 10^{-12}$ | $16 \cdot 10^{-9}$ | $3.2 \cdot 10^{-9}$ | 0 | 0 | $0.27 \cdot 10^{-6}$ |
| Air permeability K_g , s | $1 \cdot 10^{-6}$ | $7 \cdot 10^{-3}$ | $1 \cdot 10^{-5}$ | $1 \cdot 10^{-6}$ | $1 \cdot 10^{-2}$ | $1 \cdot 10^{-6}$ |
| Built-in moisture w , kg/m ³ / rh, % | 48 / 65 | 27 / 60 | 200 / 100 | 0.6 / 60 | 3.1 / 60 | 300 |

*Dry material

Table 9. Main Hygrothermal properties of Materials used in the Simulation

RESULTS

Technical Condition of External Walls

External walls of the analyzed building were composed of large-panel prefabricated concrete elements. Fourteen centimeters of wood-cement chipboard (thermal conductivity $\sim 0.12 \text{ W}/[\text{m}\cdot\text{K}]$) was used for insulation between two layers of concrete and the external surface is covered with rubble bulk. The main problems related to external walls are thermal bridges, corrosion of reinforcement, frost resistance, and large thermal transmittance.

The layer between the insulation and external concrete core is not ventilated but slightly drained (small tubes installed at the intersection of movement joints). The external core can become wet due to vapor condensation and wind-driven rain. This means that frost damage to concrete and corrosion of reinforcement can occur.

Indoor Climate

Conditions Temperature and relative humidity were measured in four apartments before and after the renovation. There was a significant difference ($P < 0.001$) in temperature measurement results, see Figure 17 left. A new adjusted heating system has

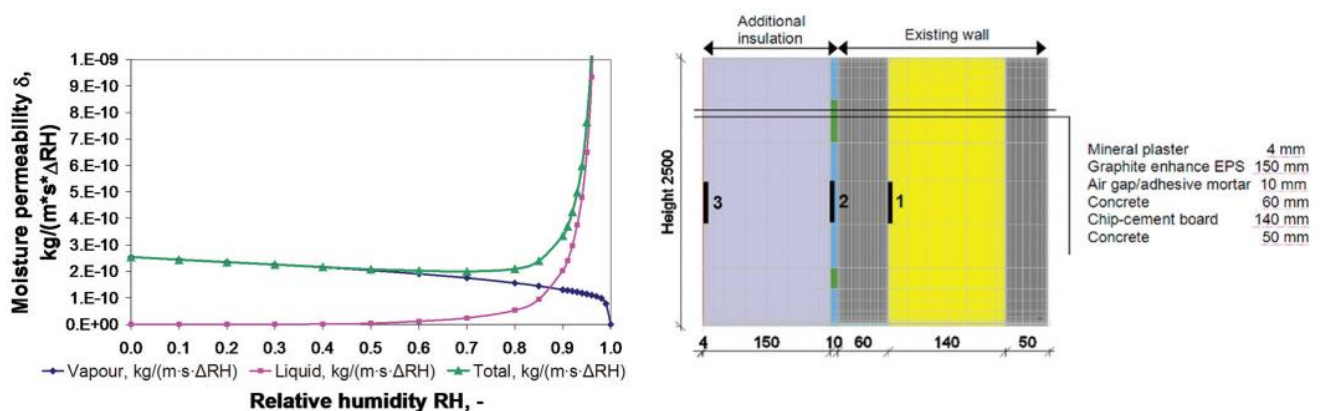


Figure 13 Moisture permeability of concrete as liquid and vapor at different RHs (left). Example of the wall section in simulation tool Delphin with measurement points of temperature and RH 1, 2, 3 (right).

even temperatures during a whole heating season after the renovation while there was a clear overheating before. There was no significant ($P = 0.3$) difference in RH before and after the

renovation. Moisture excess (the difference between vapor content of the indoor and outdoor air), v , g/m^3 was calculated from indoor and outdoor climate, Figure 17 (right).

Somewhat surprisingly, moisture excess was not lower but even higher (significant difference [$P < 0.001$]) after the renovation, especially during very cold days with outdoor air temperatures lower than -10°C . Still, the level of moisture excess being up to $\sim 3 \text{ g}/\text{m}^3$ on average and up to $\sim 4 \text{ g}/\text{m}^3$ at 90% level are lower than in these types of buildings in general.[27]

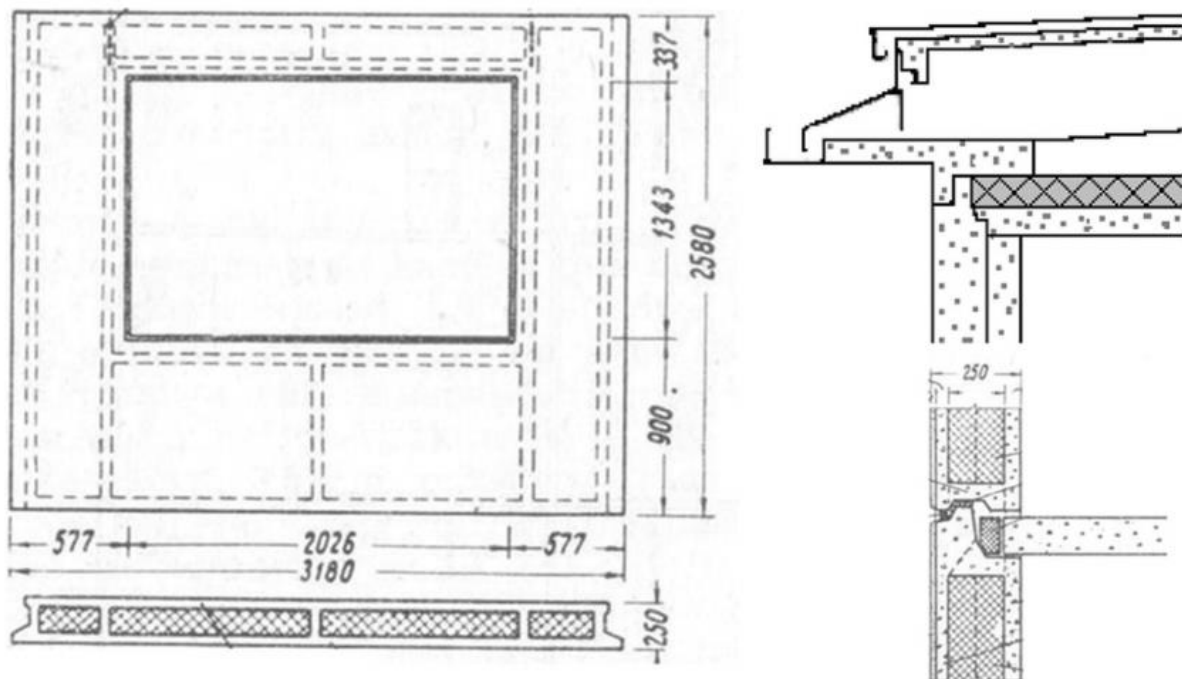


Figure 14 Original design drawing of a large panel prefabricated concrete element (left). External wall/roof junction (right-top) and external wall/inserted ceiling (right bottom).



Figure 15 Reinforcement steel between layers of concrete has started to corrode (left and middle). In principle, this steel should be cast into expanded clay concrete, but in reality, it is often not so. Cross-section of a concrete wall element (right).



Figure 16 Original drawing of an external wall/console balcony junction with a thermal bridge (left) and a picture of a degrading balcony (middle and right).

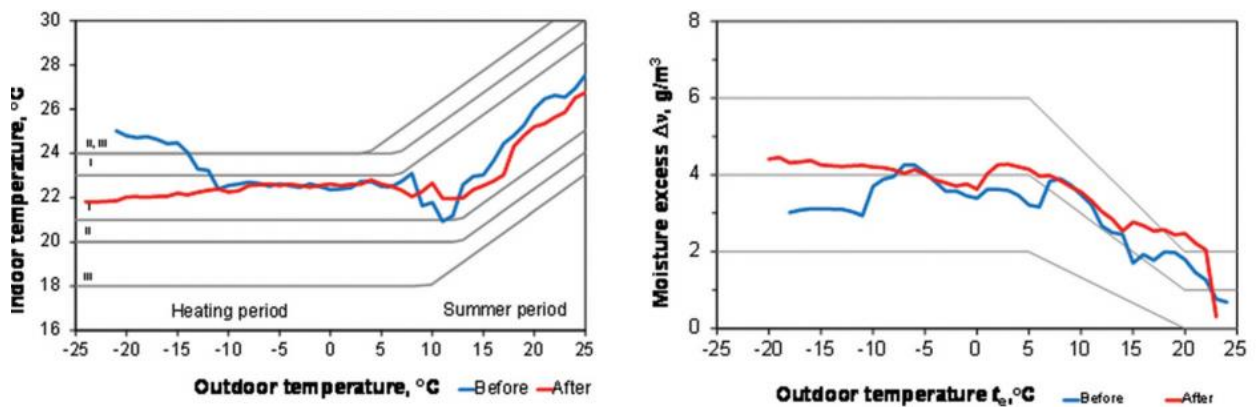


Figure 17 Measurement results of indoor air temperature (left) and moisture excess (right) depending on the outdoor air's temperature before and after the renovation.

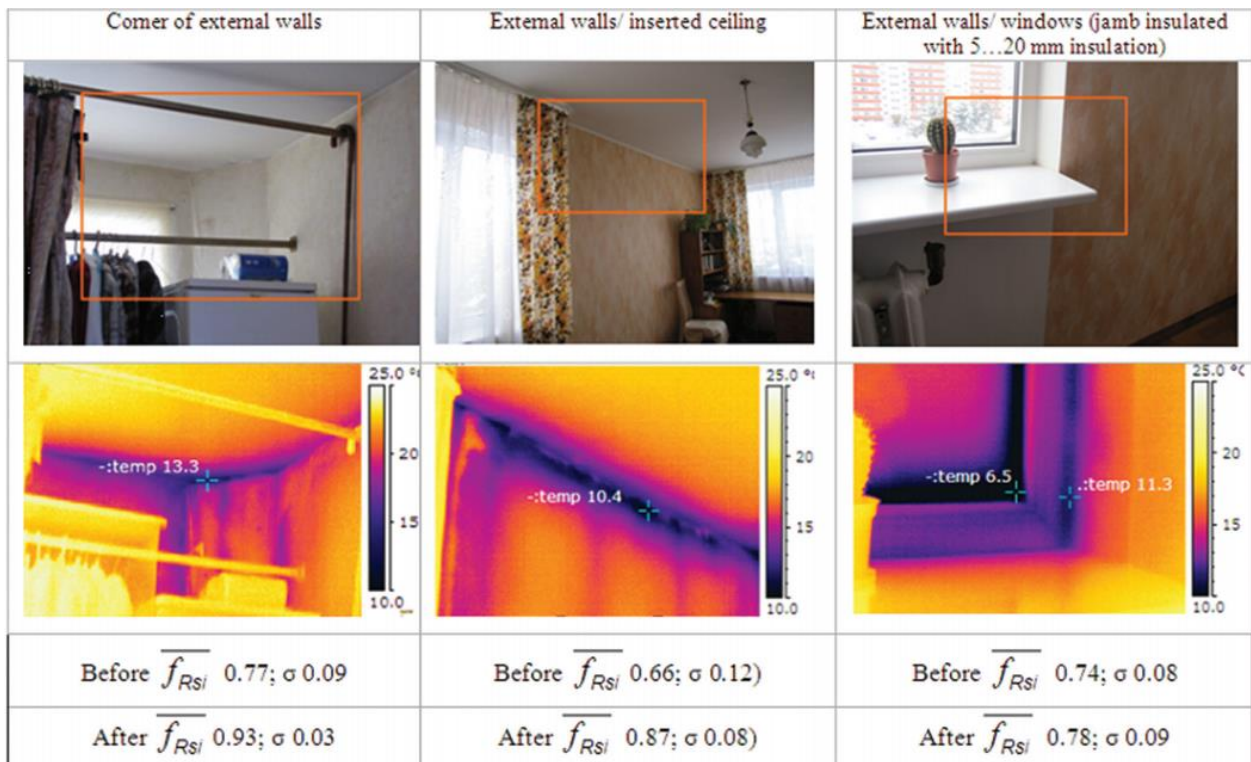


Figure 18 Measured range of temperature factor f_{Rsi} , of thermal bridges with average and standard deviation. Pictures were taken before the renovation.

Results are very sensitive to the thickness of insulation on a window's jamb (window return). It is not possible to install a sufficient layer of insulation (>30 mm) to the window jambs because of the shape of the concrete element that the windows are attached, see Figure 20. To avoid serious thermal bridges around the windows, all the windows should be placed on the external side of the existing concrete element that moves them more in line with the additional exterior insulation.[28]

Hygrothermal Performance of External Walls Temperature and RH were measured in both test walls: MW and EPS external thermal insulation composite systems (ETICS).

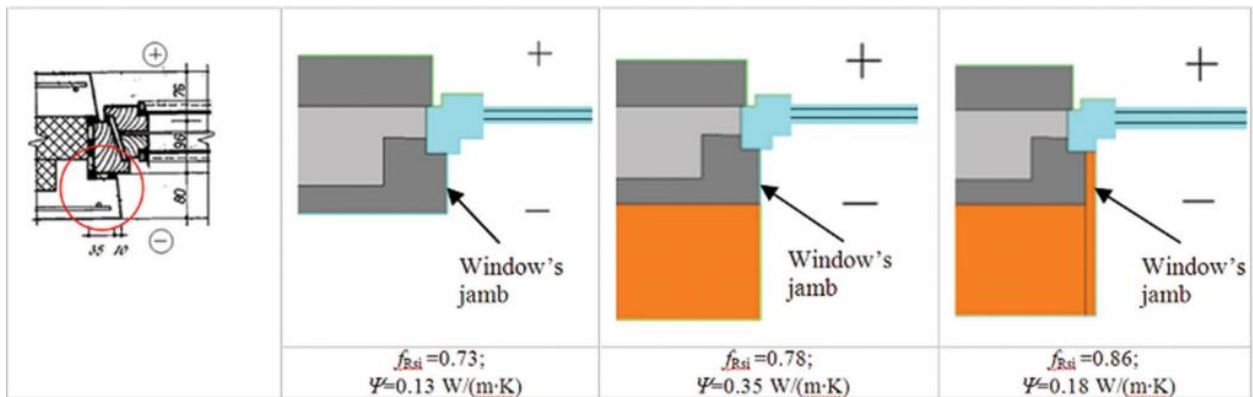


Figure 19 Calculation results of temperature factor f_{Rsi} and linear thermal transmittance of the external wall/window junction. Inside the area of the original drawing (left) the red circle shows the proportion of the jamb of a window covered.



Figure 20 Picture of an old window (left) and of new windows placed at their original position. Most of the jamb is covered and only a thin layer of insulation (5...20 mm) can be attached to the jamb

Measurements lasted for one and a half heating periods from September until December.

Hygrothermal performance of both walls was also simulated by Delphin 5.7. In general, agreement of temperature, vapor pressure, and RH between the measurements and calculations was good, except for RH between mineral wool insulation and plaster (measuring point 3, see Figure 24) where the measured value was higher. Results presented in Figure 22–Figure 24 of the cold period fit also with steady-state distributions of temperature, vapor pressure, and RH. [29]

After the first calculations, there was also a mismatch about the drying out period. According to the measurements, moisture in the wall (existing moisture in the external core and additional moisture

from adhesive mortar) dried out 3–4 months, mainly by diffusion and with minor convection. We ended up with an acceptable agreement after adding small air gaps between measurement points 1 and 2 with air pressure difference at outdoor climate conditions in cross-section 2,

The effect of moisture movement without convection can be seen in Figure 21. If in fact moisture in measuring points 1 and 2 dried out during half of the heating season it was much slower by diffusion only according to calculations. There is also some difference at the beginning of the second winter. The calculated and measured temperatures of both walls match quite well. In the case of MW, calculated temperatures at the measurement points 1 and 2 are up to 1°C lower than measured (Figure 22) and up to 1°C higher than measured in the case of EPS (Figure 25).

Measured temperatures of the two test walls are similar, maximum 0.5°C higher in the case of EPS. Also, vapor content/vapor pressures were calculated from the measured temperature and RH in both test walls and calculated with the software. Results for MW are shown in Figure 23 and for EPS in Figure 26, respectively. Vapor pressure starts to increase right after the beginning of the heating season in the second half of October but then starts to decrease. Measurement point nr 2 is not graphically presented. It behaves as point nr 1 but its level is somewhat lower. Results of measured and calculated RH are presented in Figure 24 for MW and in Figure 27 for EPS. As it

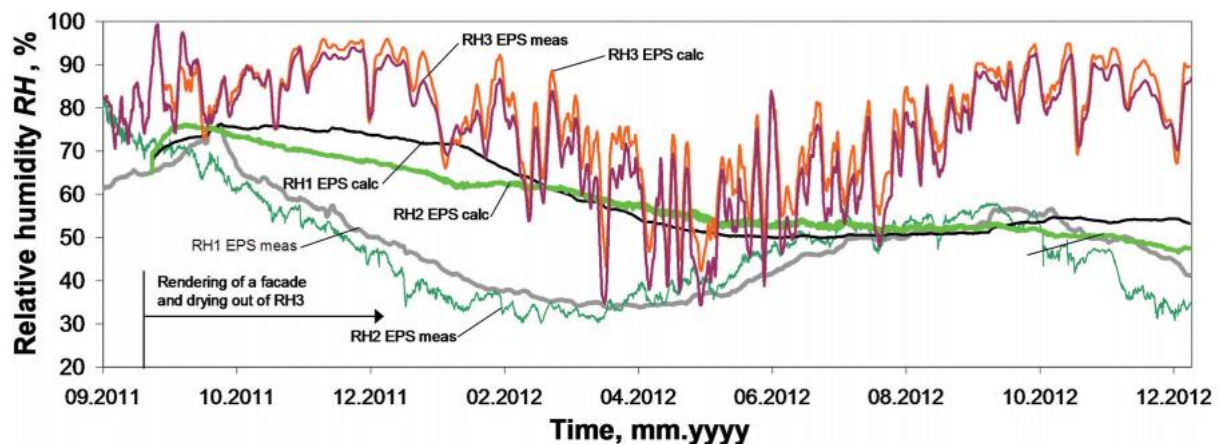


Figure 21 Comparison of measured (meas) RH and calculated (calc) RH moisture movement only by diffusion of ETICS with graphite enhanced EPS.

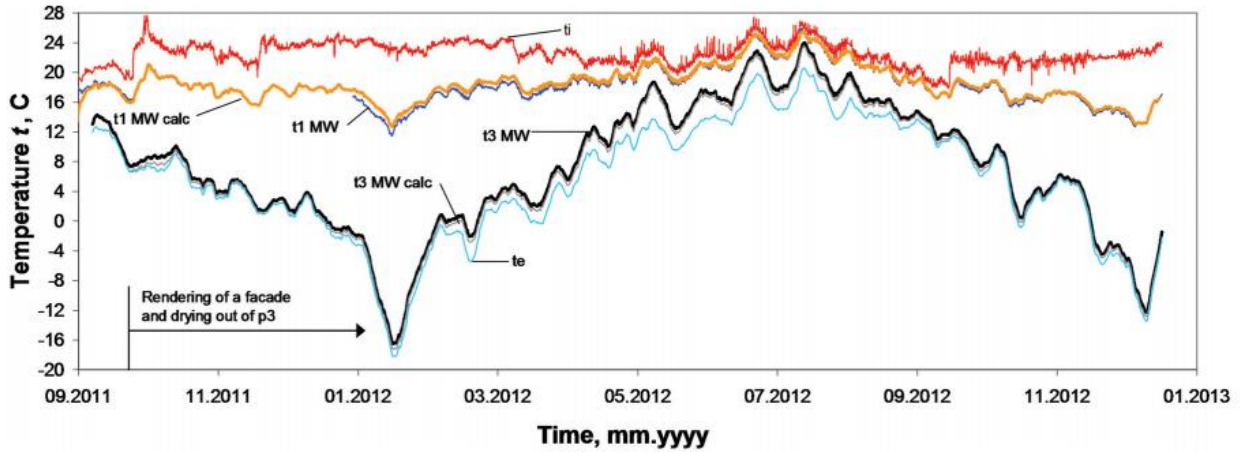


Figure 22 Measured and calculated temperature (t) in the wall additionally insulated with MW.

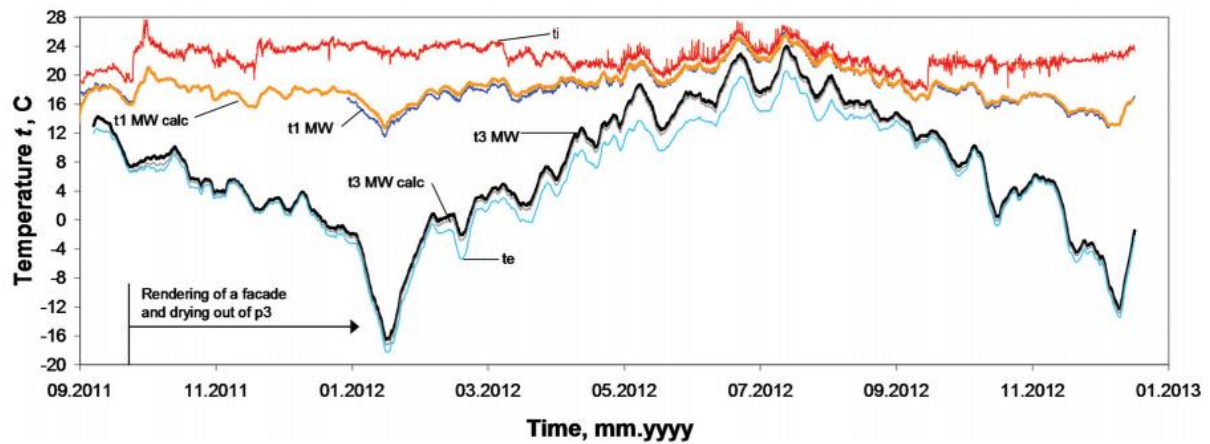


Figure 23 Measured and calculated vapor pressure (p) in the wall additionally insulated with MW

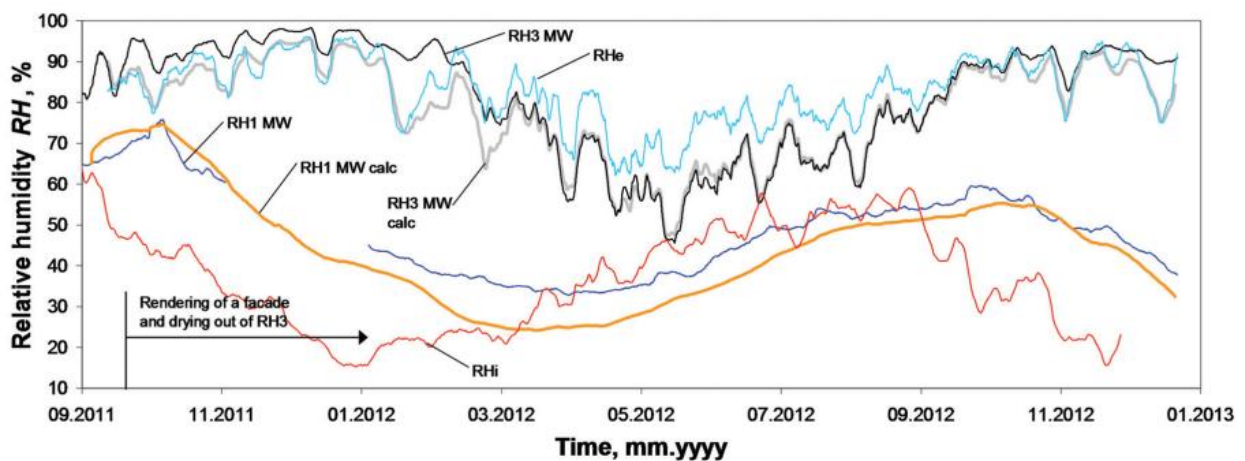


Figure 24 Measured and calculated RH in the wall additionally insulated with MW

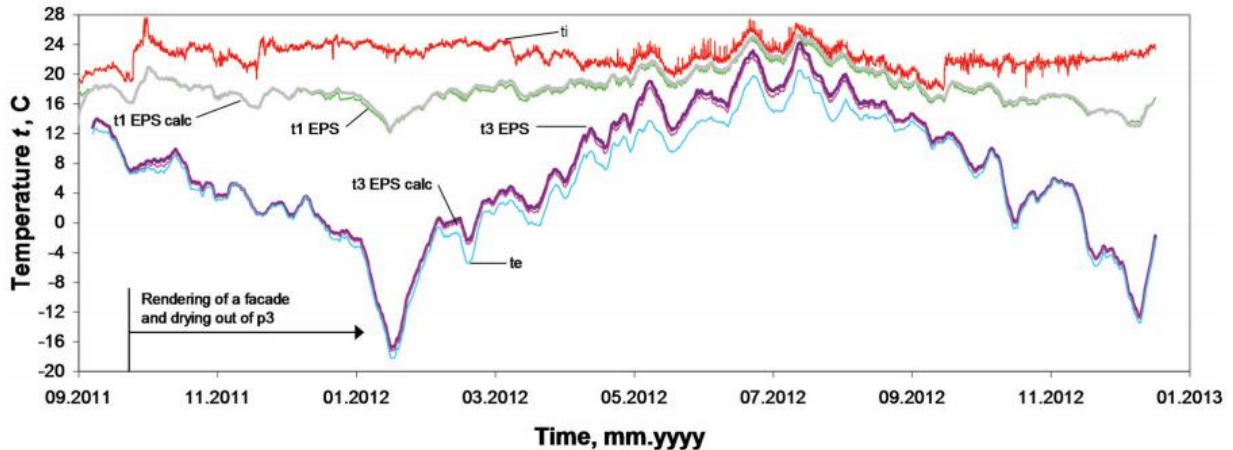


Figure 25 Measured and calculated temperature in the wall additionally insulated with expanded polystyrene (EPS). Location of measurement points see in Figure 12.

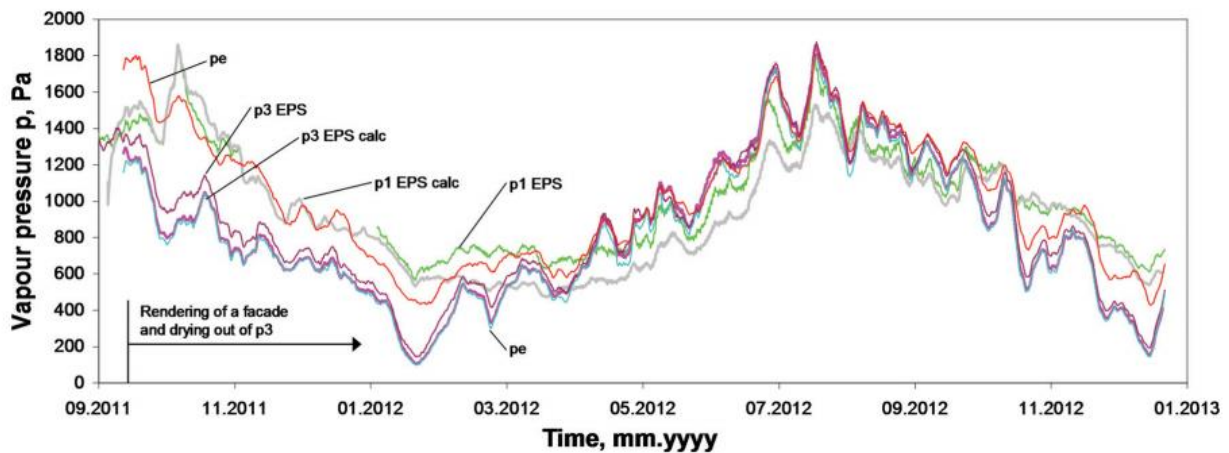


Figure 26 Measured and calculated vapor pressure in the wall additionally insulated with EPS appears, measured RH at point 3 with MW is somewhat higher than calculated during winter period.

In spring measured RH at point 1 is somewhat higher than calculated with both insulation materials. Correlation in the summer period is very good, especially in the case of MW. To the contrary, agreement with EPS is better in wintertime. Results of measuring point 2 follow the results of point 1 but at 10%–15% lower level. That is a result of higher vapor pressure at point 1 compared to point 2 at almost same temperatures. Results of thermal transmittance of walls are presented in Figure 28. It can be seen that the calculated thermal transmittance of MW is substantially higher than the rest of the three lines. Fluctuation of measurement results appears probably because solar radiation affects the temperature of the external surface of the wall. Average thermal transmittances in winter months are $0.17 \text{ W}/(\text{m}^2 \cdot \text{K})$ for EPS and $0.19 \text{ W}/(\text{m}^2 \cdot \text{K})$ for MW.[30]

DISCUSSION

Indoor Climate and Thermal Comfort Indoor climate measurements before and after the retrofit showed small improvement at air temperatures, where no overheating appears at very cold periods because of better adjustment of a new heating system. Natural passive stack ventilation was changed into mechanical exhaust ventilation with an exhaust air heat pump. Recovered heat was used for domestic hot water and heating. The air change did not improve after the renovations. It can be seen from moisture excess (Figure 27 right). There are several reasons that are more or less related to each other. First, the exhaust fan was set to minimum speed soon after the installation due to energy saving, lower sound level, and better thermal comfort. Also, building fabric became more airtight with new windows and additional insulation that decreased infiltration

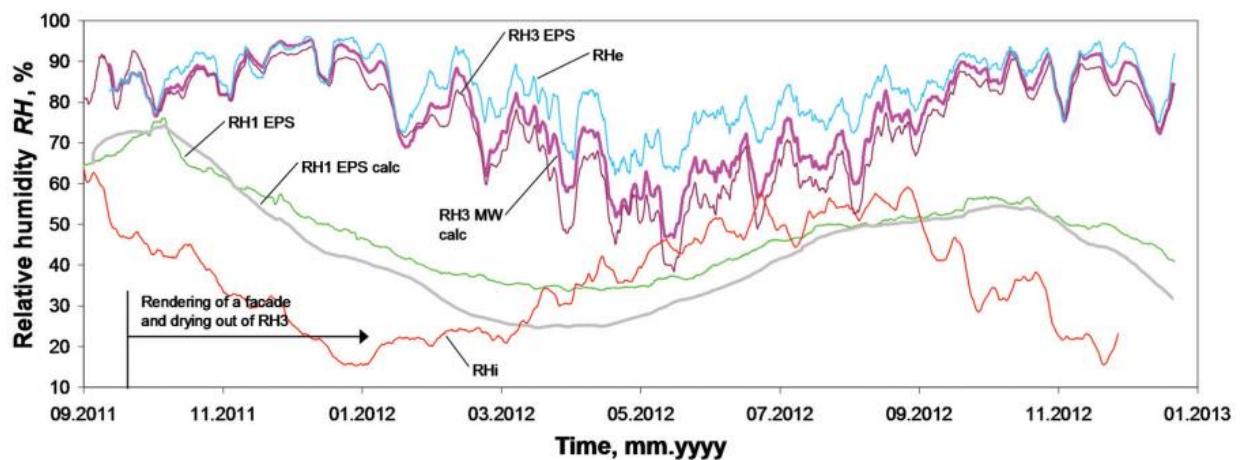


Figure 27 Measured and calculated RH in the wall additionally insulated with EPS.

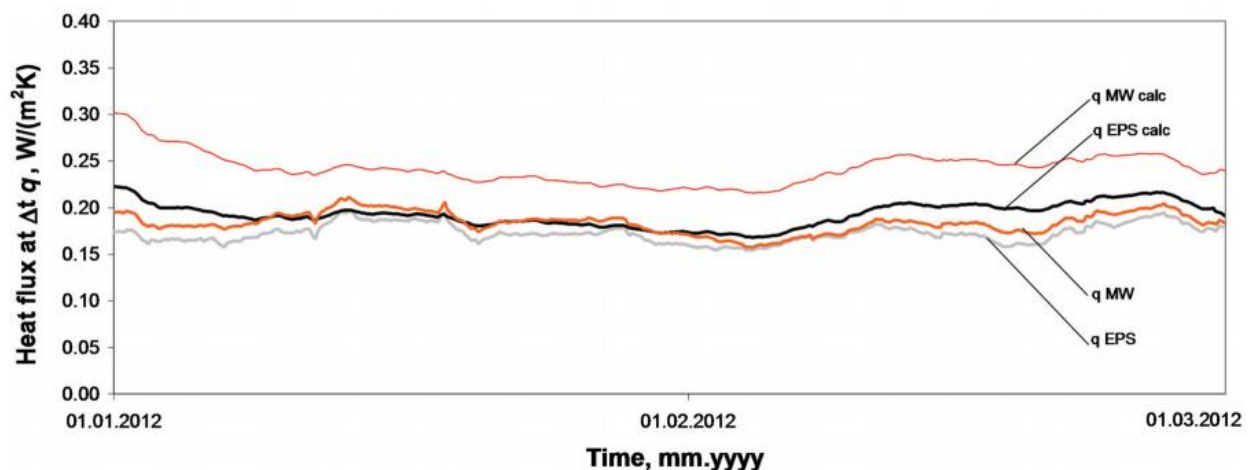


Figure 28 Measured and calculated thermal transmittances in the wall additionally insulated with EPS and MW. Lines

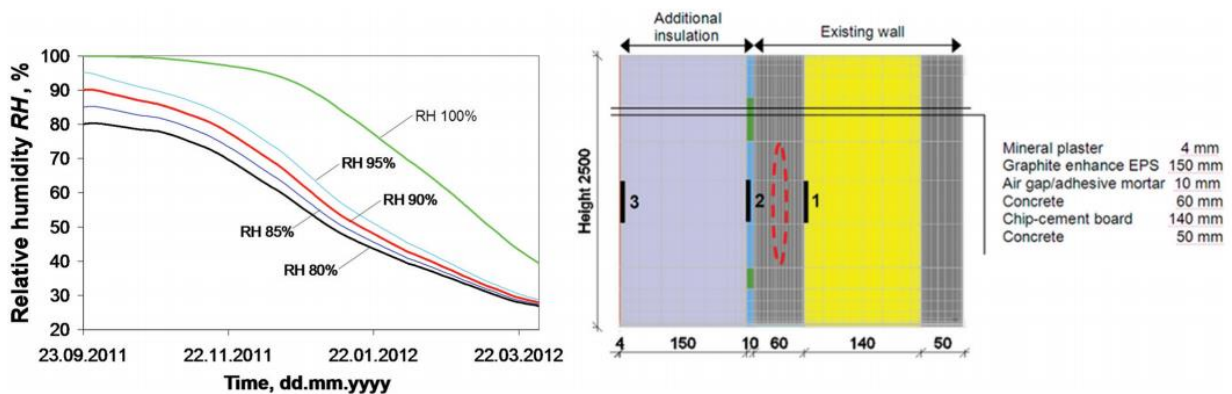


Figure 29 Moisture drying out time from the external layer of concrete between measuring points 1 and 2 (right) with different initial moisture.

The indoor moisture excess 2–3 g/m³ after the renovation indicates an average indoor humidity load level. This means that moisture production/living density had been relatively low. There was a problem with low floor temperatures on the first floor. The floor was not insulated from the bottom side (cellar’s ceiling) because of lack of finance, the low height of the cellar, and impracticability of workmanship (pipes, lighting, cables, etc. attached to the cellar’s ceiling).

Thermal Bridges

During typical low-budget energy renovation, only old wooden windows are replaced and previously replaced windows remain in the same location. Since the thickness of additional insulation into walls is typically 150–200mm, windows become located 200–270 mm inside the surface of the facade instead of 50–70mm originally. This is a problem because of esthetics and architecture, reduced daylighting, energy efficiency, and mainly thermal bridges around the windows. The negative impact is greater in the case of small and narrow windows. Generally, some insulation is recommended to be placed at the window’s jamb, but in practice this is complicated and often only 5–20mm is achievable. If the temperature factor f_{Rsi} does not change much, then the linear thermal transmittance is very sensitive to the jamb’s insulation.

Heat loss through thermal bridges around the windows compared to the rest of a wall is often at a similar scale. In the future, moving all the windows outside is advisable. Also, most of the windows

installed about 10 years ago can be replaced again since selective covering was not yet common then and remarkable development of windows has taken place during the last years. Another thermal bridge that remained after the renovation is the external wall/balcony junction. It could be eliminated by insulating a balcony slab from the bottom and top. The technical condition of concrete balconies and awning is sometimes problematic and steel elements, including reinforcement mesh, are sometimes corroded. Since after additional insulation the original 1 m width of a balcony becomes only about 0.8 m, removal of all existing balconies should be considered. New, durable, and wider balconies containing minor thermal bridges would be a sustainable investment. [31]

Hygrothermal Performance of ETICS on a Concrete Element

One of the main goals of this study was to analyze the hydrothermal performance of an external wall insulated additionally with mineral wool and expanded polystyrene ETICS. Initial simulation results considering only diffusion showed a remarkable mismatch during the first heating season. Although the adhesive mortar/air gap was sealed with PU foam at the basement wall and roof, there was probably some air leakage. Air leakage between the insulation and original wall (measurement point 2) is possible because of rubble bulk covered with particles of different sizes. This is contact with adhesive mortar did not assure a totally airtight connection. The air pressure difference created by the stack effect enabled some air movement along the wall. Calculations show that a narrow 0.5–1 mm opening below and above the wall is able to transport more moisture than by diffusion. Cracks with such a small width could originate from shrinkage of monetization concrete connecting prefabricated elements or those could be in the elements produced from three layers.

The impact of air convection between the additional thermal insulation and the original wall is small enough not to appear in the results of thermal transmittance of the wall in practice, see Figure 28. Higher calculated thermal transmittance might be caused by air leakage through MW insulation. Slightly higher thermal transmittance in the case of MW can be explained by the lower thermal conductivity of EPS, having declared value = $0.032 \text{ W}/(\text{m}\cdot\text{K})$ compared to = $0.038 \text{ W}/(\text{m}\cdot\text{K})$ in the case of MW. The addition of 150 mm of additional EPS/ MW insulation contributes more than 2/3 to the total thermal resistance of the wall. [32]

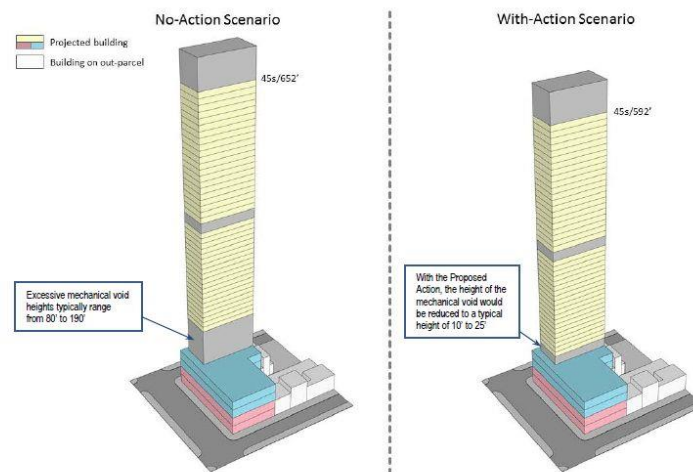


Measurements and calculations showed that moisture in the analyzed wall dried out in half of the heating season (see Figure 21 and Figure 29), approximately 3–4 months. If dried only by diffusion, it would have taken about a year for most of the moisture and the rest of it would have dried out during the second year. In the analyzed case with convection totally wet, an external layer would have dried out from most of the moisture also within 3–4 months but in that case, large moisture flux through the wall and possible condensation behind the plaster would be a threat.

Different aspects of the hygrothermal performance of ETICS have been studied for decades. There should be a separate viewpoint between ETICS on concrete/masonry and wooden structures. Although it has been found to be a functioning solution in principle it is very sensitive to driving-rain-caused water leakage from cracks in the finishing layer.

The performance of ETICS walls depends on the design and materials choice, connections between plaster and other materials in joints, workmanship, technology, and quality. In the cold climate of Finland, poor frost resistance of ETICS is a problem, and testing methods and criteria according to ETAG 004 worked out in central Europe might not be proper. Tested walls had also minor driving rain loads since it was sheltered by a neighboring higher building and because of other factors of the surrounding environment. Performance of ETICS walls under high driving rain loads and in the case of higher buildings must be handled as another field of research that was not the aim of this paper. Also,

durability and factors impacting it in addition to climate loads (content and type of plaster, vapor permeability, water uptake coefficient, adhesion, cracking, frost resistance, etc.) is a field of future research. During maintenance of ETICS, one should also consider a possible layer of paint that might be added later. General Success of Current Energy-Renovation Pilot Project The main progress of the current energy renovation pilot project was its better design and workmanship quality. [33]



It must be noticed that since it was a pilot project, workmanship under strict supervision was probably somewhat better than usual. From now on, similar renovations can be started with existing know-how about success and problems. In addition to lower heating bills, renovation should lead also to better durability, the longer service life of structures, and better indoor climate and aesthetics. These all have also a positive impact on the value of real estate. One should also move on towards the next more progressive steps by modernizing older housing stock. Often renovation is conducted in many stages without a holistic approach. Main renovation solutions employed are typical: additional external insulation and changing of old wooden windows. Together with the change of membrane waterproofing, additional thermal insulation is added to the roof. The renovation of balconies and awnings depends on damages.

The overall success of this example project can acquire satisfactory evaluation avowals. A novel solution in this pilot project was a holistic approach and an air heat pump for heat recovery of the new mechanical ventilation. Attitudes of inhabitants to the renovation varied both before and after renovation. In the current pilot project, people were somewhat more tolerant since approximately half of the whole investment came from sponsors and subsidizers. Still, there were complaints about designed solutions, execution of workmanship, and some unfamiliar changes.

CONCLUSIONS This case-study analysis studied measured and calculated hygrothermal performance of a mineral wool (MW) and graphite enhanced expanded polystyrene (EPS) external thermal insulation composite systems (ETICS/EIFS). Also, indoor climate, air leakage rate, and thermal bridges were measured before and after the low-budget energy renovation of an existing concrete large panel elements apartment building. Indoor climate measurements showed no major changes in moisture excess, mostly because mechanical ventilation airflows were decreased by the operator. Overheating that existed before was avoided after the renovation with a new adjusted heating system.

The airtightness of the building fabric improved only in apartments where old leaky windows were replaced. Additional external insulation solves the serious problem of thermal bridges, except at external wall/window junction if windows remain at their original position and also at external wall/balcony and external wall/foundation wall junction.

Therefore, windows should be attached to the external side of the existing façade. The measured hygrothermal performance of both walls was good and correlation existed with the calculated temperature, vapor pressure, and RH distributions. Built-in moisture of the whole wall (measuring spots 1 and 2 on both sides of the external layer of concrete) dried out during the first heating season, achieving RH values below 50%. Moisture in thin plastering (measuring spot 3 between insulation and plaster) dried out within a few days but stayed quite high, especially in the case of mineral wool, being over 90%. It means that the content and properties of the external finishing plaster must be carefully designed to achieve low enough vapor permeability and low water uptake.

This becomes even more crucial at a greater vapor flow due to material with higher vapor permeability instead of concrete. The average measured thermal transmittance U during the winter was $0.17 \text{ W}/(\text{m}^2 \cdot \text{K})$ in the case of graphite enhanced EPS and $0.19 \text{ W}/(\text{m}^2 \text{ K})$ for mineral wool. This is close to the expected value calculated from a producer's data and allows us to make positive conclusions about thermal performance.

Hygic performance was also satisfactory and moisture dried out during the first heating season. Measurements and calculations showed that there had been some convection of moist air in the wall. A drying out process by diffusion only would have been much slower. Short-term hygrothermal performance of ETICS is normal when proper design and workmanship are performed, in particular,

related to joints. Additional insulation lowers the RH inside the existing wall which stops the corrosion process and frost damage. Long term performance and durability of ETICS in a cold climate and under-driving rain loads need to be further investigated with special attention to content and properties of render, frost resistance, cracking, staining, maintenance, and repainting.

Chapter 3

Thermal design of ETICS made with cementitious foam

-Model characteristics

-Base Case High Mass Building

The basic test building (Figure 1) is a rectangular single zone (8 m wide x 6 m long x 2.7 m high) with no interior partitions and 2 of windows on the **south exposure**.

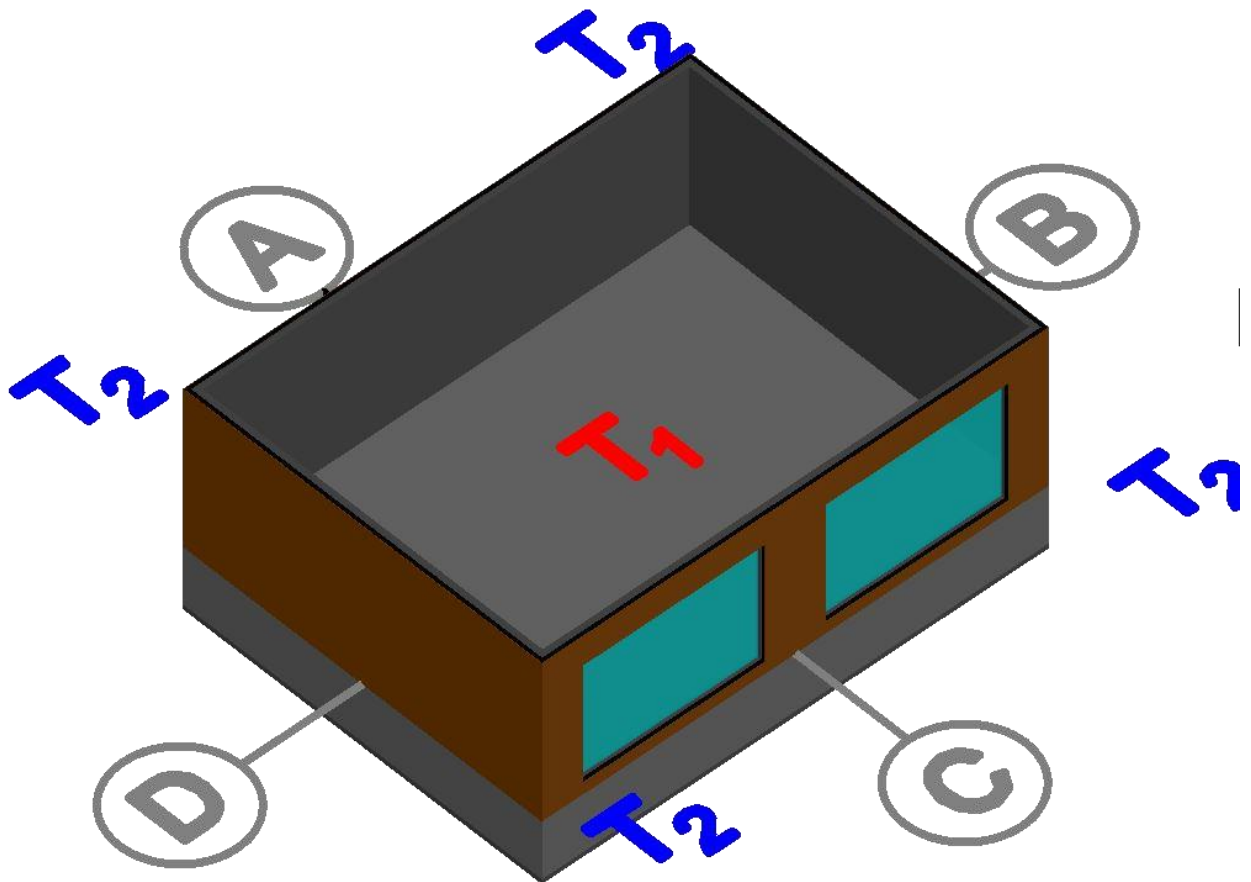


Figure 30 Base Building – Isometric View of Southeast corner with Windows on South Wall.

I will do heat transfer analysis for the Wall construction, all required data are given in the table below, then I will do same analysis but with different wall cross-section layers and different Foam insulation layer characteristics

ETICS anchors are potential thermal bridges and may promote heat transfer in an insulated component, depending on the quality of the anchor. By using premium anchors with low heat conductivity, you may not require further insulation measures.

I will use different density of Foam insulation layer. The new values for Foam section is given in the Table 1 below.

| Wall Construction (heavy weight mass) | | | | | | |
|---------------------------------------|---------------------------------|---------------|-----------------------------------|-----------------------------------|---|-----------------------------------|
| Element | $k \left(\frac{W}{mK} \right)$ | Thickness (m) | $U \left(\frac{W}{m^2K} \right)$ | $R \left(\frac{m^2K}{W} \right)$ | Density $\left(\frac{kg}{m^3} \right)$ | $Cp \left(\frac{J}{kgK} \right)$ |
| Int. Surface Coeff. | | | 8.290 | 0.121 | | |
| Concrete Block | 0.510 | 0.100 | 5.100 | 0.196 | 1400 | 1000 |
| Foam Insulation | 0.040 | 0.0615 | 0.651 | 1.537 | 10 | 1400 |
| Wood Siding | 0.140 | 0.009 | 15.556 | 0.064 | 530 | 900 |
| Ext. Surface Coeff. | | | 29.300 | 0.034 | | |
| Overall, air-to-air | | | 0.512 | 1.952 | | |

Floor Construction (heavy weight mass)

| Element | $k \left(\frac{W}{mK} \right)$ | Thickness (m) | $U \left(\frac{W}{m^2K} \right)$ | $R \left(\frac{m^2K}{W} \right)$ | Density $\left(\frac{kg}{m^3} \right)$ | $Cp \left(\frac{J}{kgK} \right)$ |
|---------------------|---------------------------------|---------------|-----------------------------------|-----------------------------------|---|-----------------------------------|
| Int. Surface Coeff. | | | 8.290 | 0.121 | | |
| Concrete Slab | 1.130 | 0.080 | 14.125 | 0.071 | 1400 | 1000 |
| Insulation | 0.040 | 1.007 | 0.040 | 25.175 | | |
| Overall, air-to-air | | | 0.039 | 25.366 | | |

Table 10 The characteristics of the heavier mass wall and floor are as follows

Roof Construction (light weight mass)

| Element | $k \left(\frac{W}{mK} \right)$ | Thickness (m) | $U \left(\frac{W}{m^2K} \right)$ | $R \left(\frac{m^2K}{W} \right)$ | Density $\left(\frac{kg}{m^3} \right)$ | $Cp \left(\frac{J}{kgK} \right)$ |
|---------------------|---------------------------------|---------------|-----------------------------------|-----------------------------------|---|-----------------------------------|
| Int. Surface Coeff. | | | 8.290 | 0.121 | | |
| Plasterboard | 0.160 | 0.010 | 16.000 | 0.063 | 950 | 840 |
| Fiberglass Quilt | 0.040 | 0.1118 | 0.358 | 2.794 | 12 | 840 |
| Roof Deck | 0.140 | 0.019 | 7.368 | 0.136 | 530 | 900 |
| Ext. Surface Coeff. | | | 29.300 | 0.034 | | |
| Overall, air-to-air | | | 0.318 | 3.147 | | |

Window Properties

| | |
|---|------------------------|
| Extinction coefficient | 0.0196/mm |
| Number of panes | 2 |
| Pane thickness | 3.175mm |
| Air-gap thickness | 13mm |
| Index of refraction | 1.526 |
| Normal direct-beam transmittance through one pane | 0.86156 |
| Thermal Conductivity of glass | $1.06 \frac{W}{mK}$ |
| Conductance of each glass pane | $333 \frac{W}{m^2K}$ |
| Combined radiative and convective coefficient of air gap | $6.297 \frac{W}{m^2K}$ |
| Exterior combined surface coefficient | $21.00 \frac{W}{m^2K}$ |
| Interior combined surface coefficient | $8.29 \frac{W}{m^2K}$ |
| U-value from interior air to ambient air | $3.0 \frac{W}{m^2K}$ |
| Hemispherical infrared emittance of ordinary uncoated glass | 0.9 |
| Density of glass | $2500 \frac{kg}{m^3}$ |
| Specific heat of glass | $750 \frac{J}{kgK}$ |
| Interior shade devices | None |
| Double-pane shading coefficient at normal incidence | 0.907 |
| Double-pane solar heat gain coefficient at normal incidence | 0.789 |

There is 0.2 m of wall below the window and 0.5 m of wall above the window.

Table 11. Experimental data according to the experiments at TU Darmstadt

Infiltration: 0.5 air change/hour

Internal Load: 200 W continuous, 60% radiative, 40% convective, 100% sensible

Mechanical System: 100% convective air system, 100% efficient with no duct losses and no capacity limitation, no latent heat extraction, nonproportional- type dual setpoint thermostat with dead band, heating $<20^{\circ}\text{C}$, cooling $>27^{\circ}\text{C}$

Soil Temperature: 10C continuous

For all the heat transfer analysis I use the following temperatures T1 inside temperature and T2 outside temperature.

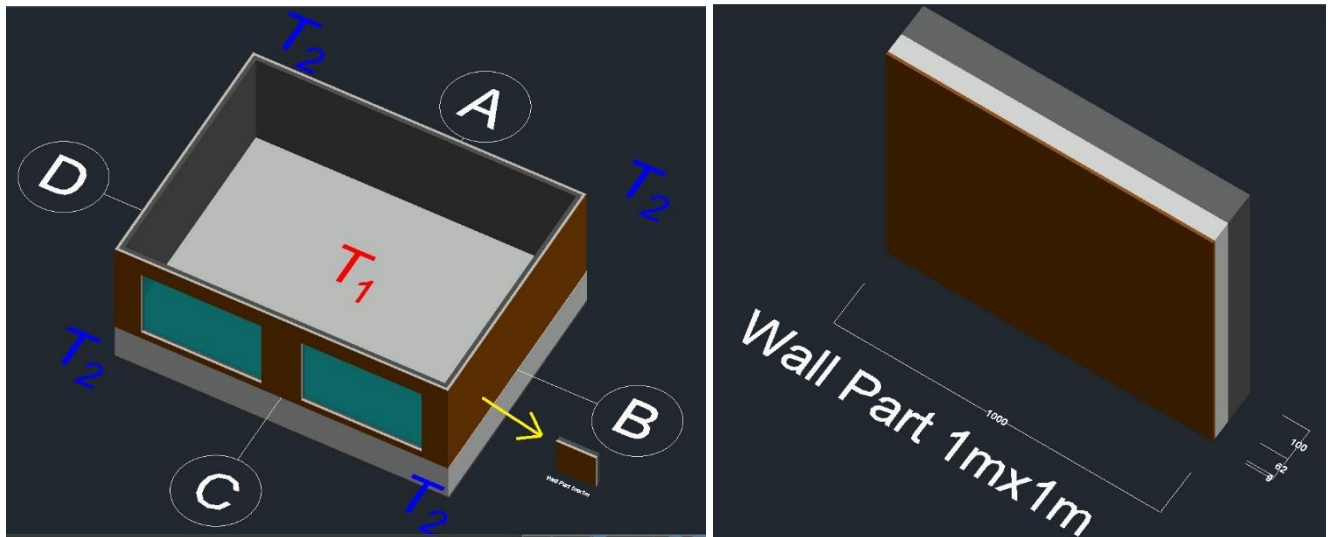
T1= $+30^{\circ}\text{C}$

T2= -30°C

Analysis 1

Perspective view of the building

Small part for analysis



Figures 31 A/B

Now, I will do the heat transfer analysis 3 time in Abaqus by changing thickness of layers and replacing heat transfer characteristics of Foam Insulation layer with the data from the table 1 below

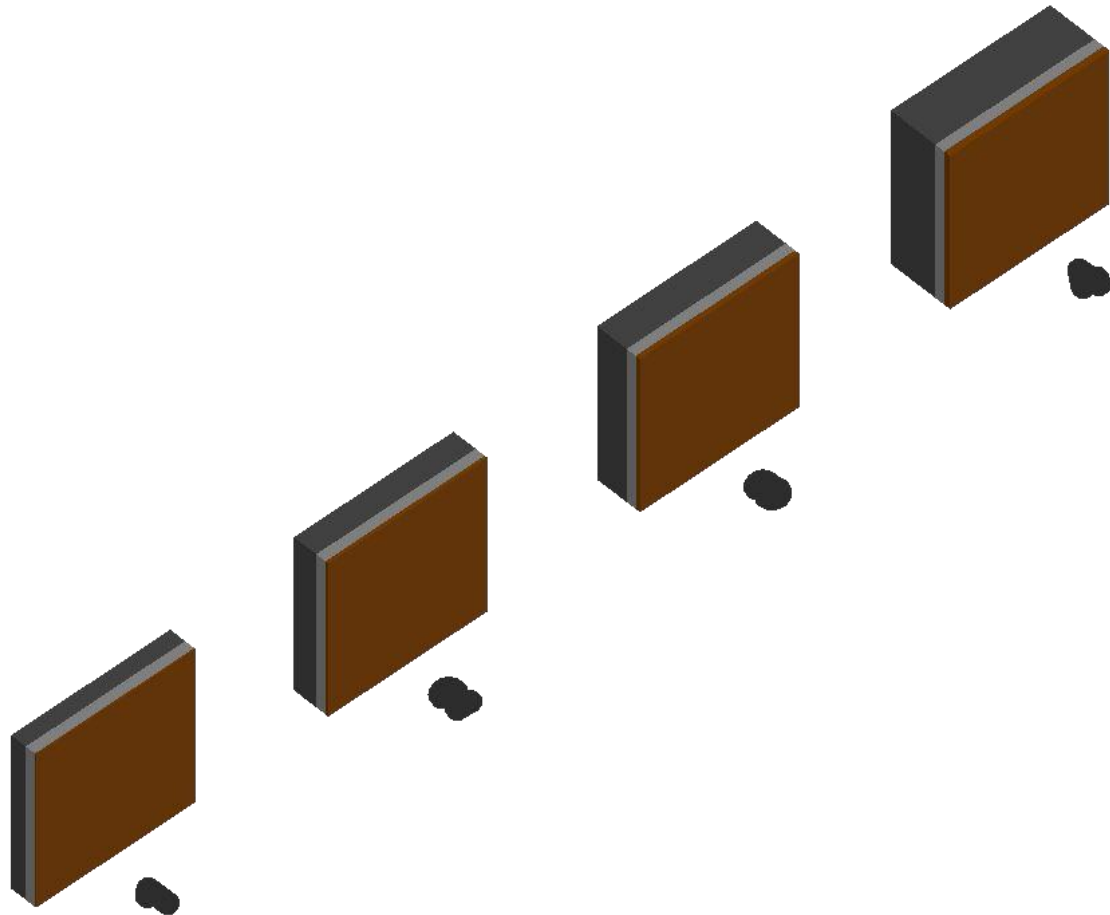


Figure 32. Wall parts with different thickness

| NRG-FOAM | | RVE | | CEMENT PASTE | | | EFFECTIVE | | | |
|----------------------------|---------------------------|--|----------|--------------|---------------------------------|--|--|---------------------------|--|---|
| # | ID | ID | Porosity | ID | k_{cement} [W/(mK)] | ρ_{cement} [kg/m ³] | ρC_{cement} [J/(m ³ K)] | k_{eff} [W/(mK)] | ρc_{eff} [J/(m ³ K)] | α_{eff} [m ² /s] |
| 1 | R4C1 | R4 | 51,1% | C1 | 0,588 | 1624,5 | 1,284E+06 | 0,237 | 6,281E+05 | 3,779E-07 |
| 2 | R4C2 | R4 | 51,1% | C2 | 0,643 | 1704,0 | 1,484E+06 | 0,258 | 7,258E+05 | 3,548E-07 |
| 3 | R4C3 | R4 | 51,1% | C3 | 0,732 | 1895,0 | 1,527E+06 | 0,290 | 7,468E+05 | 3,886E-07 |
| 1 | R6C1 | R6 | 70,3% | C1 | 0,588 | 1624,5 | 1,284E+06 | 0,140 | 3,816E+05 | 3,662E-07 |
| 2 | R6C2 | R6 | 70,3% | C2 | 0,643 | 1704,0 | 1,484E+06 | 0,150 | 4,410E+05 | 3,412E-07 |
| 3 | R6C3 | R6 | 70,3% | C3 | 0,732 | 1895,0 | 1,527E+06 | 0,168 | 4,537E+05 | 3,697E-07 |
| 1 | R8C1 | R8 | 84,7% | C1 | 0,588 | 1624,5 | 1,284E+06 | 0,070 | 1,978E+05 | 3,528E-07 |
| 2 | R8C2 | R8 | 84,7% | C2 | 0,643 | 1704,0 | 1,484E+06 | 0,073 | 2,284E+05 | 3,215E-07 |
| 3 | R8C3 | R8 | 84,7% | C3 | 0,732 | 1895,0 | 1,527E+06 | 0,079 | 2,350E+05 | 3,376E-07 |
| AIR | | | | | | | | | | |
| ρ [g/m ³] | c_{air} [J/(gK)] | ρc_{air} [J/(m ³ K)] | | | | | | | | |
| 1225 | 1 | 1225 | | | | | | | | |

Table 12. Chemico-physical characteristics of foam concrete from experimental data of TU Darmstadt
Then I can make a comparison between 4 different wall layer thicknesses.

Analysis 1

Let's create a 3D model space, with the deformable material type. Solid material with extrusion type.
Wall part geometry for the analysis

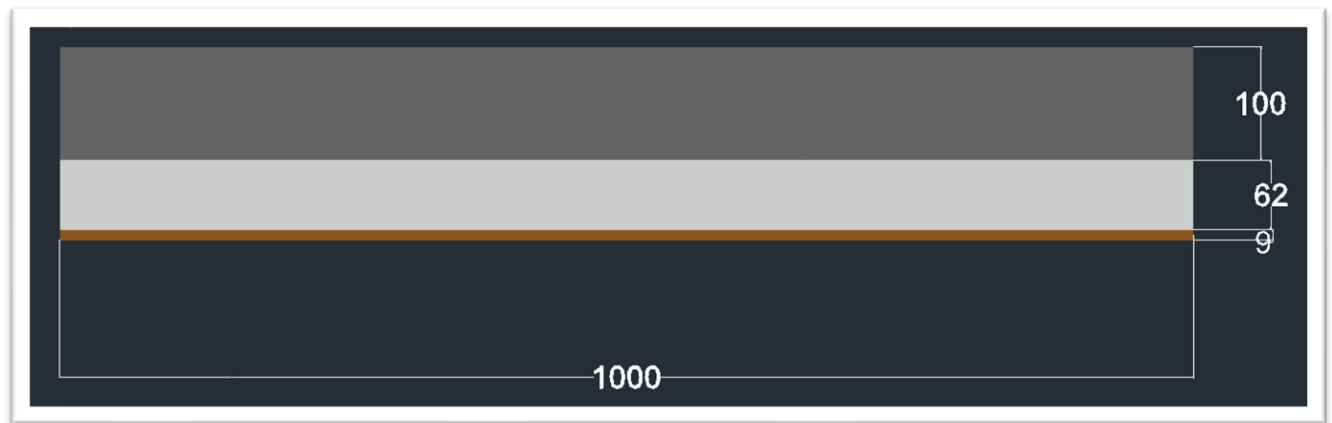


Figure 33. Abaqus software used to create 3D model of the wall with 3 different layers. Below 3D model is presented

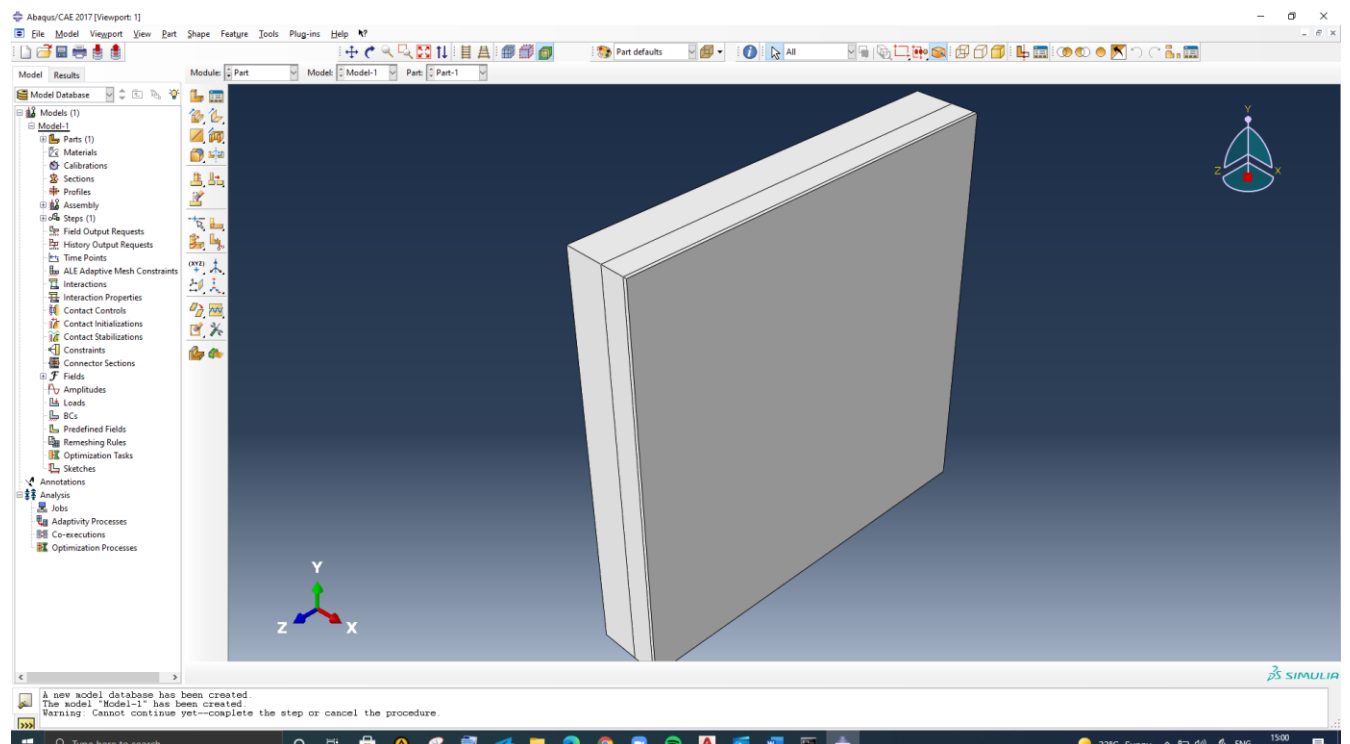


Figure 34. Second step creating material for each layer. Each material has thermal conductivity then we divide into section and assign material properties

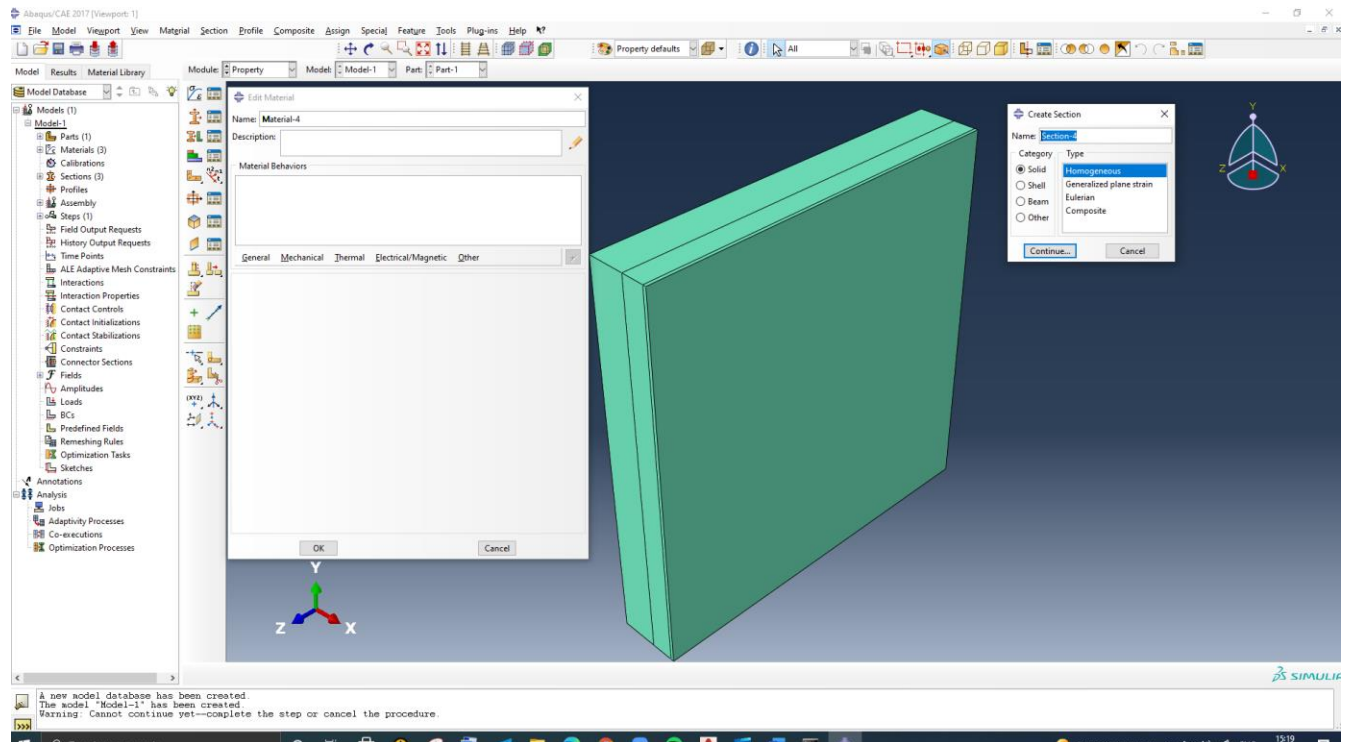


Figure 35. Assembly

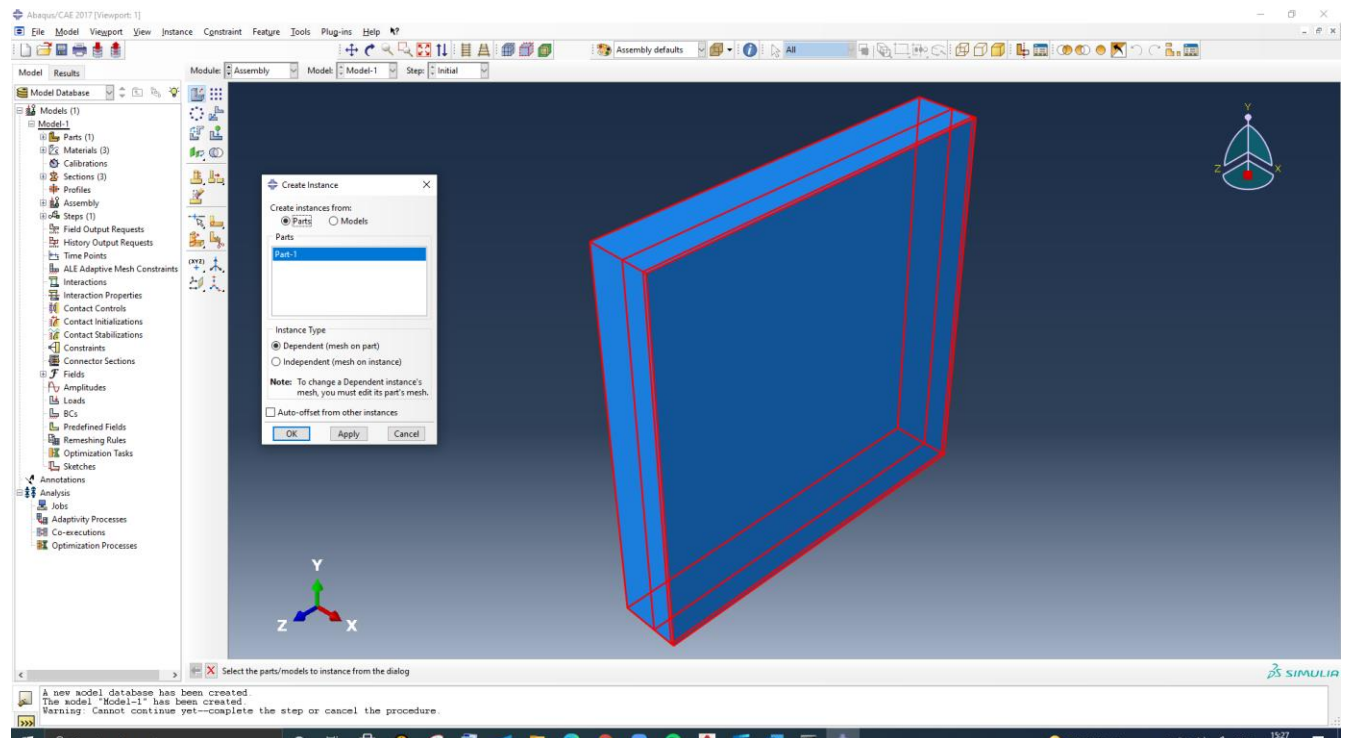
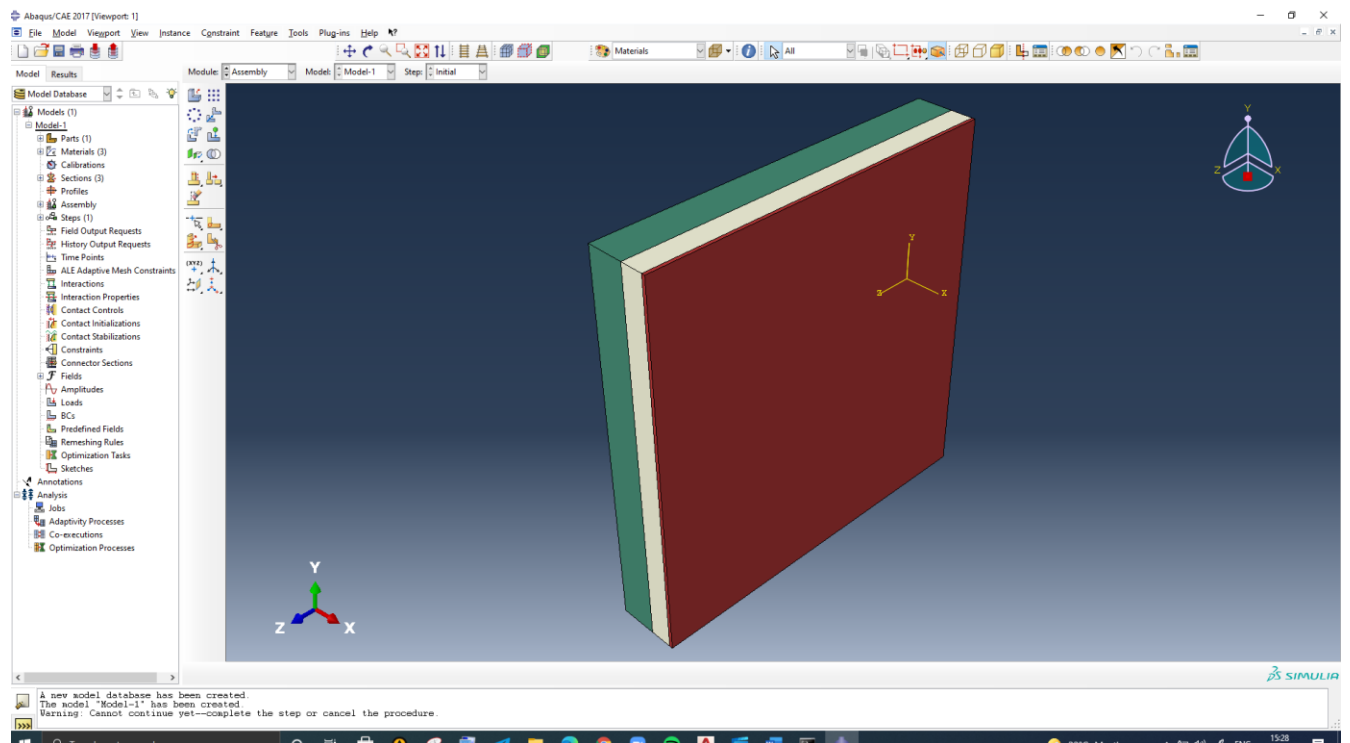


Figure.36 It can be visualized with different materials for each layer



The next step is initial conditions with an Increment size of 100 in steady-state conditions with time period of 6000.

The history output request Thermal/FTEMP, Facet temperature, HTL time-integrated HFL

Load boundary condition

The highlighted red area illustrates the thermal influence zone of Temperature from inside of the structure with the value of $T_1=30C$

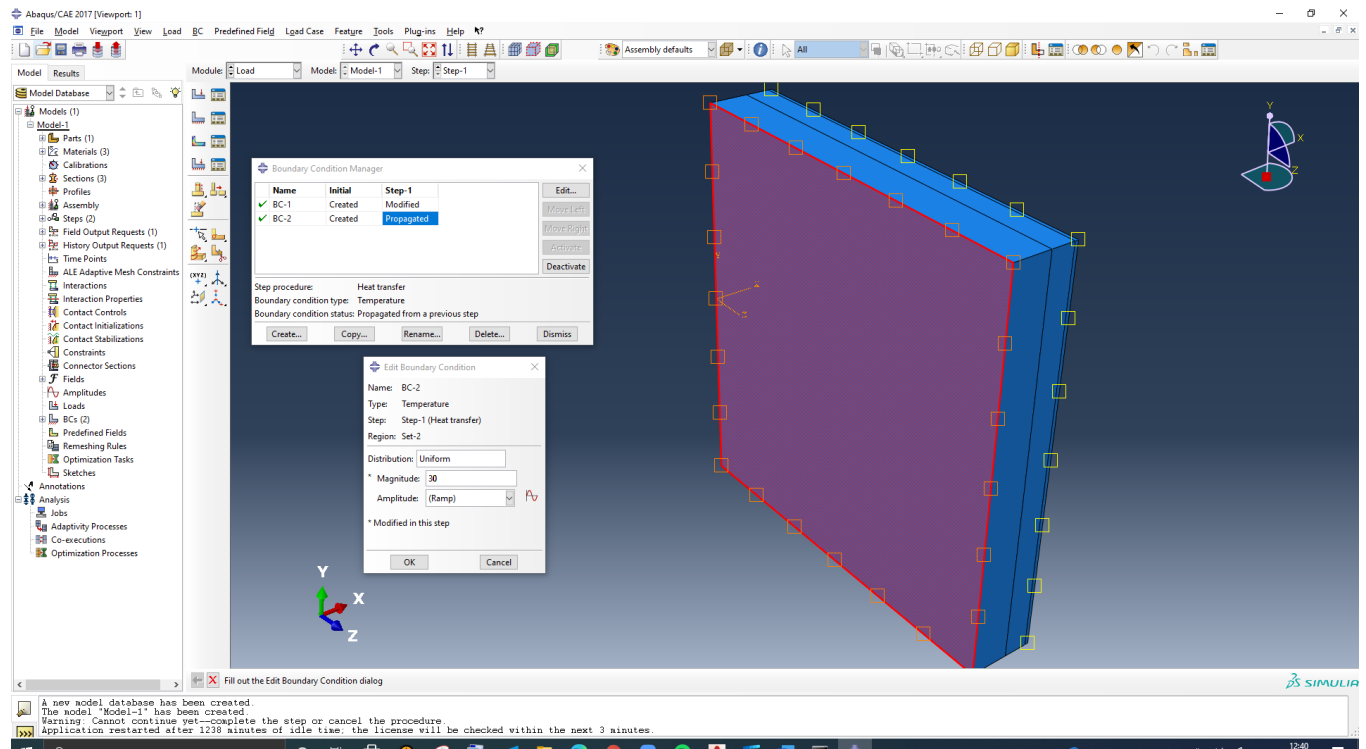


Figure 37& 38. Red highlighted area illustrates effect of Temperature T2 to the outer surface of wall, With a value $T_2 = -30$

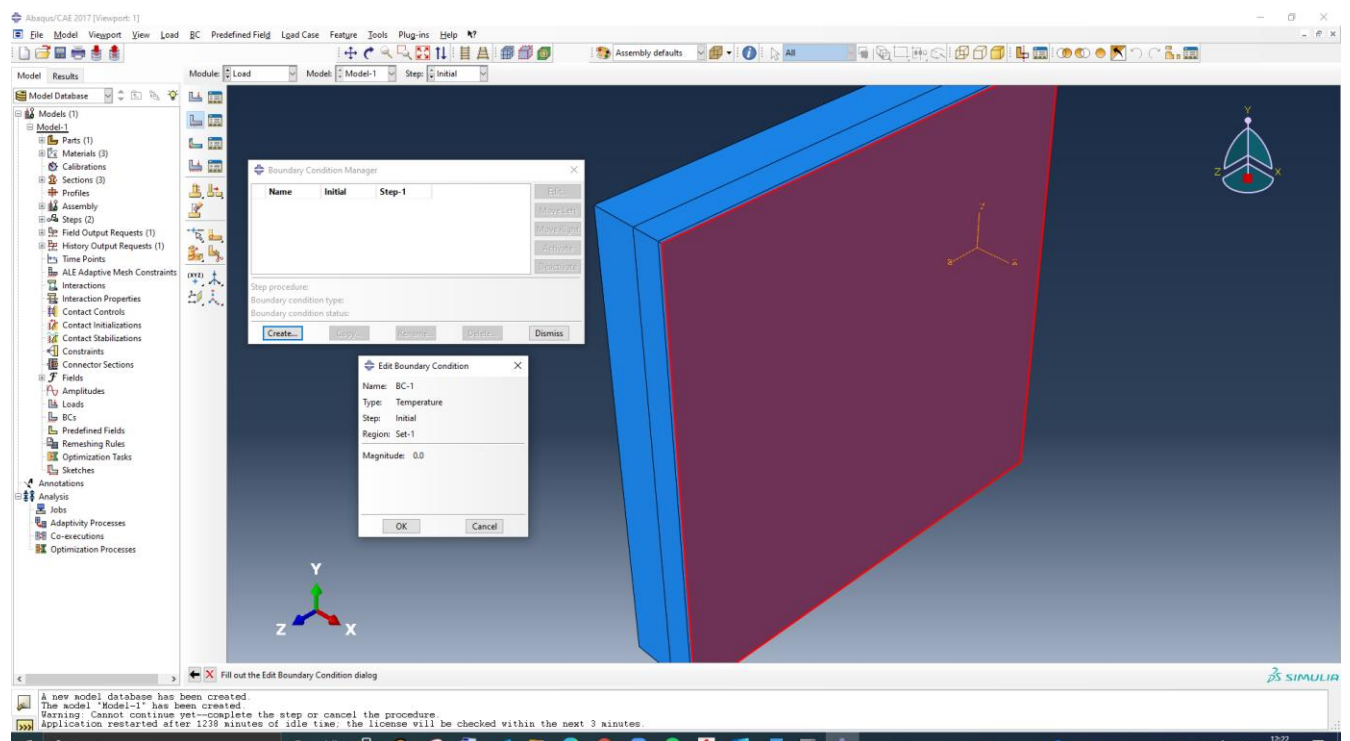


Figure 39. Global seeds size for Mesh is 0.02, in order to get better and accurate result after influence of temperature, It is better to use lower values for seeds size

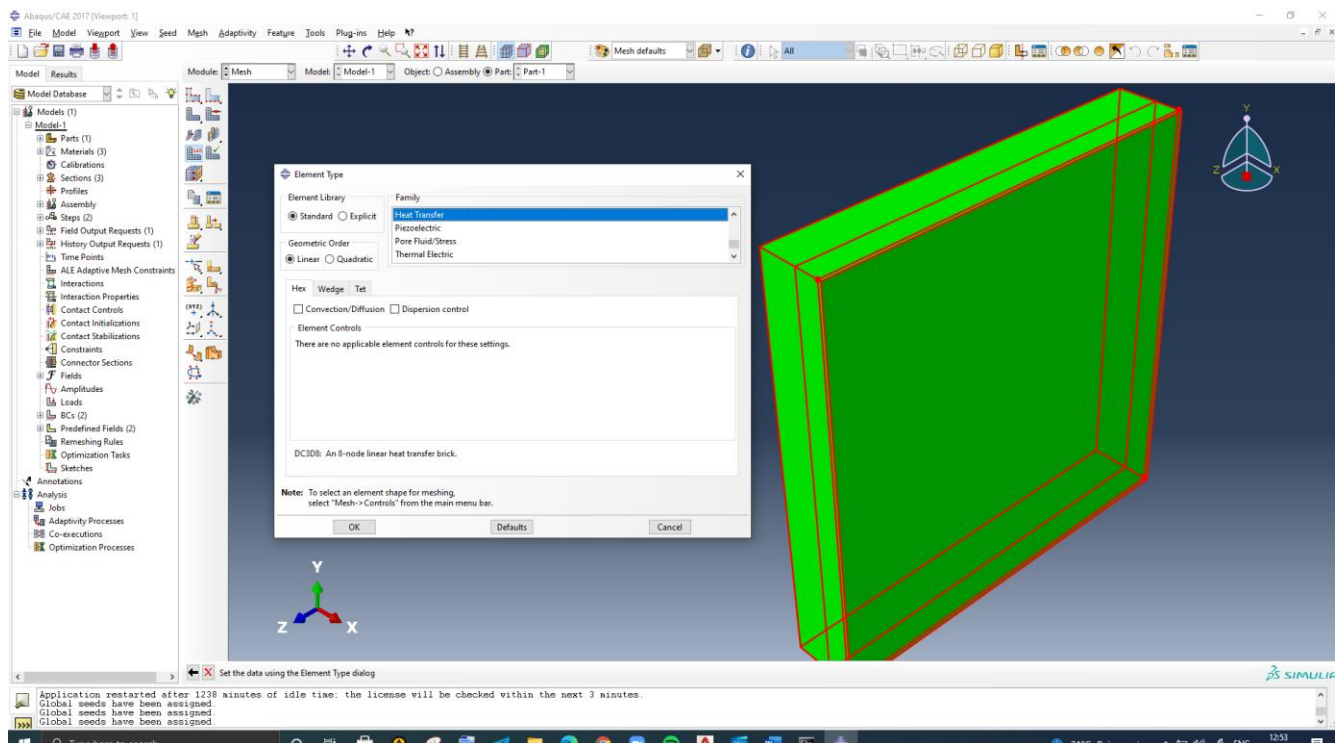
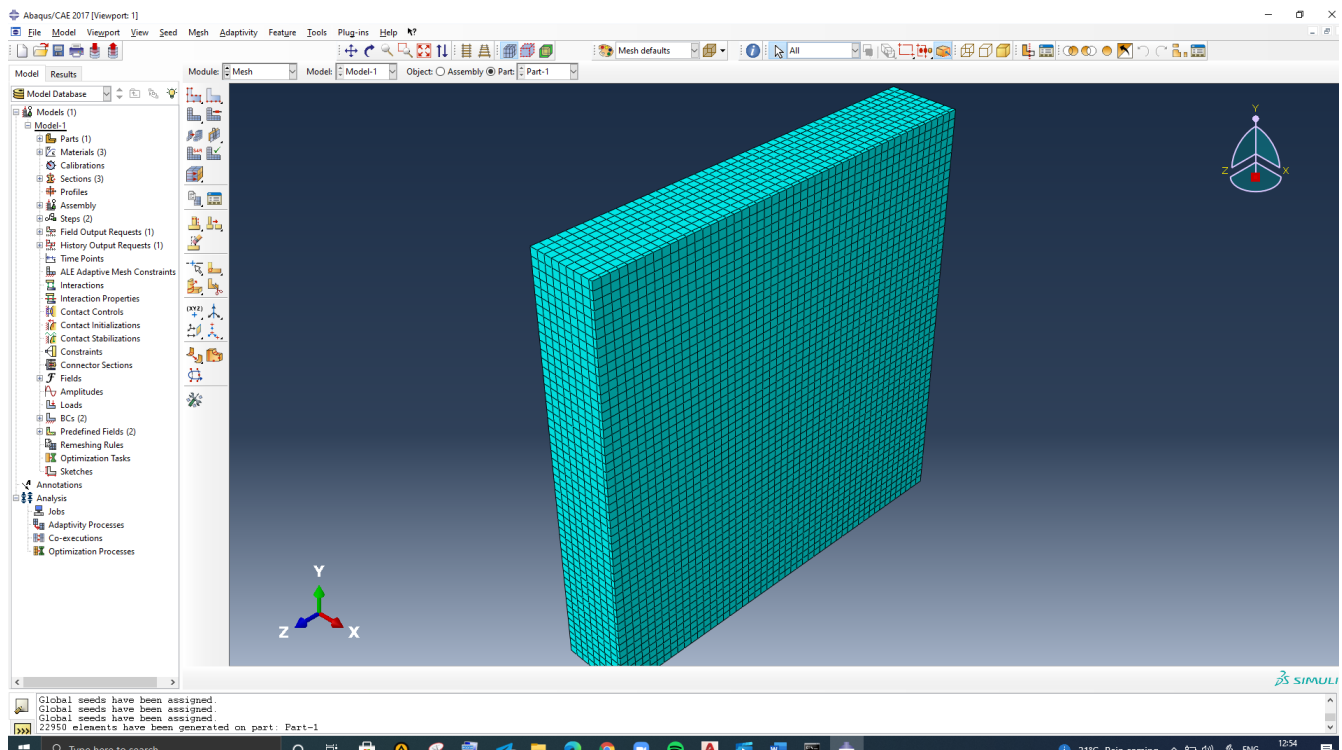


Figure 40. The wall meshes, so now we can apply the thermal effect of Temperature and see the deformation of the wall after applying temperature.



After modeling and inputting all the required data, It is required to submit job in Abaqus software. The software automatically makes all nessery colculation, after that procees the fallowing heat transfer through the wall was obtained in 3D format

Figure 41. 3D heat transfers from 3D model

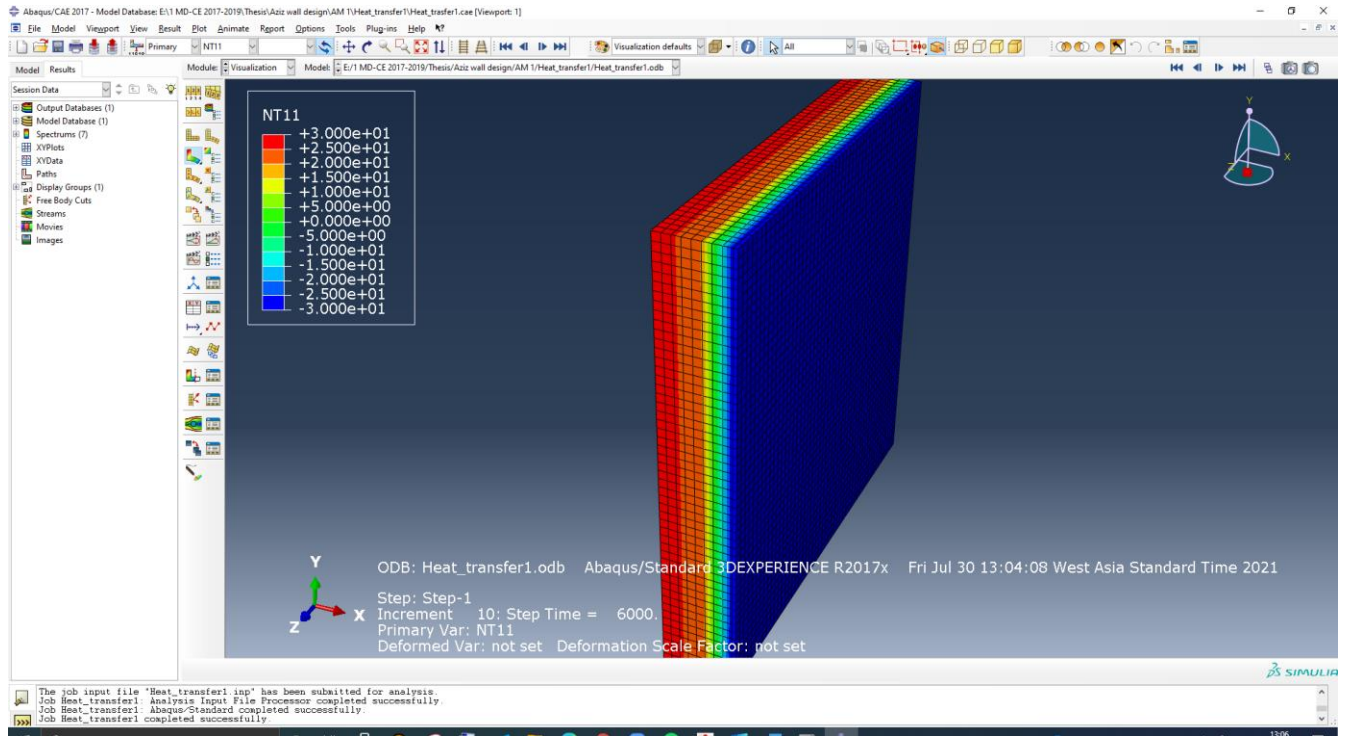
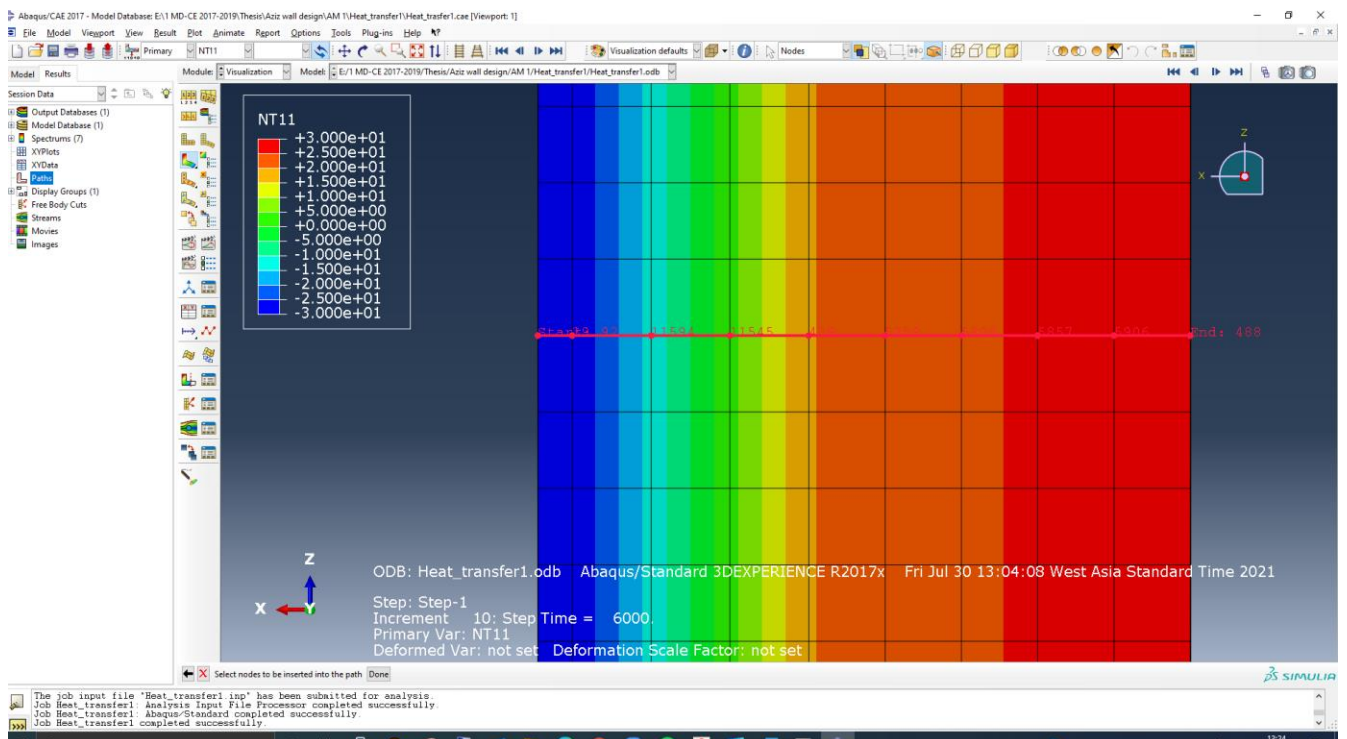


Figure 42. heat transfer line path through the wall



In order to get numerical values and a graph of heat transferring through the wall, It is required to select notes that pass through the wall, and by using Abaqus software plot we can get the

Figure 43. Temperature and true distance graph. From this graph numerical values in each node can be easily obtained

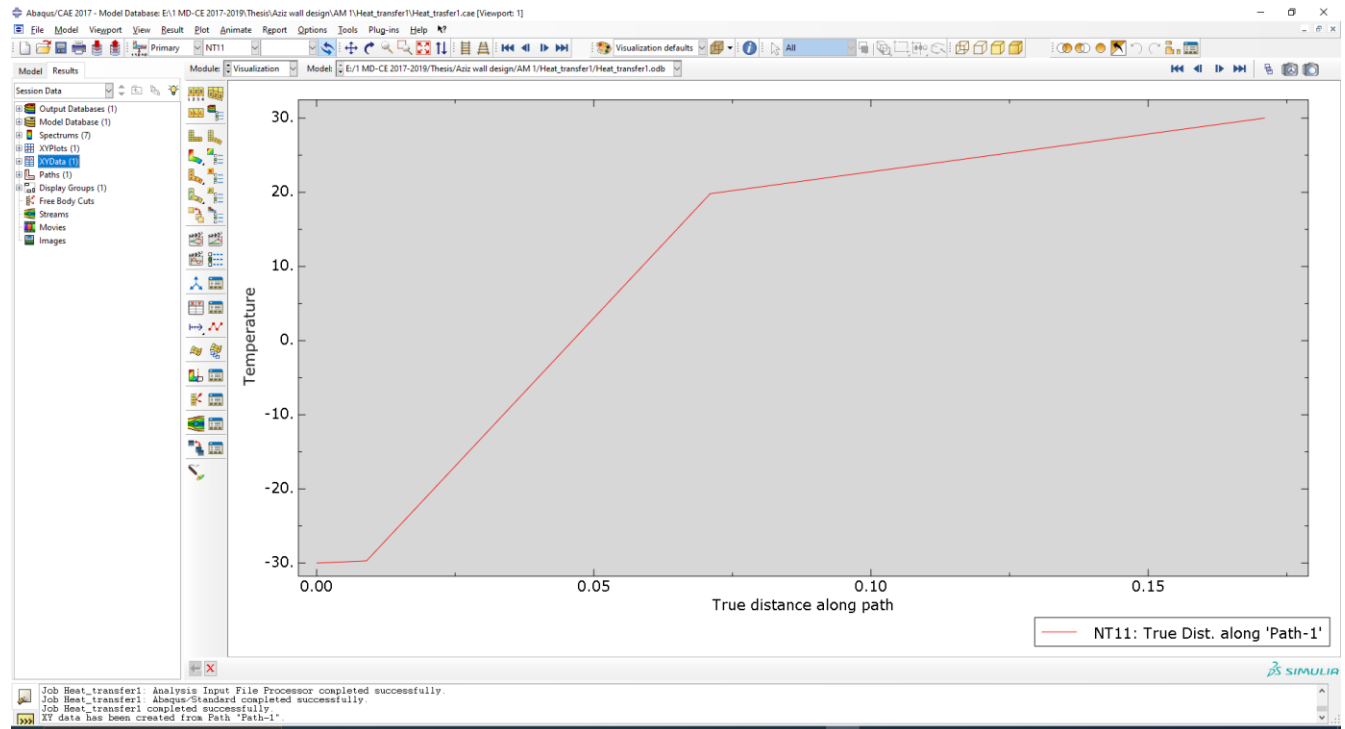


Table 14. The numerical value of Temperature in the true distance through the wall cross-section.

| Analysis1 | | |
|-----------|----------|---------|
| X[m] | Y {T[C]} | |
| | 0 | -30 |
| 0.009 | | -29.699 |
| 0.0296667 | | -13.197 |
| 0.0503333 | | 3.305 |
| 0.071 | | 19.807 |
| 0.091 | | 21.846 |
| 0.111 | | 23.884 |
| 0.131 | | 25.923 |
| 0.151 | | 27.961 |
| 0.171 | | 30 |

Analysis 2

Let`s perform the same analysis with different geometry. There is no change in the Foam insulation layer geometry throughout all analyses Meanwhile Thermal property of the Foam insulation layer will change in each analysis.

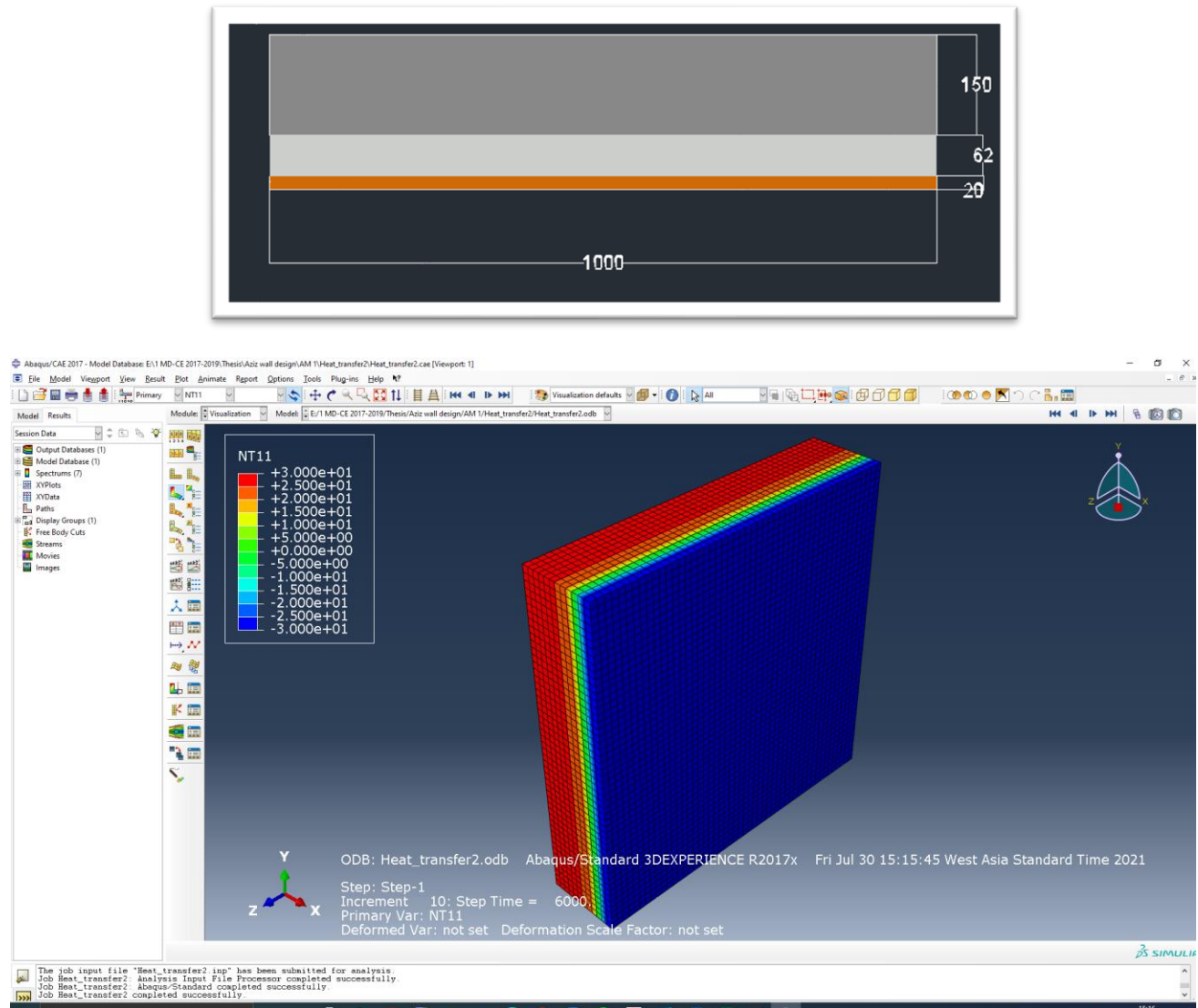


Figure 44. Heat transfer through the wall for the 2 nd analysis

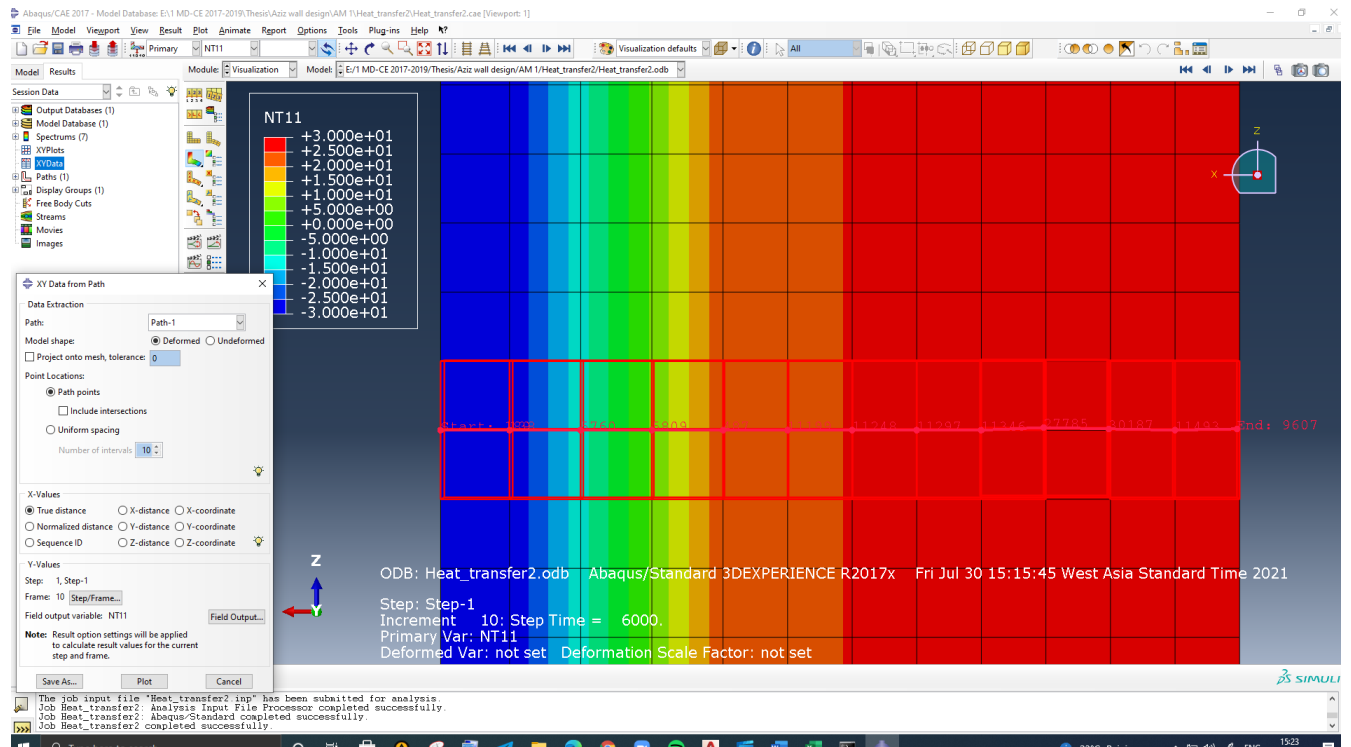


Figure 45. Heat transfer path data collection line

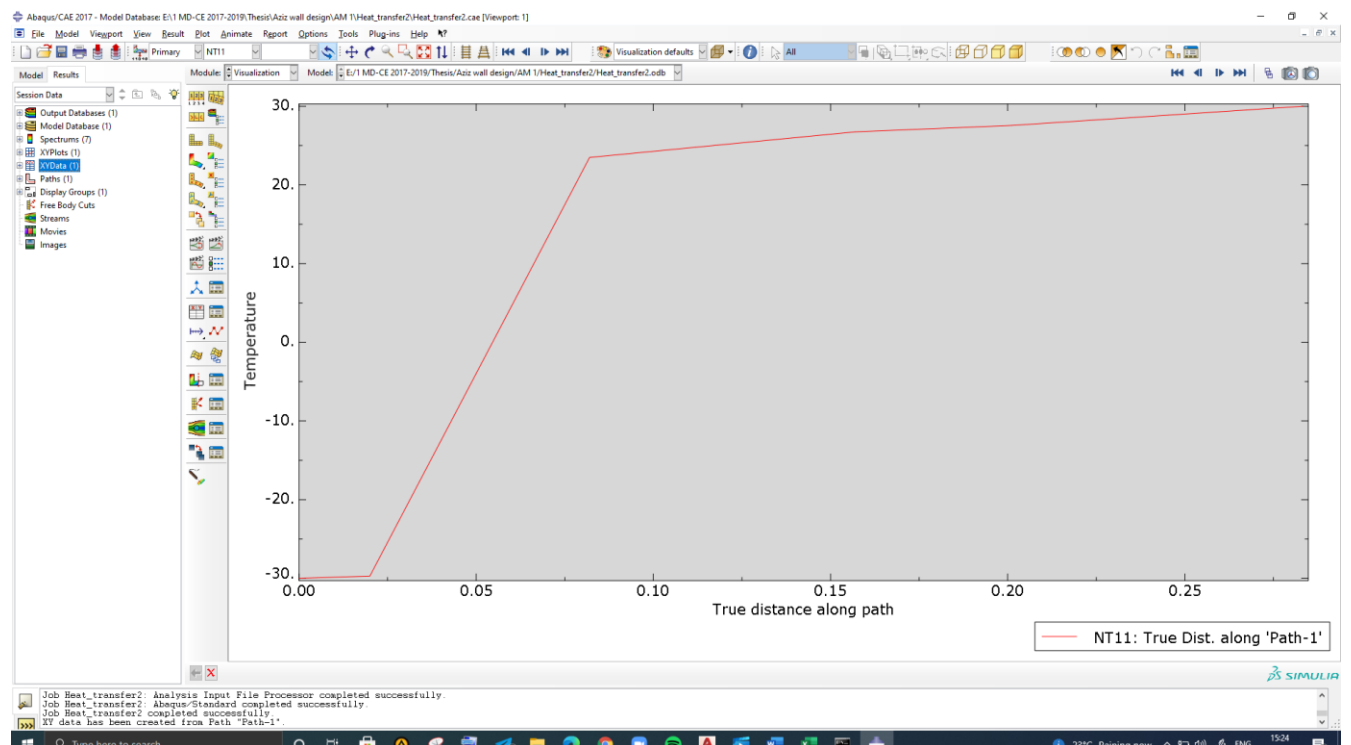


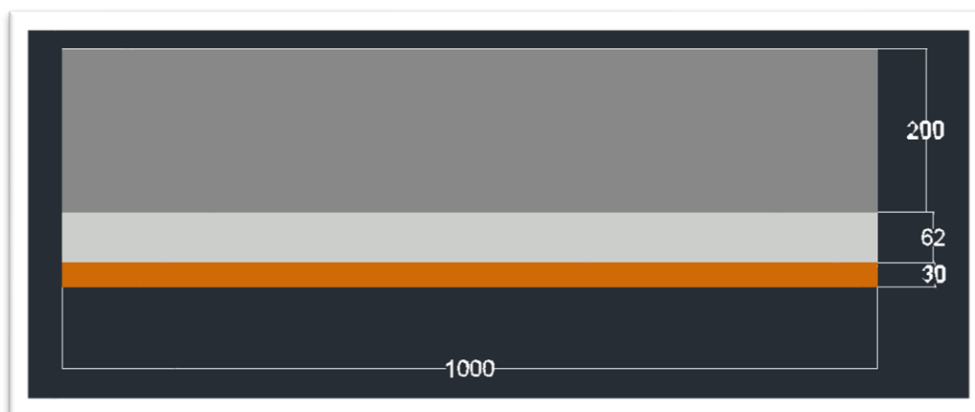
Figure 46. Graphical representation of the heat transfer path a long the wall

Table 15. Numerical values of the heat along the path below.

| Analysis2 | |
|-----------|---------|
| X [m] | Y [C] |
| | 0 -30 |
| 0.02 | -29.715 |
| 0.0406667 | -11.980 |
| 0.0613333 | 5.753 |
| 0.082 | 23.488 |
| 0.10075 | 24.302 |
| 0.1195 | 25.116 |
| 0.13825 | 25.930 |
| 0.157 | 26.744 |
| 0.201176 | 27.558 |
| 0.228591 | 28.372 |
| 0.256006 | 29.186 |
| 0.28342 | 30 |

Analysis 3

Let`s perform the same analysis with different geometry. There is no change in the Foam insulation layer geometry throughout the analysis, Meanwhile Thermal property of the Foam insulation layer will change in each analysis.



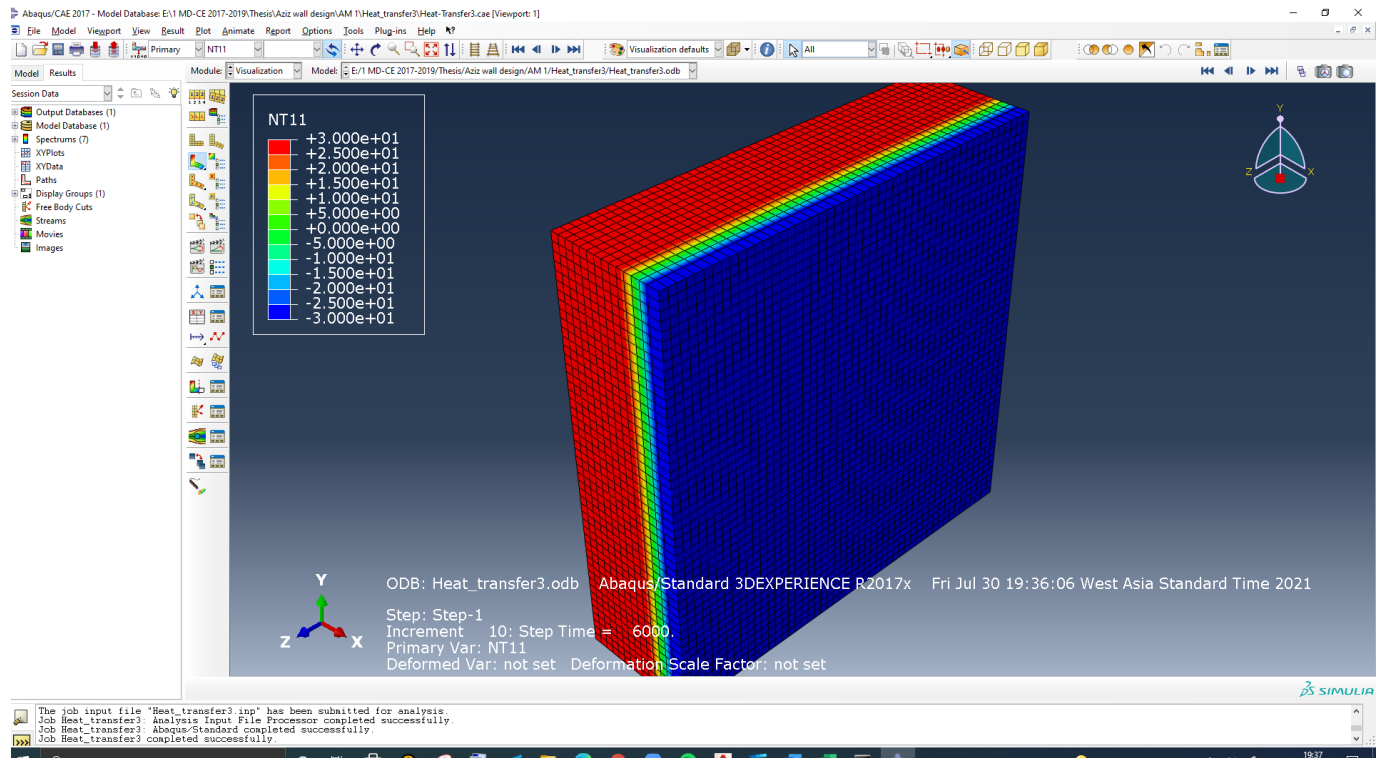


Figure 47. Heat transfer through the wall for the 3rd analysis

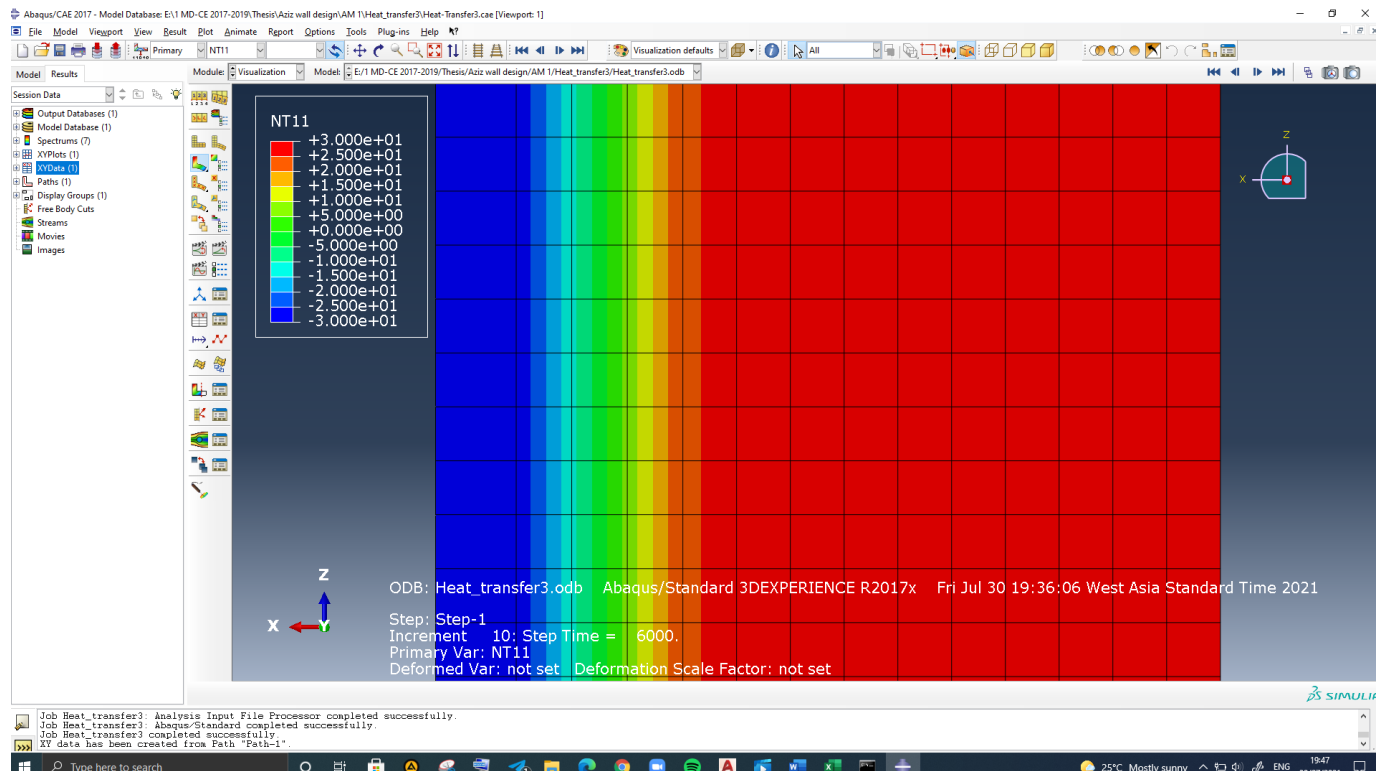


Figure 48. Heat transfer path data collection line for 3rd analysis

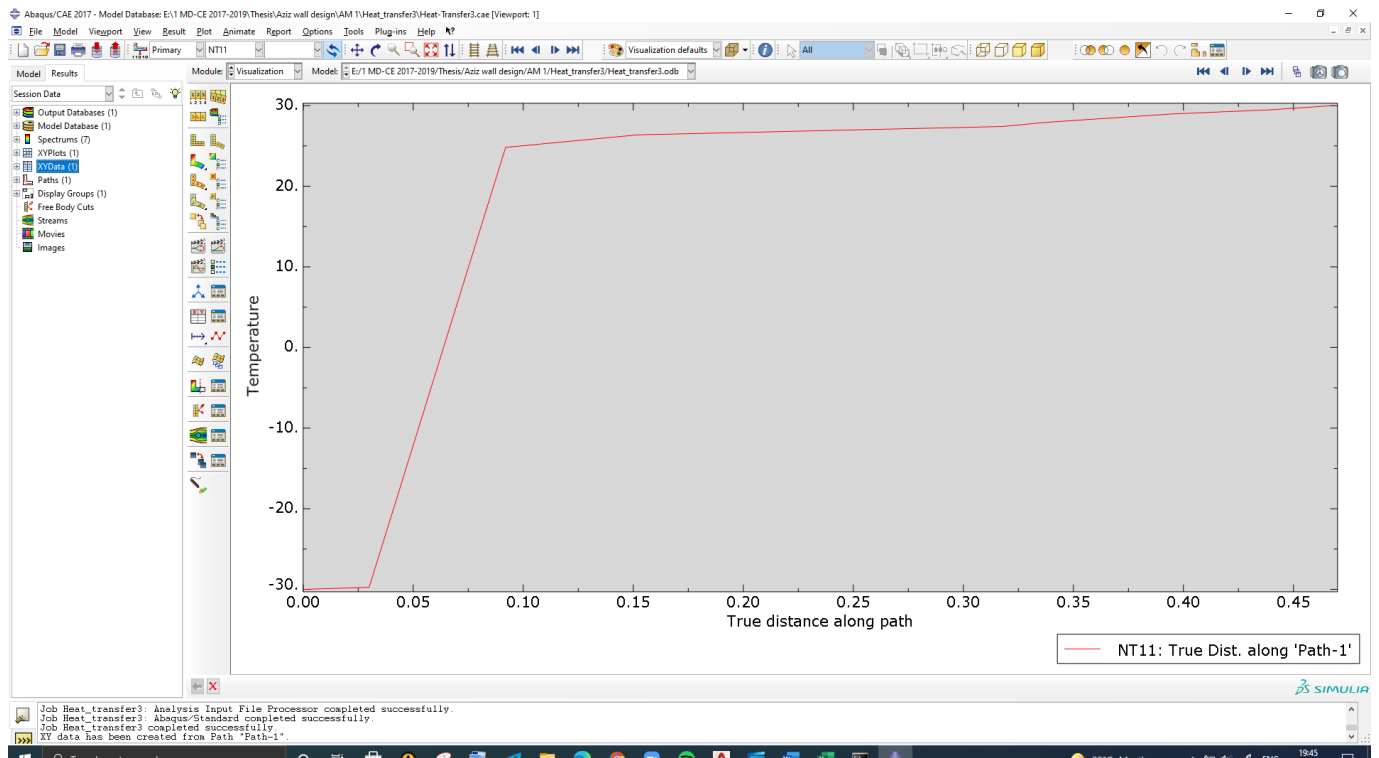


Figure 49. Graphical representation of the heat transfer path a long the wall

Table 16. Numerical values of the heat a long the path below.

| Analysis3 | |
|-----------|---------|
| X [m] | Y [C] |
| 0 | -30 |
| 0.03 | -29.745 |
| 0.0506667 | -11.556 |
| 0.0713333 | 6.633 |
| 0.092 | 24.822 |
| 0.112 | 25.340 |
| 0.132 | 25.858 |
| 0.152 | 26.375 |
| 0.23485 | 26.893 |
| 0.3177 | 27.411 |
| 0.3377 | 27.929 |
| 0.366055 | 28.446 |

| | |
|----------|--------|
| 0.394411 | 28.964 |
| 0.439311 | 29.482 |
| 0.467666 | 30 |

Analysis 4

Let`s perform the same analysis with the different geometry. There is not change in the Foam insulation layer geometry through the all analysis, Meanwhile Thermal property of Foam insulation layer will change in each analysis.

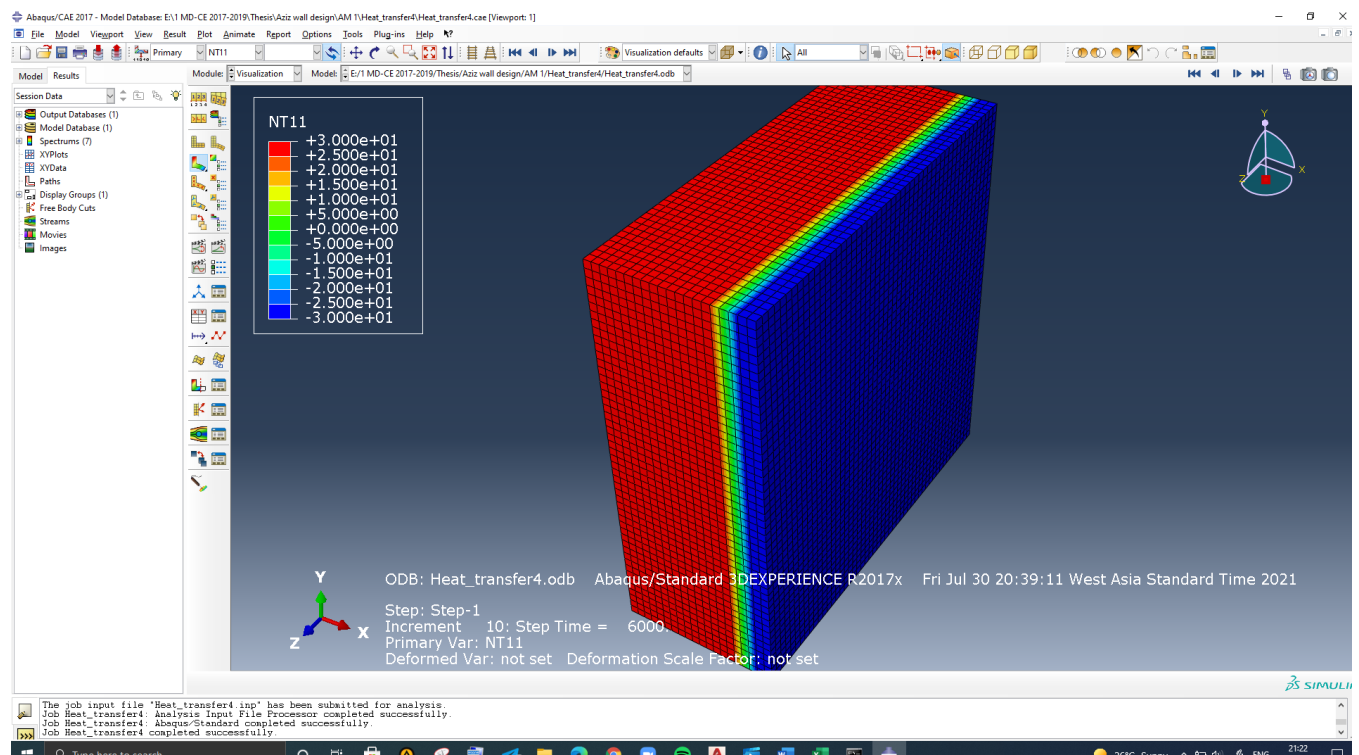


Figure 50. Heat transfer through the wall for the 3 nd analysis

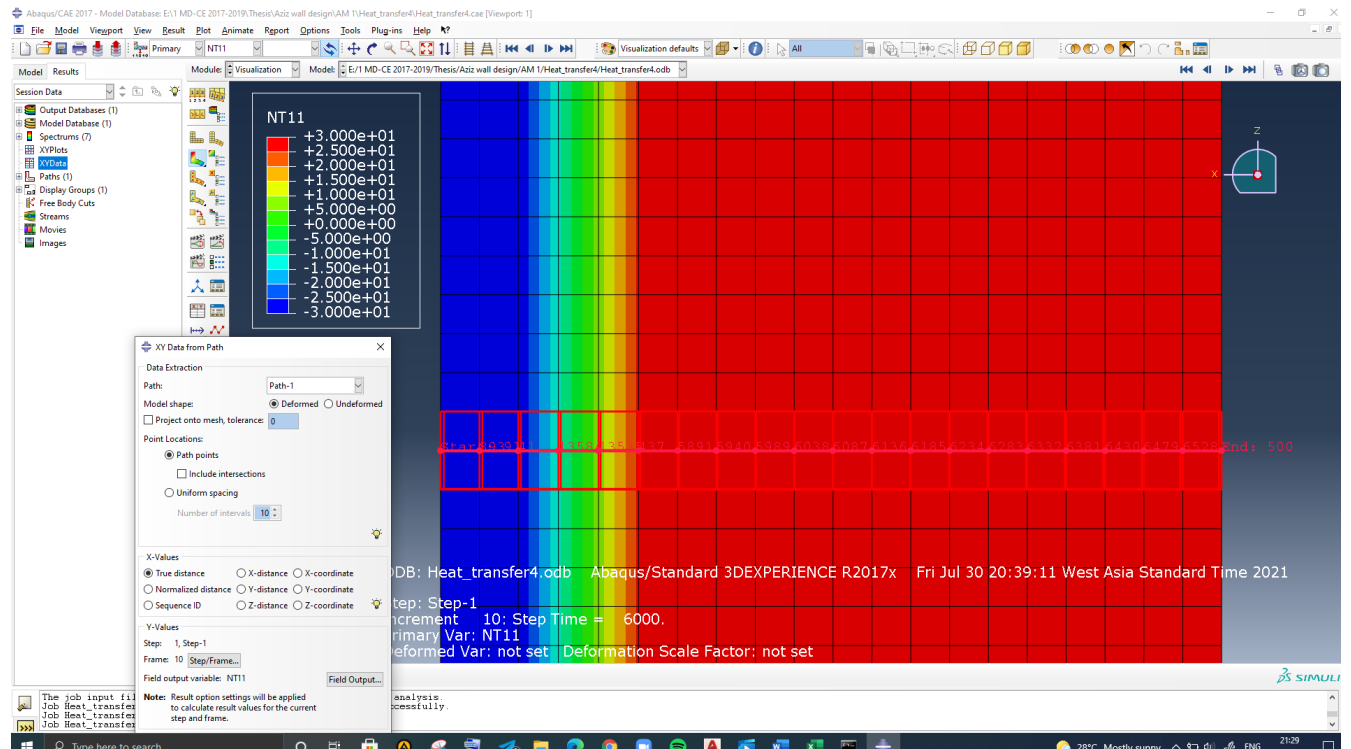


Figure 51. Heat transfer path data collection line for 4th analysis

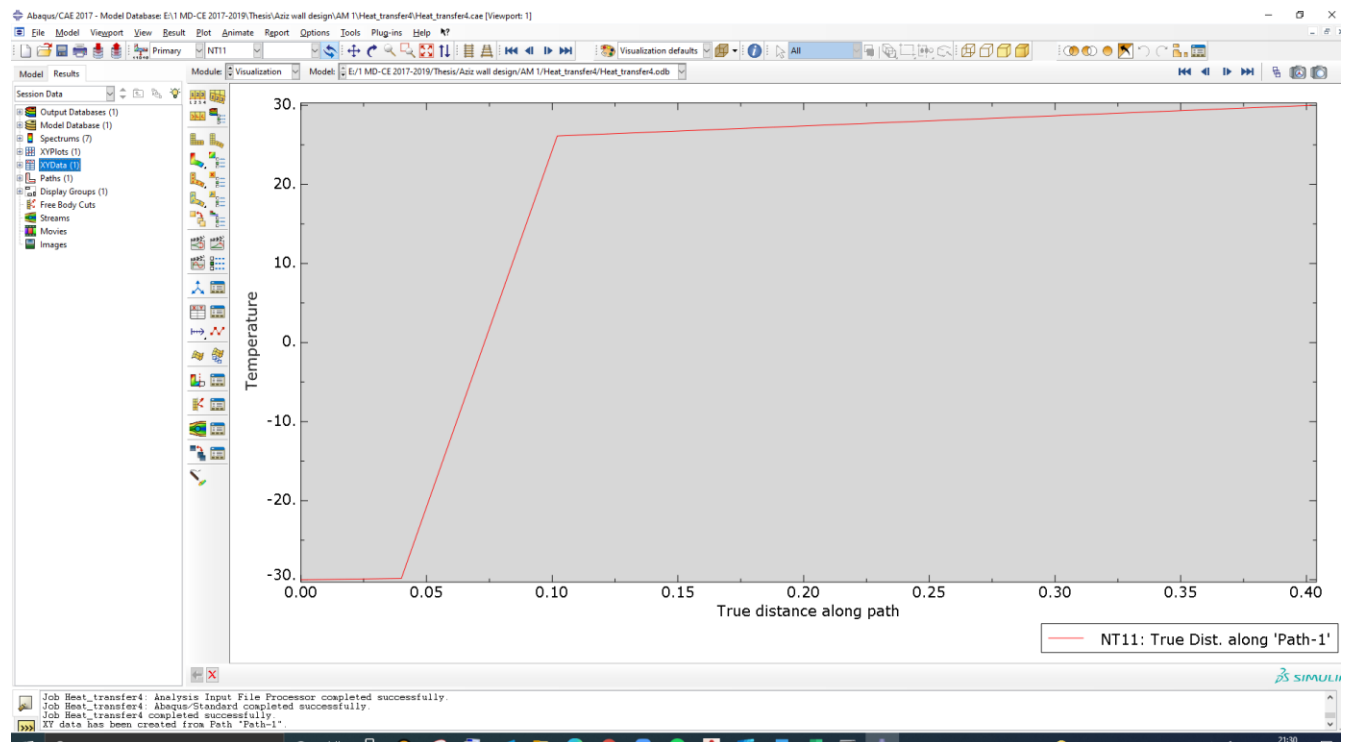
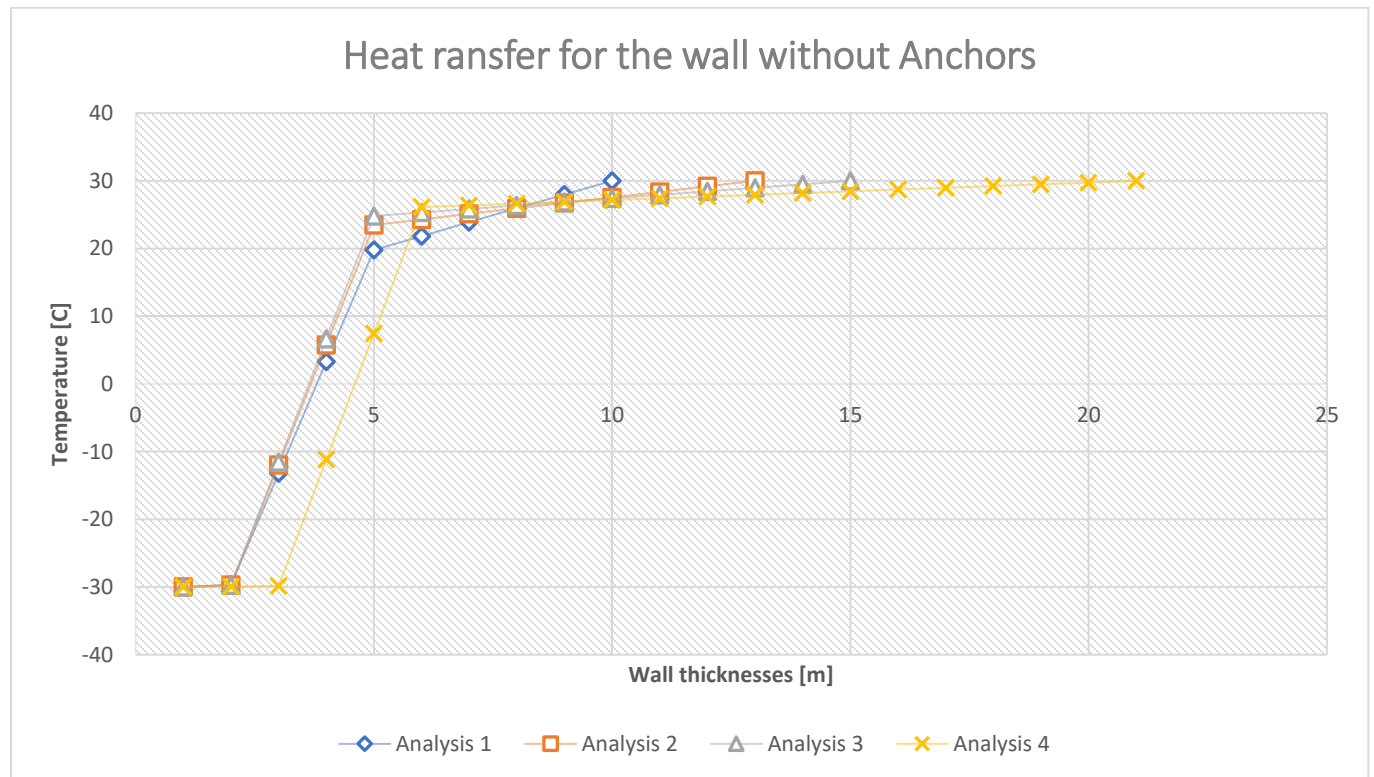


Figure 52. Graphical representation of the heat transfer path a long the wall

Table 17. Numerical values of the heat a long the path below.

| Analysis4 | |
|-----------|---------|
| X [m] | Y [C] |
| | 0 |
| | -30 |
| 0.02 | -29.915 |
| 0.04 | -29.830 |
| 0.0606667 | -11.178 |
| 0.0813333 | 74.728 |
| 0.102 | 26.124 |
| 0.122 | 26.382 |
| 0.142 | 26.641 |
| 0.162 | 26.899 |
| 0.182 | 2.715 |
| 0.202 | 27.416 |
| 0.222 | 27.674 |
| 0.242 | 27.933 |
| 0.262 | 28.191 |
| 0.282 | 28.449 |
| 0.302 | 28.708 |
| 0.322 | 28.966 |
| 0.342 | 29.224 |
| 0.362 | 29.483 |
| 0.382 | 29.741 |
| 0.402 | 30 |

The graph below illustrates Heat transfer analysis of four walls with different thicknesses. In the following case study, we consider wall without anchors.



I can repeat the same calculations above by adding Anchors to the wall with 4 different ways of distribution them on the Wall outer surface. As final conclusion I can make heat transfer table for the wall and wall with anchors.

Together with the insulation material used, ETICS anchors have a significant influence on the heat loss through house facades. The amount of heat that anchors transfer from inside a building is measured at specific points using the Chi value. The basic principle is that the smaller the Chi value of an ETICS anchor the lower the impact of an anchor on a component's U-value. Furthermore, the number of anchors per square metres also affects the value. A low number has a positive impact on the U-value. The U-value is a specific value that compares the insulation properties of components. It indicates how much heat per square metres flows through a component. A low U-value gives an indication that the components used allow for little heat to transfer from the interior to the exterior. Consequently, a building stays warm for a longer time.

Analysis 1 of the wall with Anchors

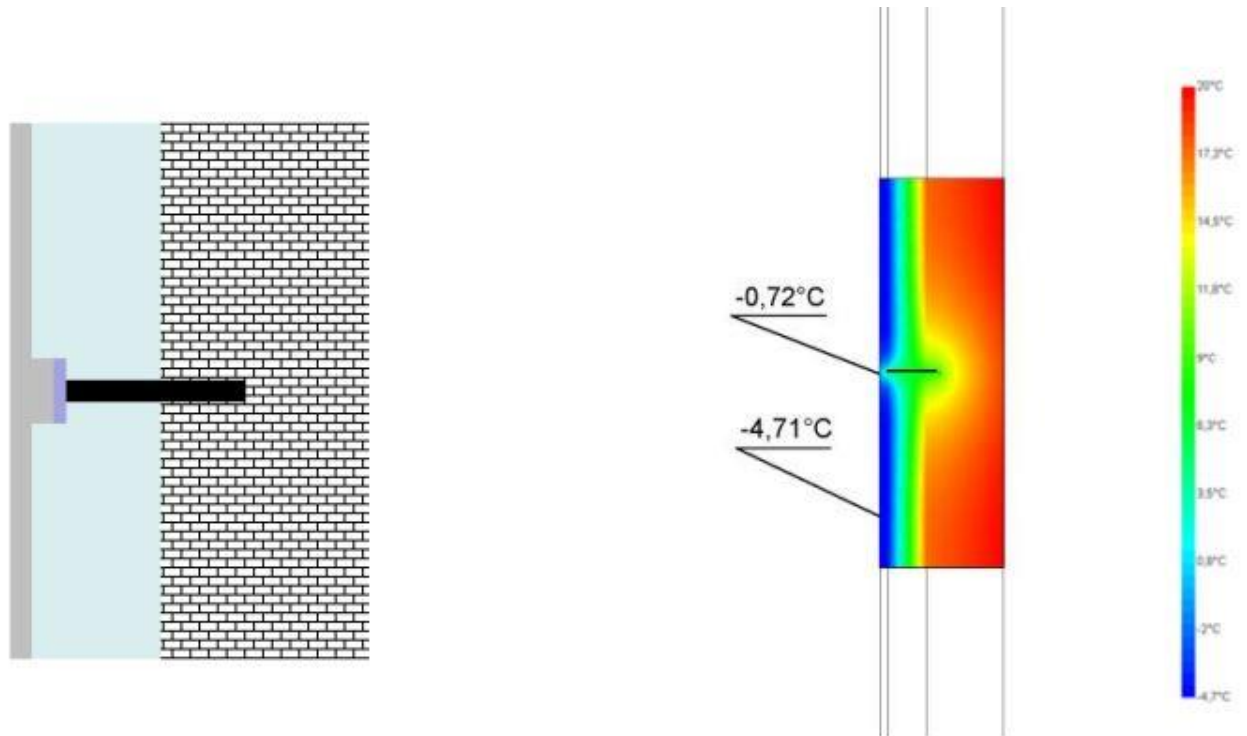


Figure 53. Schematic representation of anchor on the wall and its Thermal effect.

Let's perform the same wall heat transfer analysis with anchors. For the 1st analysis, I will use 16 anchors, geometrical data for fixing anchors are illustrated in the image below.

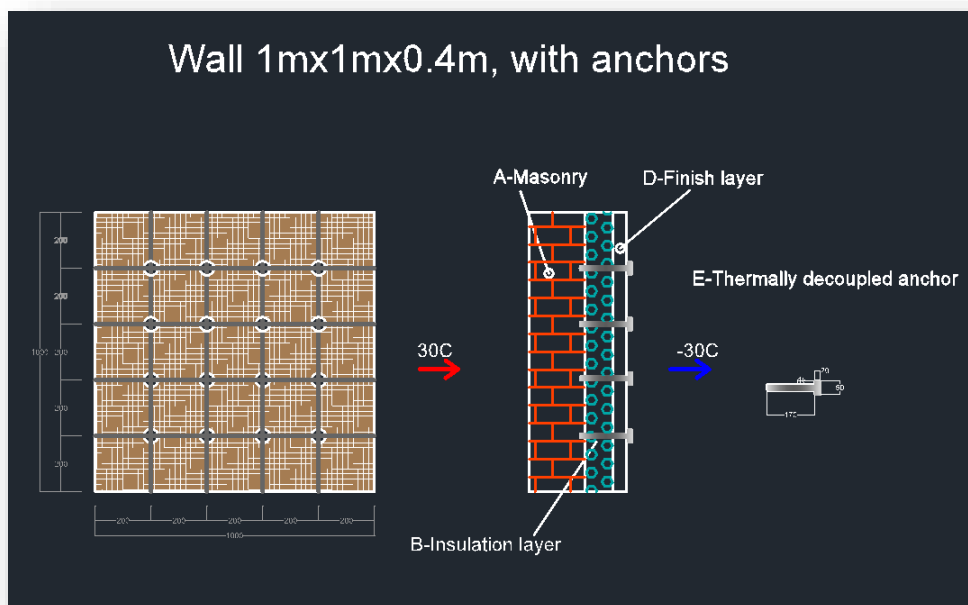


Figure 54. Wall part with anchors represented by AutoCAD

I have created the model of Anchor in part section of Abaqus. The Anchor has a thermal conductivity of $45\text{W}/[\text{mK}]$. The same anchor with geometry and property will be used for that analysis.

Figure 55. Model of anchor with all properties in Abaqus

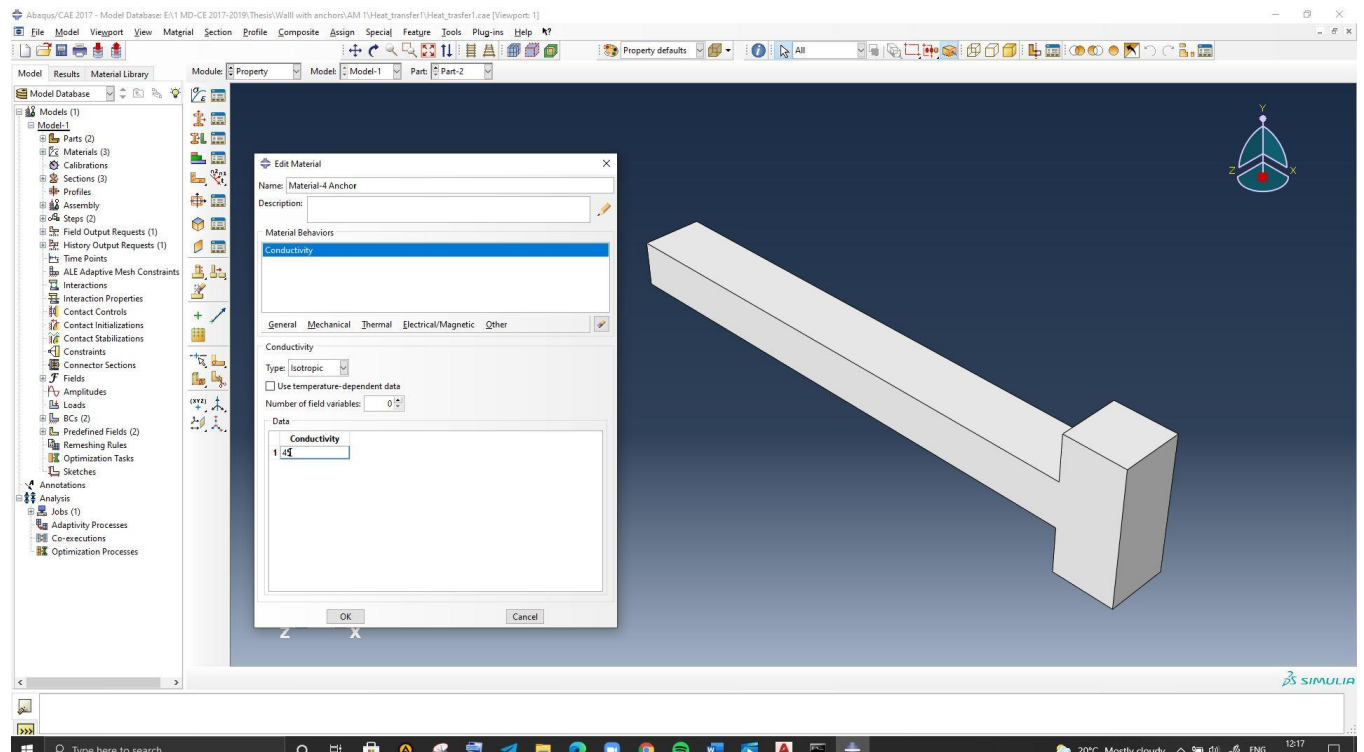


Figure 56. Distribution of 16 anchors to the wall outer face.

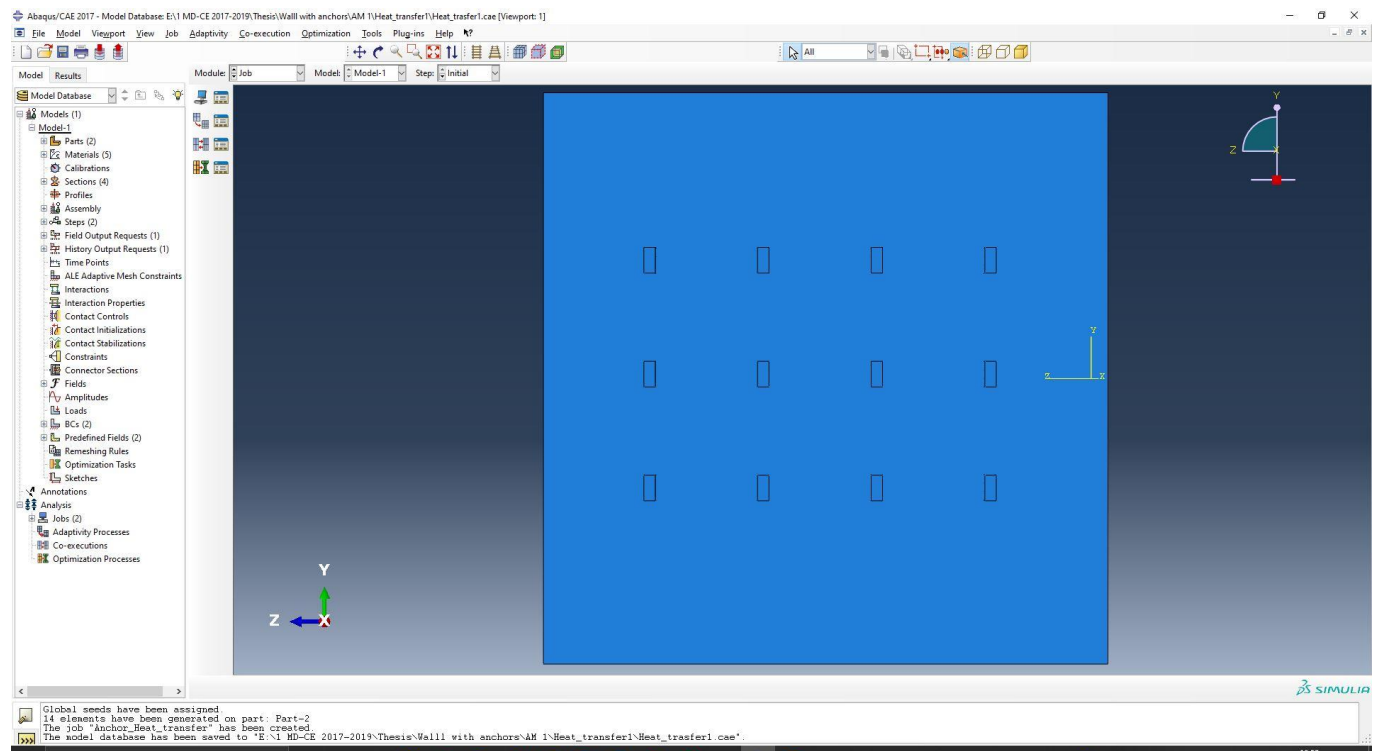


Figure 57. After submitting model in Abaqus I have got the following heat transfer model through the wall.

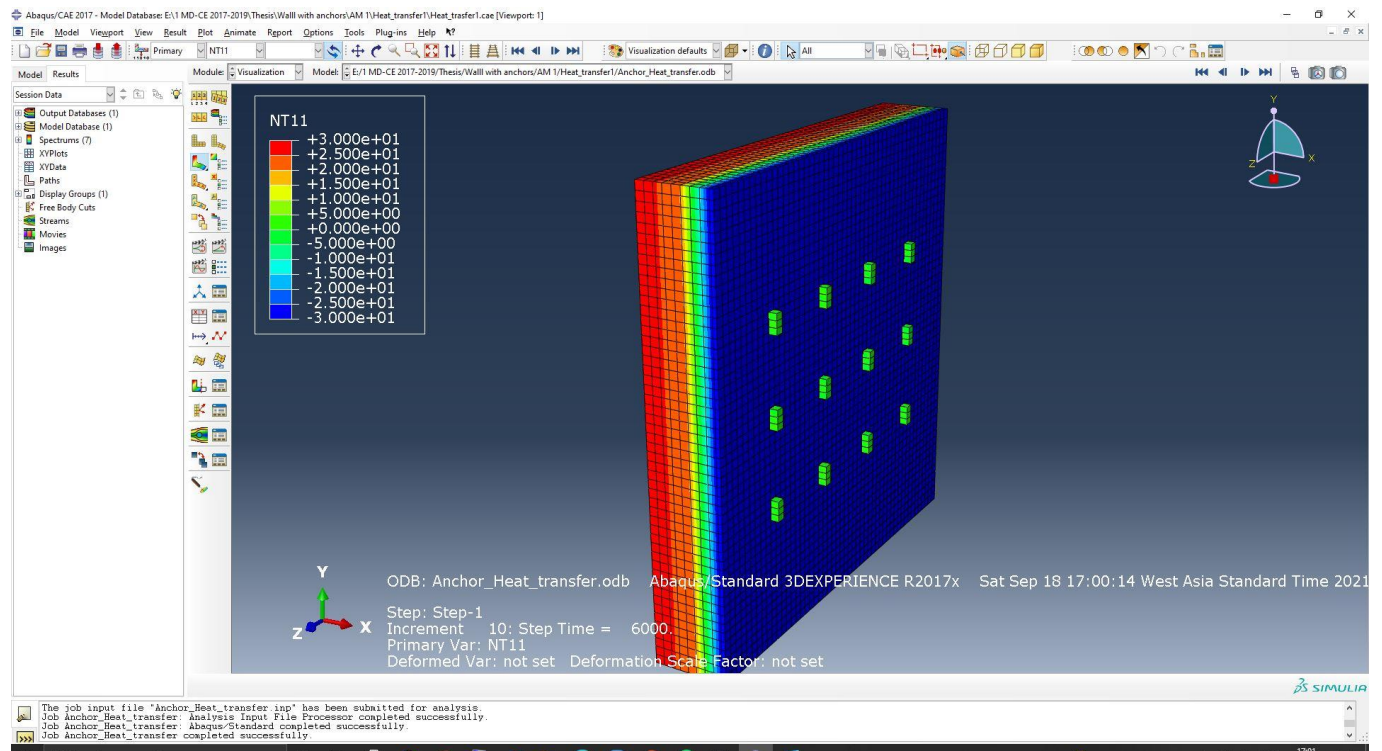


Figure 58. The graphical representation of heat transfer through the wall.

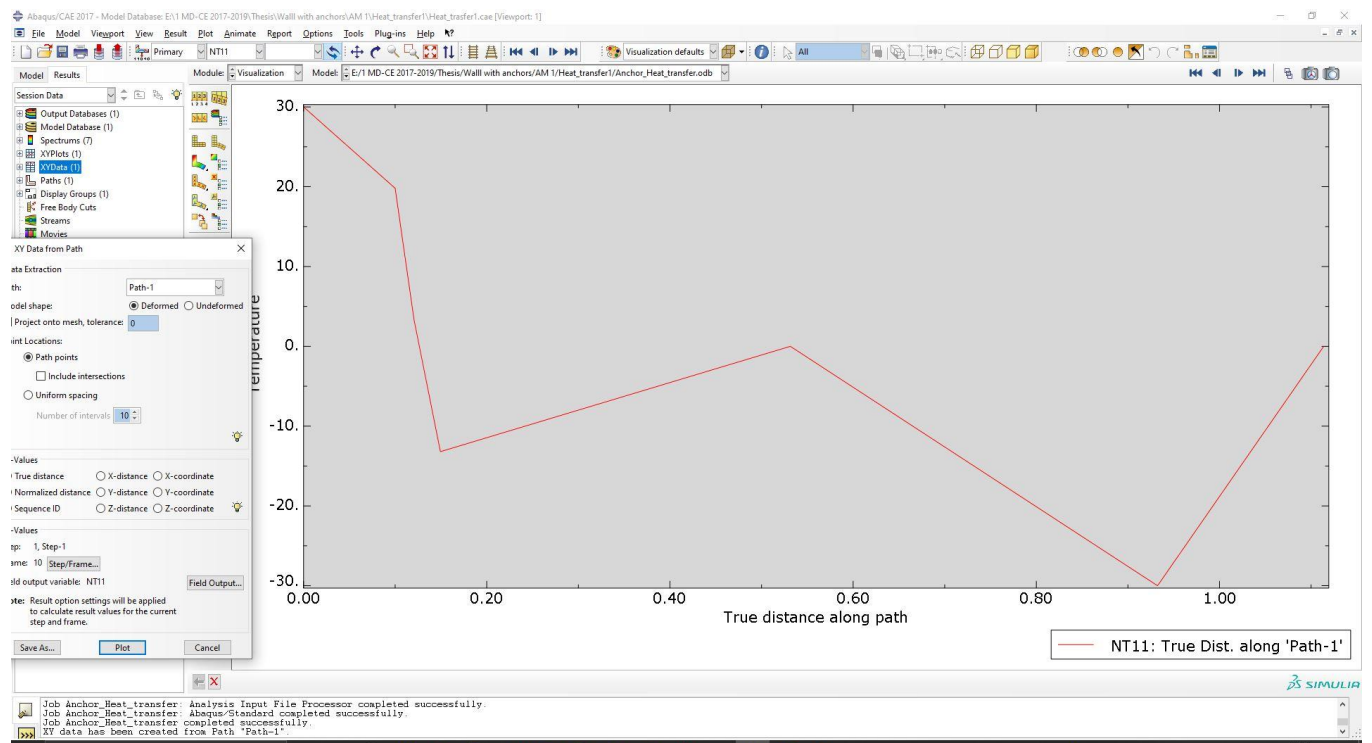


Table 18. The table below is numerical values of Temperature in the different point along the cross-section of the wall.

| With Anchor Analysis1 | |
|-----------------------|---------|
| X | Y |
| 0 | 30 |
| 0.02 | 27.961 |
| 0.04 | 25.923 |
| 0.06 | 23.884 |
| 0.08 | 21.846 |
| 0.10 | 19.807 |
| 0.12 | 3.305 |
| 0.14 | -13.197 |
| 0.53 | 0 |
| 0.93 | -30 |
| 1.11 | 0 |

Analysis 2 of wall with Anchors

Let`s perform the same wall heat transfer analysis with anchors. For the 2nd analysis, I will use 9 anchors, geometrical data for fixing anchors are illustrated in the image below.

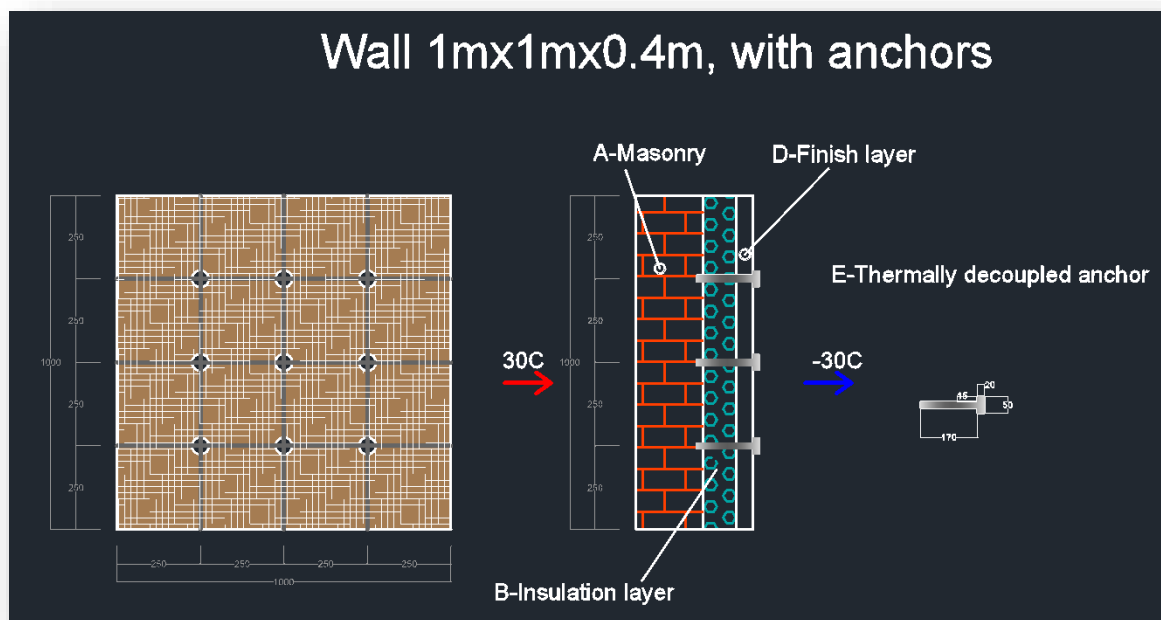


Figure 59. Distribution of 9 anchors to the wall outer face.

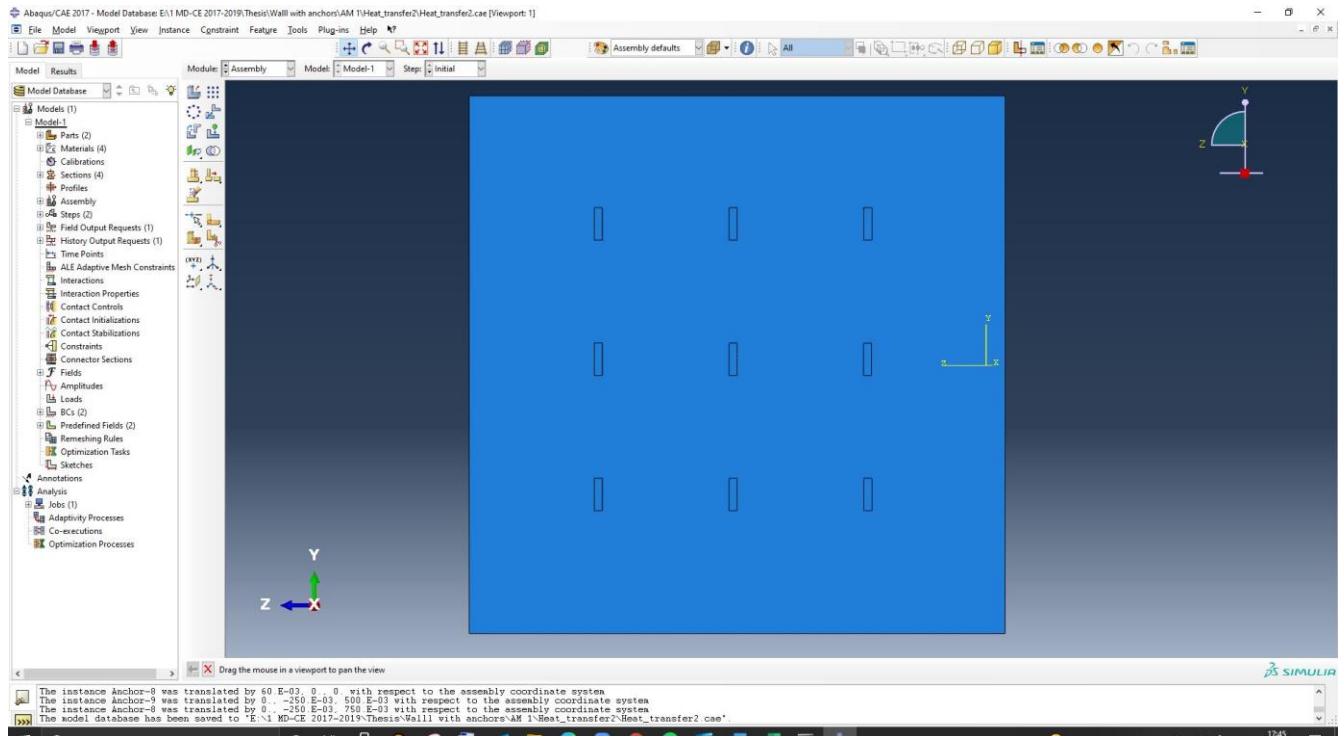
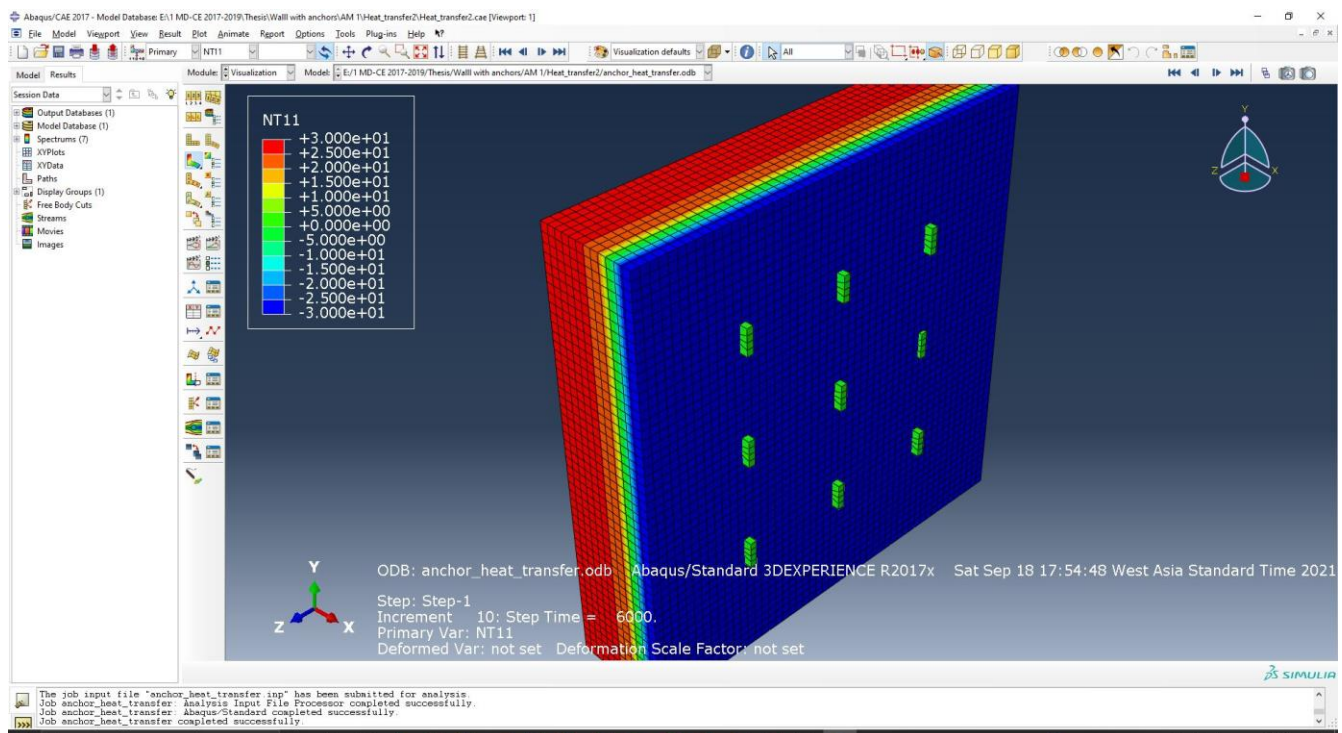


Figure 60.



The PATH for the temperature distribution through the wall, the path can be selected randomly. For

the case distribution had been chosen in the same line as on of the anchors. The chosen distribution illustrated below.

Figure 61.

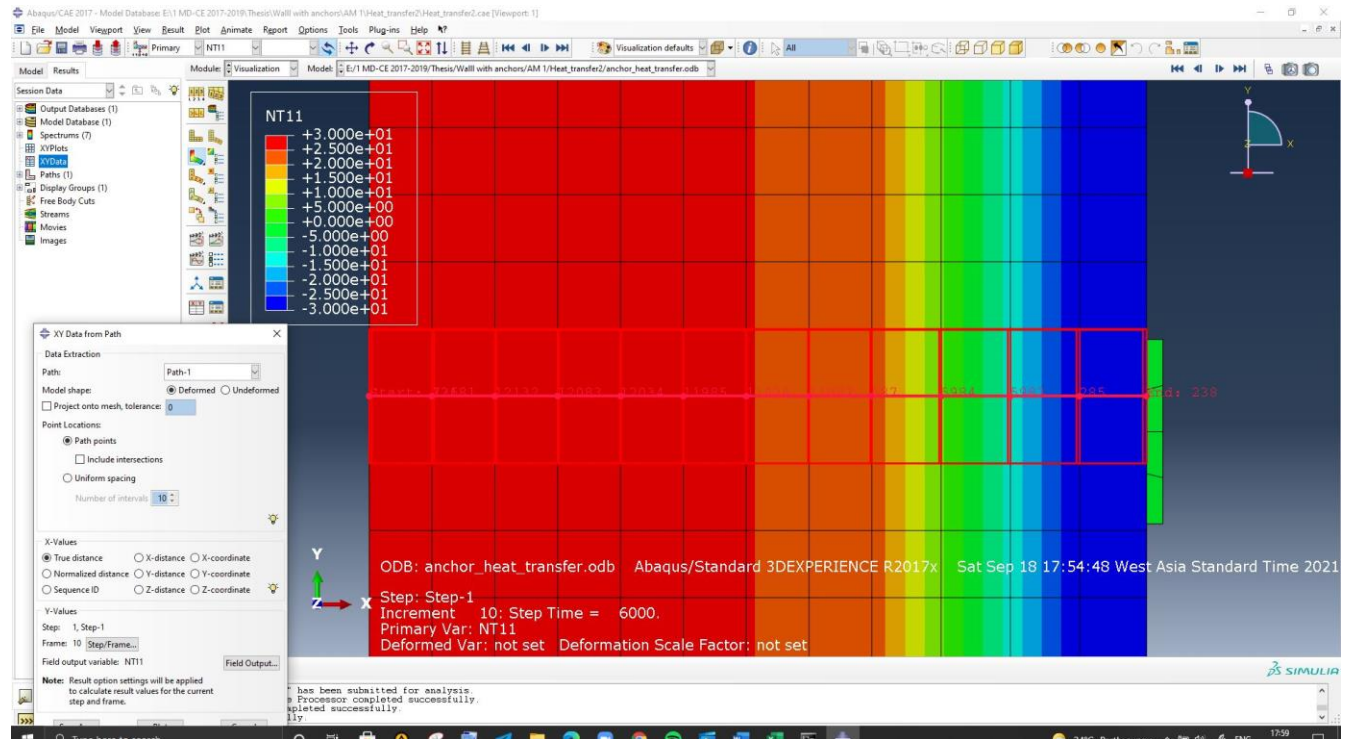
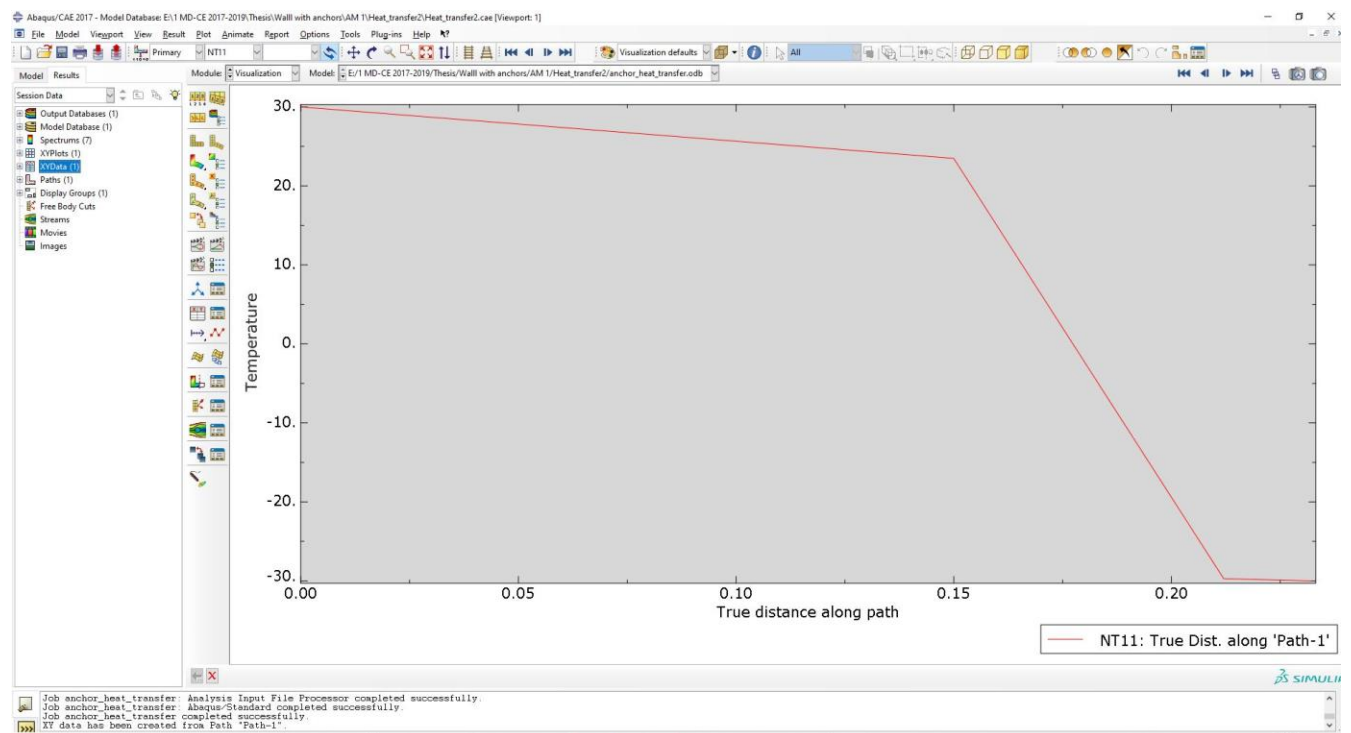


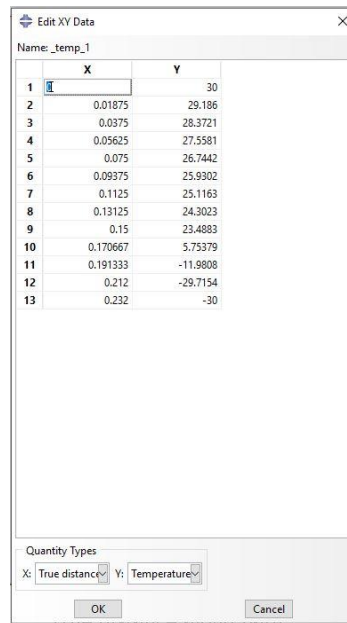
Figure 66. The graphical representation of heat transfer through the wall.



The table below is numerical values of Temperature in the different point along cross-section of the wall.

Table 19. The table on the right real values, that Abaqus software represented

| With Anchor Analysis2 | |
|-----------------------|---------|
| X | Y |
| | 0 30 |
| 0.018 | 29.186 |
| 0.037 | 28.372 |
| 0.056 | 27.558 |
| 0.075 | 26.744 |
| 0.093 | 25.930 |
| 0.112 | 25.116 |
| 0.131 | 24.302 |
| 0.15 | 23.488 |
| 0.170 | 5.753 |
| 0.191 | -11.980 |
| 0.212 | -29.715 |
| 0.232 | -30 |



Analysis 3 of the wall with Anchors

Let`s perform the same wall heat transfer analysis with anchors. For the 3rd analysis, I will use 4 anchors, geometrical data for fixing anchors are illustrated in the image below.

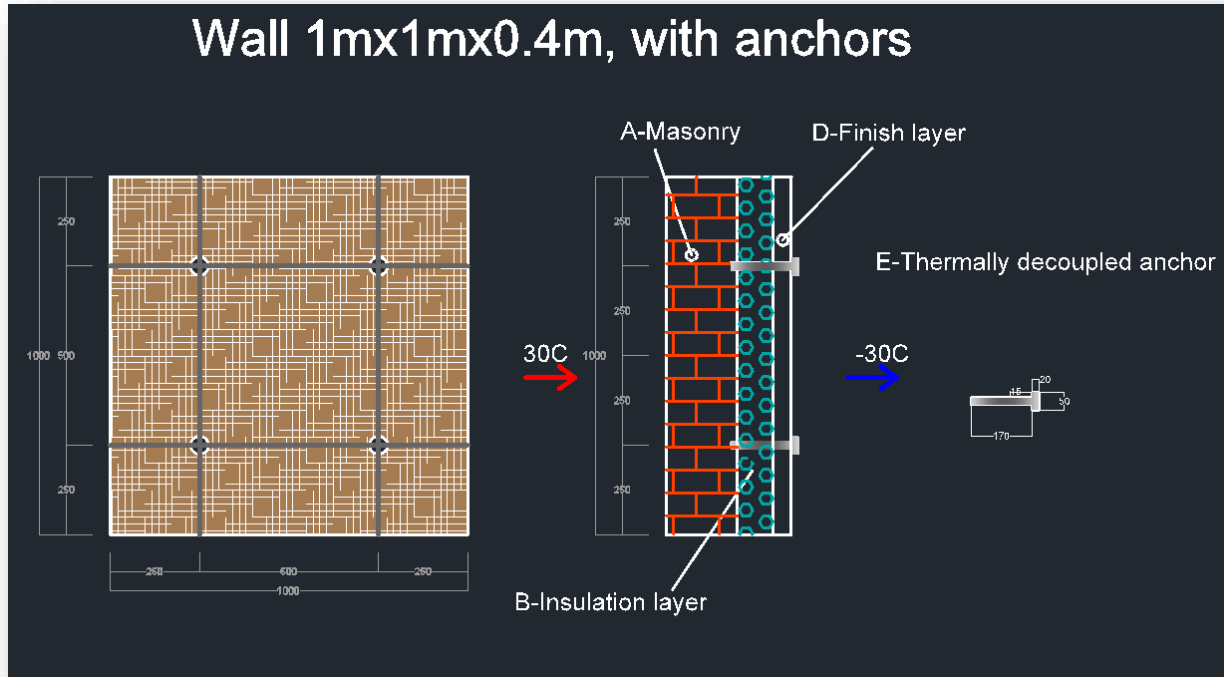
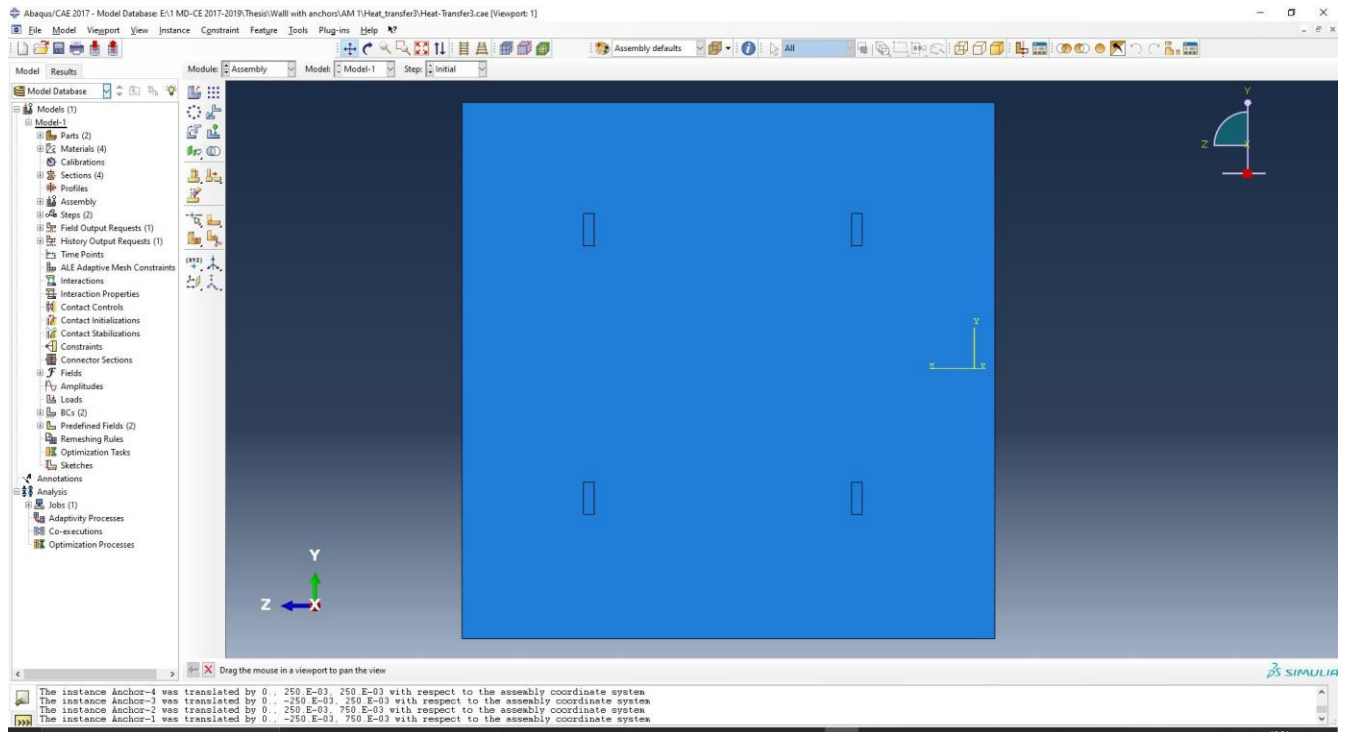


Figure 67. Distribution of 4 anchors to the wall outer face.



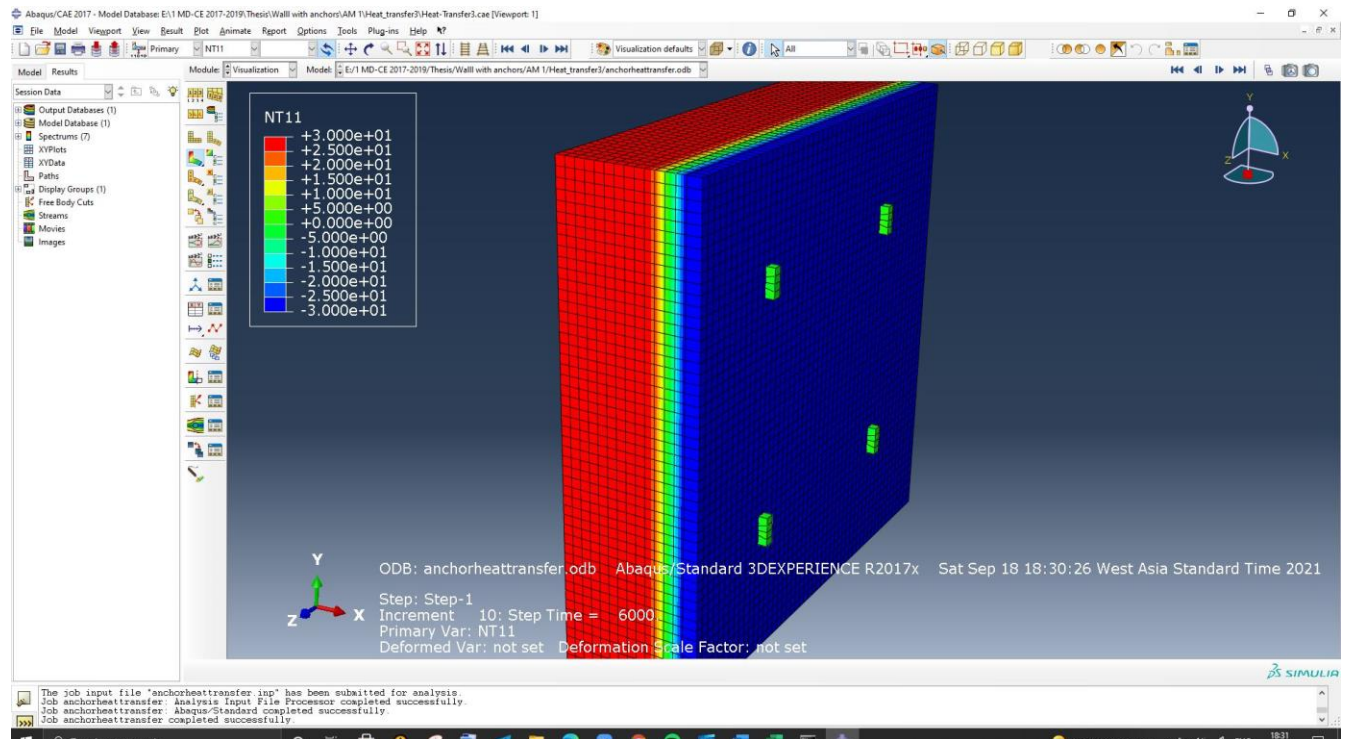


Figure 68.

The PATH for the temperature distribution through the wall, the path can be selected randomly. For the case, distribution had been chosen in the same line as one of the anchors. The chosen distribution is illustrated below.

Figure 69.

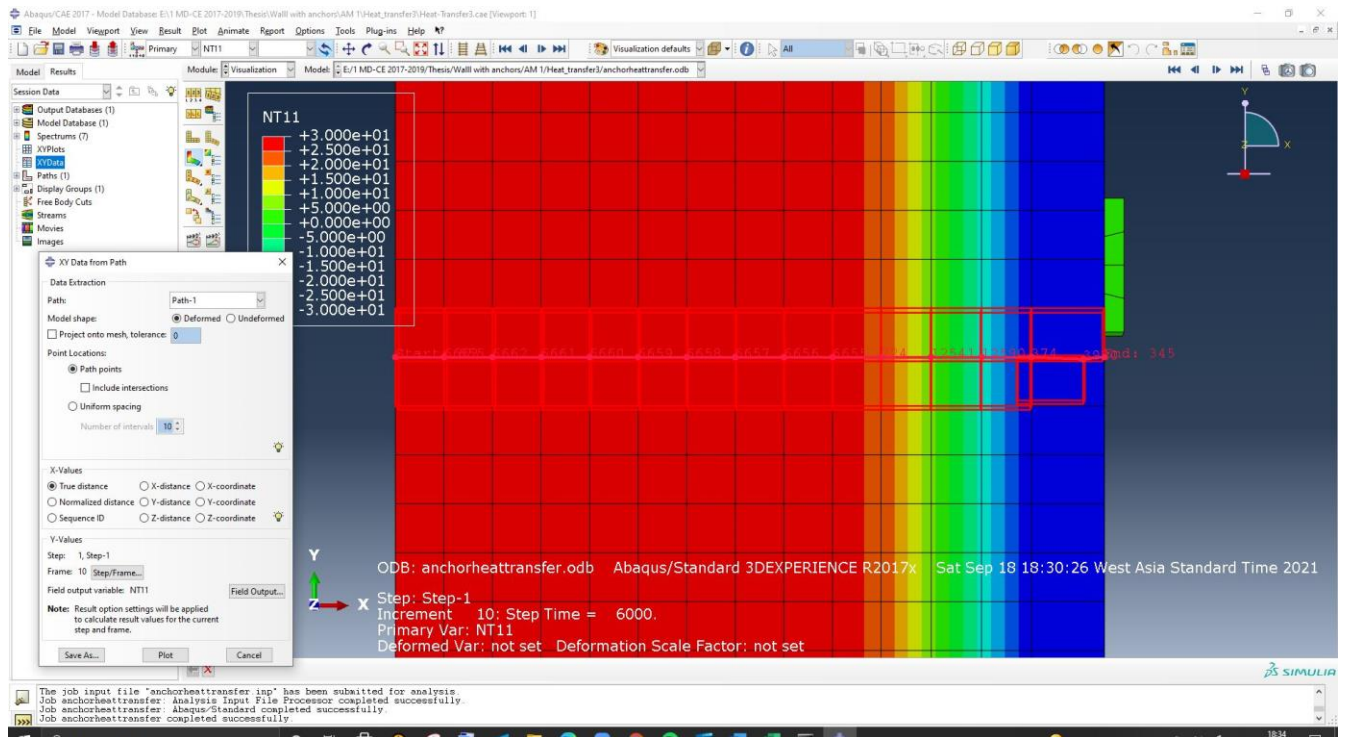
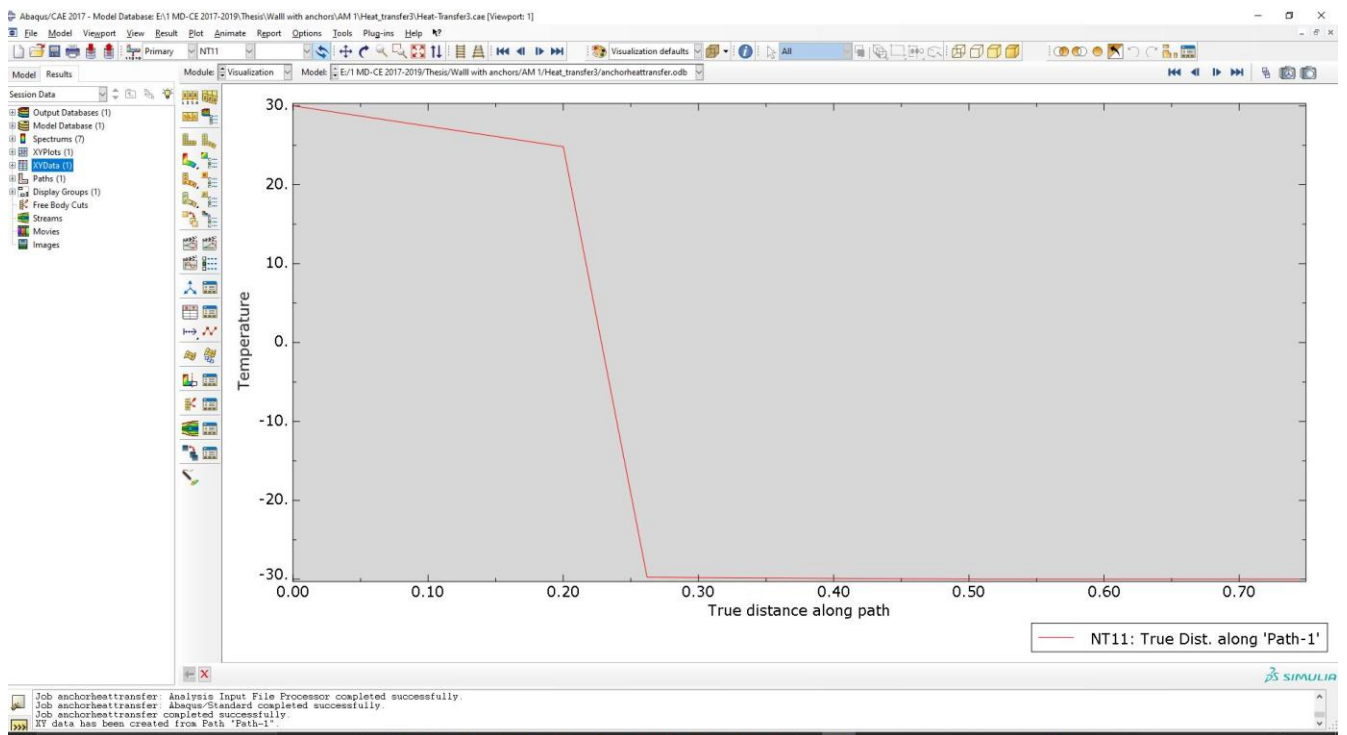


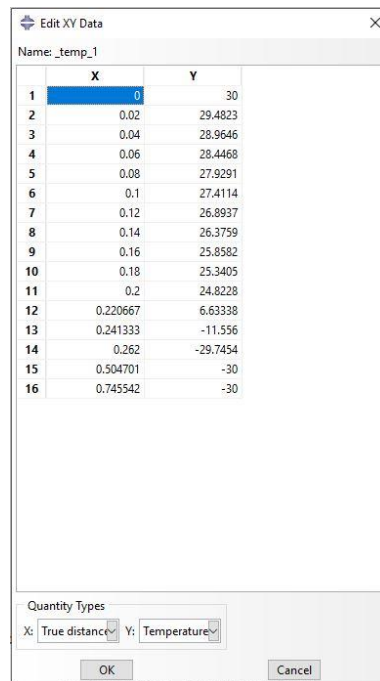
Figure 70. The graphical representation of heat transfer through the wall.



The table below is numerical values of Temperature in the different point along cross-section of the wall.

Table 20. The table on the right real values, that Abaqus software represented

| With Anchor Analysis3 | |
|-----------------------|---------|
| X | Y |
| 0 | 30 |
| 0.02 | 29.482 |
| 0.04 | 28.964 |
| 0.06 | 28.446 |
| 0.08 | 27.929 |
| 0.10 | 27.411 |
| 0.12 | 26.893 |
| 0.14 | 26.375 |
| 0.16 | 25.858 |
| 0.18 | 25.340 |
| 0.20 | 24.822 |
| 0.22 | 6.633 |
| 0.24 | -11.556 |
| 0.26 | -29.745 |
| 0.50 | -30 |
| 0.74 | -30 |



Analysis 4 of the wall with Anchors

Let`s perform the same wall heat transfer analysis with anchors. For the 4th analysis, I will use 1 anchors, geometrical data for fixing anchors are illustrated in the image below.

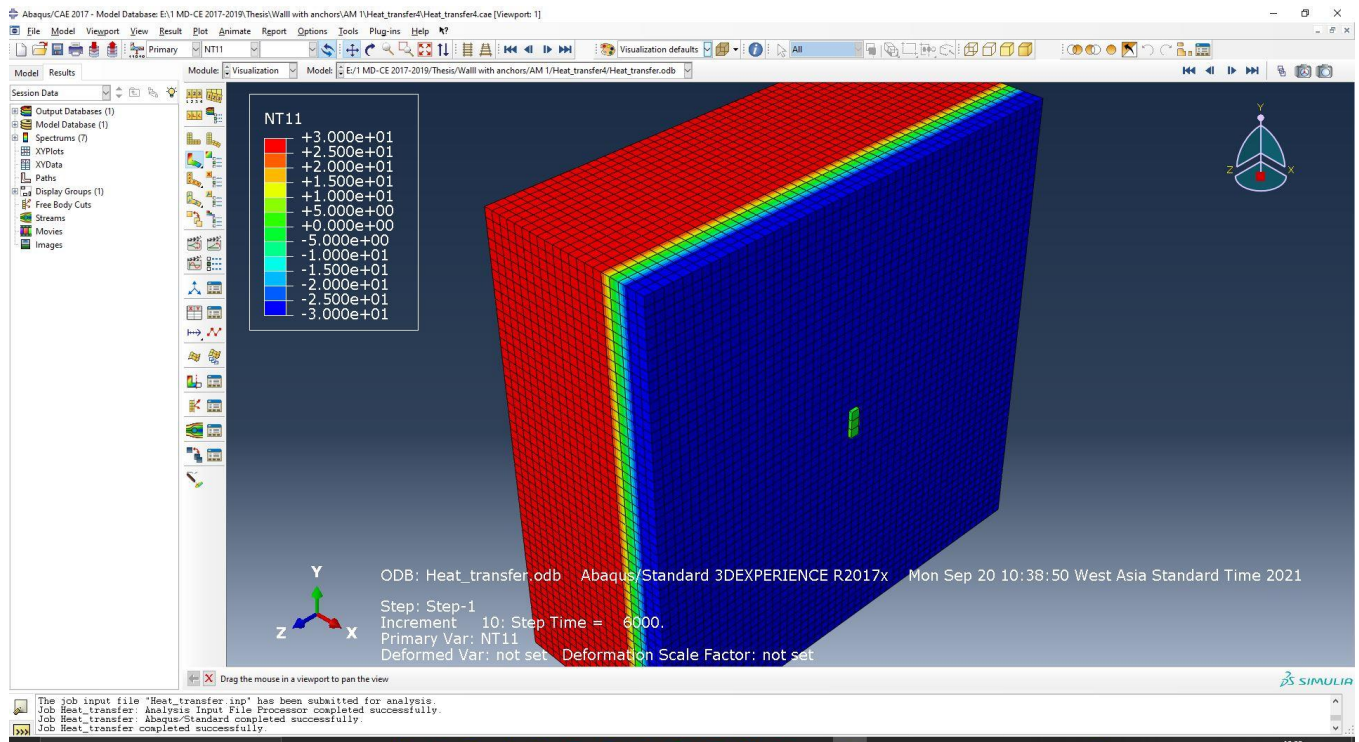
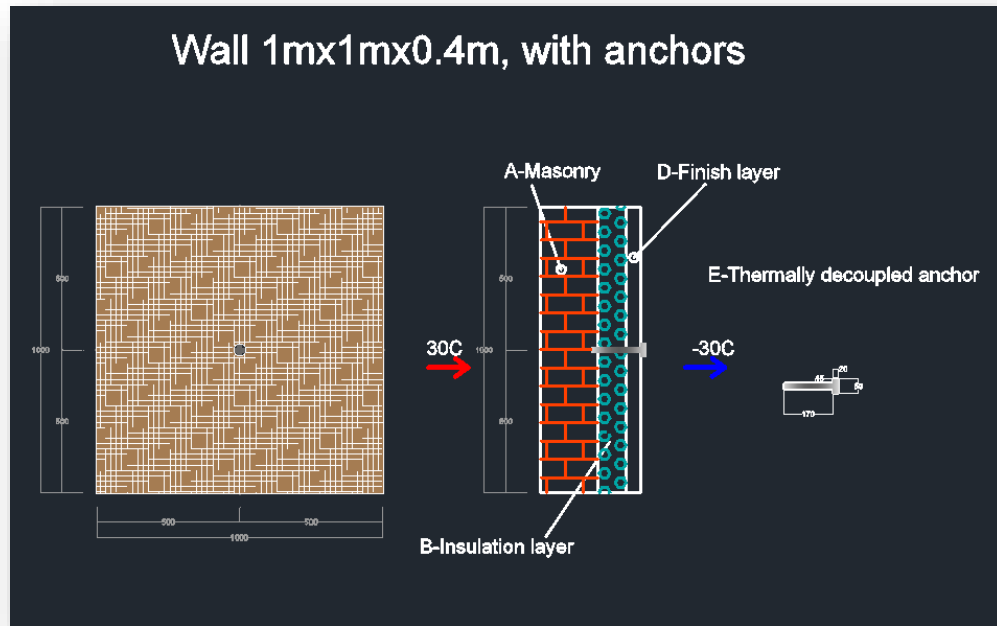


Figure 71.

The PATH for the temperature distribution through the wall, the path can be selected randomly. For the case distribution had been chosen in the same line as on of the anchors. The chosen distribution illustrated below.

Figure 72.

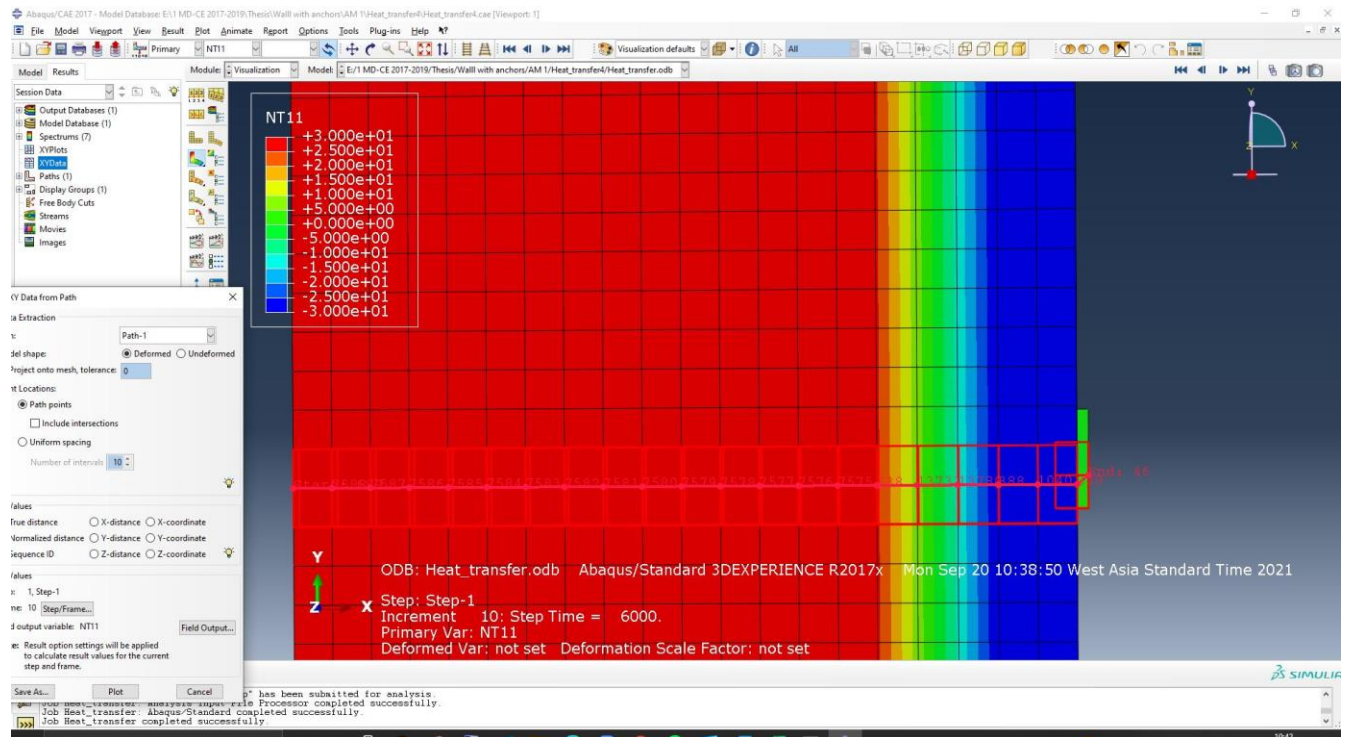
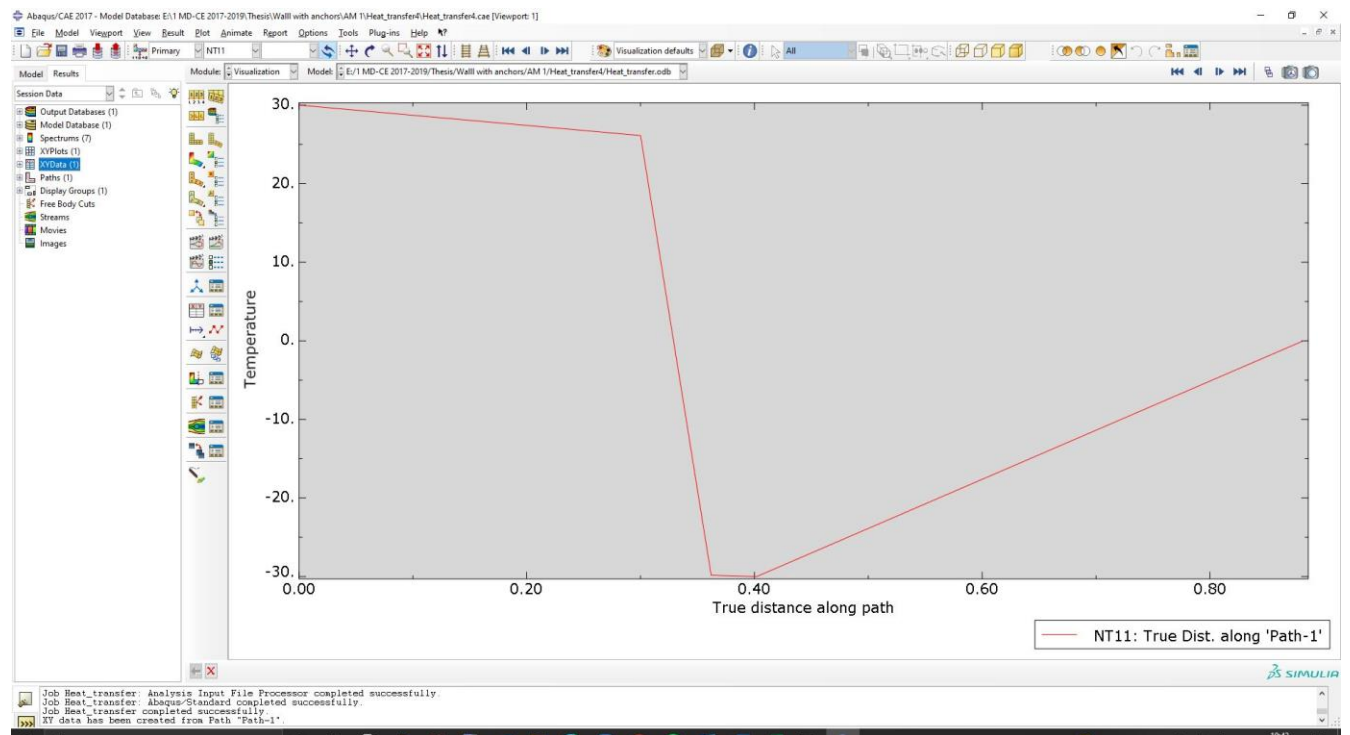


Figure 72. The graphical representation of heat transfer through the wall.



The table below is numerical values of Temperature in the different point along cross-section of the wall.

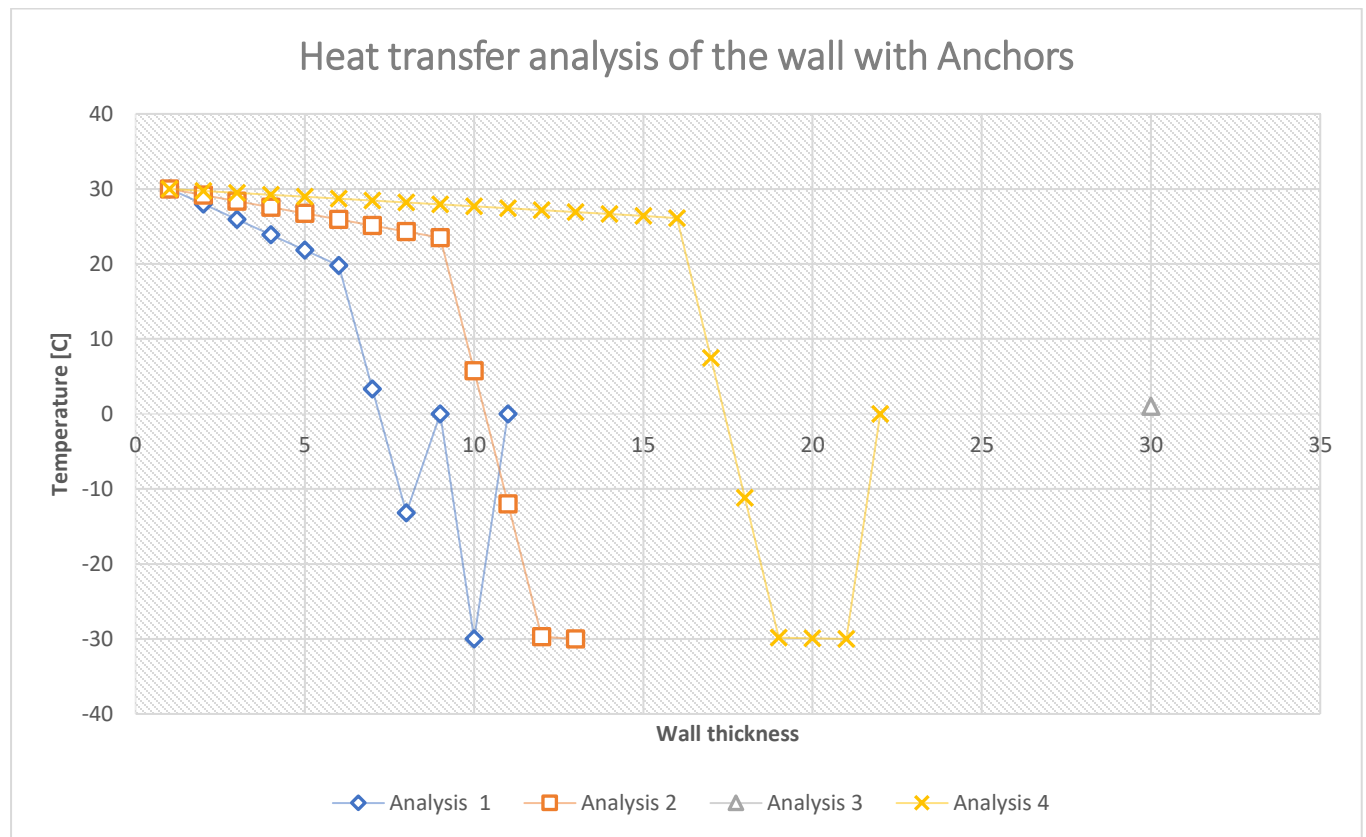
Table 21. The table on the right real values, that Abaqus software represented

| With Anchor Analysis4 | | |
|-----------------------|---|---------|
| X | Y | |
| | 0 | 30 |
| 0.02 | | 29.741 |
| 0.04 | | 29.483 |
| 0.06 | | 29.224 |
| 0.08 | | 28.966 |
| 0.10 | | 28.708 |
| 0.12 | | 28.449 |
| 0.14 | | 28.191 |
| 0.16 | | 27.933 |
| 0.18 | | 27.674 |
| 0.2 | | 27.416 |
| 0.22 | | 27.152 |
| 0.24 | | 26.899 |
| 0.26 | | 26.641 |
| 0.28 | | 26.382 |
| 0.3 | | 26.124 |
| 0.32 | | 7.472 |
| 0.34 | | -11.178 |
| 0.36 | | -29.830 |
| 0.38 | | -29.915 |
| 0.40 | | -30 |
| 0.88 | | 0 |

| | X | Y |
|----|----------|----------|
| 1 | 0 | 30 |
| 2 | 0.02 | 29.7416 |
| 3 | 0.04 | 29.4833 |
| 4 | 0.06 | 29.2249 |
| 5 | 0.08 | 28.9665 |
| 6 | 0.1 | 28.7082 |
| 7 | 0.12 | 28.4498 |
| 8 | 0.14 | 28.1915 |
| 9 | 0.16 | 27.9331 |
| 10 | 0.18 | 27.6747 |
| 11 | 0.2 | 27.4164 |
| 12 | 0.22 | 27.152 |
| 13 | 0.24 | 26.8996 |
| 14 | 0.26 | 26.6413 |
| 15 | 0.28 | 26.3829 |
| 16 | 0.3 | 26.1245 |
| 17 | 0.320667 | 7.47283 |
| 18 | 0.341333 | -11.1789 |
| 19 | 0.362 | -29.8306 |
| 20 | 0.382 | -29.9153 |
| 21 | 0.402 | -30 |
| 22 | 0.882067 | 0 |

Quantity Types
 X: True distance Y: Temperature

The table below shows graphical representation of Heat transfer analysis in numerical way through the wall with four different thicknesses and for all the cases Anchors were used with different repositioning for each case



As a summary we can conclude that Heat transfer increases in the case of anchors if increase the number of anchors with short spacing it will significantly influence to the heat transfer. For better keeping temperature it is recommended to Minimize the number of anchors with convenience spacing since two short distances between anchors increases transmittance of the wall. As a result, it can negatively affect to the Thermal performance and property of the walls.

Thermally-isolating wall anchors and reinforcement devices and anchoring systems employing the same are disclosed for use in masonry cavity walls. A thermally-isolating coating is applied to the wall anchor, which is interconnected with a wire formative veneer tie. The thermally-isolating coating is selected from a distinct grouping of materials, that are applied using a specific variety of methods, in one or more layers and cured and cross-linked to provide high-strength adhesion. The thermally-coated wall anchors provide an in-cavity thermal break that severs the thermal threads running throughout the cavity wall structure, reducing the U- and K-values of the anchoring system by thermally-isolating the metal components.

Conclusion

The heat transfer analysis of two condition wall with anchors and without illustrate that thin wall require a fewer number of anchors to reduce heat transfer through the wall meanwhile for thick walls there is no big effect for heat transfer. For the wall with the same material property.

In general, the presence of air spaces or pockets increases the insulating value of walls built of heavy clay products. Furring materially increases the insulating value of ordinary types of walls. The differences in insulating value between the various types of hallow tile walls tested are unimportant.

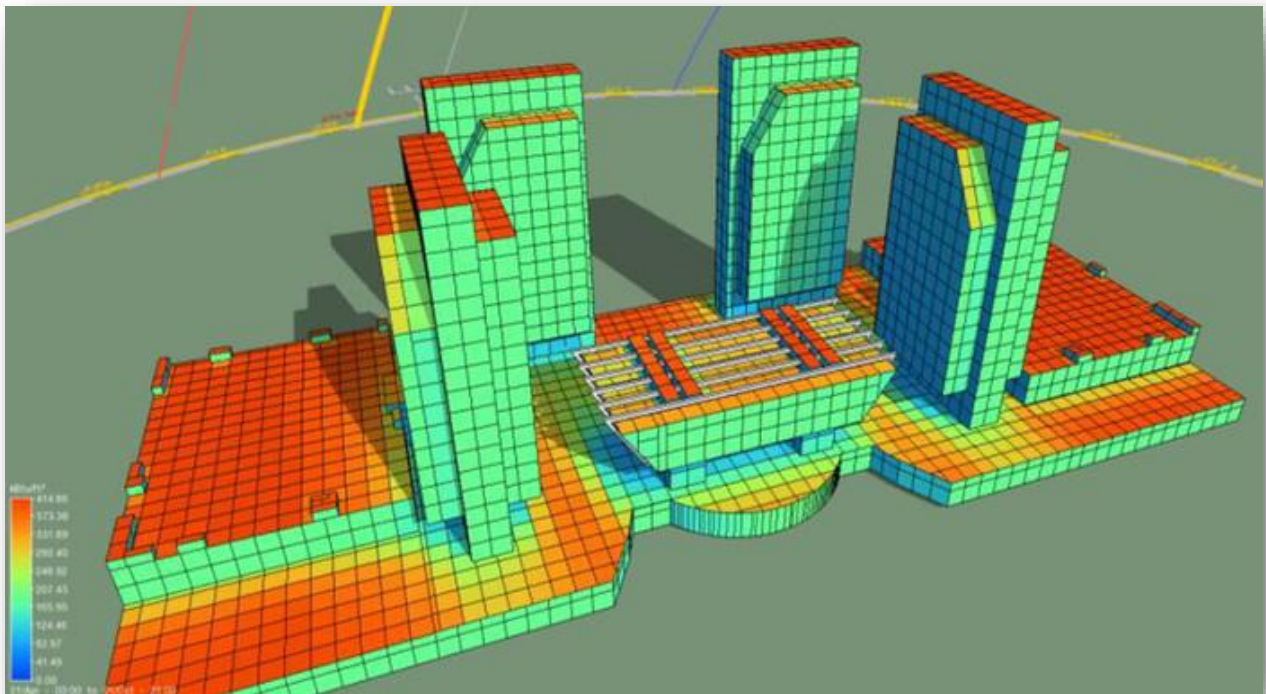


Figure 74. Understanding Energy Modeling and Building Simulation

Energy Modeling and Building Simulation

Judging by test on two kinds of brick, representing approximately two extremes in common brick manufacture, the kind of brick used in a brick wall is of little importance from the insulation standpoint alone.

The type of workmanship in a masonry wall may make a considerable difference in the insulating value, depending chiefly on the degree of filling of the mortar joints. Solidly filled vertical joints are not so effective from the insulation standpoint as partially filled joints.

The Insulating value of all walls tested increases with decreasing temperature, the increase, in general, being more repeat with hollow walls than with solid walls.

The investigation pointed out that air infiltration through finished walls plays a minor role in heat loss from building. The possibilities of heat loss by partial air penetration into hollow walls are discussed at some length and it may be inferred that there is always a possibility that an individual wall of this type may be subjected to air penetration effects of appreciable magnitude.

[]

In conclusion, it might be emphasized that in an actual building, heat loss through windows, doors and roof tend to level out the effect of differences in the walls themselves to a verify considerable extent. It may therefore be said that there are considerable differences in the insulating values of the various types of walls tested the magnitude of these differences is not sufficient to make them a very important factor in the choice of building wall types, except perhaps in the case relatively thin solid masonry without air space where discomfort may be caused or moisture condensation produced by abnormally cold interior wall surface. As an illustration from another angle of the observed differences in an uninsulated wall type, walls showing the lower insulating value, by addition half inch of good insulation material be endowed with a thermal resistance approximately as great as those showing the higher insulating values in the tests. The difference between poorest and best wall from the viewpoint of thermal insulation representing the extremes in ordinary uninsulated construction is equivalent to approximately $\frac{3}{4}$ inch of good insulating material

REFERENCES

- 1- P. Favaretto, G. E. N. Hidalgo, C. H. Sampaio, R. D. A. Silva, and R. T. Lermen, "Characterization and use of construction and demolition waste from south of Brazil in the production of foamed concrete blocks," *Applied Sciences*, 2017
- 2- S. Mindess, *Developments in the Formulation and Reinforcement of Concrete*, Woodhead publishing limited, Cambridge, UK, 2008
- 3- M. R. Jones and A. Mccarthy, "Preliminary views on the potential of foamed concrete as a structural material," *Magazine of Concrete Research*, vol. 57, no. 1, pp. 21–31, 2005.
- 4- Y. H. M. Amran, N. Farzadnia, and A. A. A. Abang, "Properties and applications of foamed concrete: a review," *Construction and Building Materials*, 2015.
- 5- M. A. O. Mydin and Y. C. Wang, "Structural performance of lightweight steel-foamed concrete–steel composite walling system under compression," *@in-Walled Structures*, 2011.
- 6- K. Ramamurthy, K. K. K. Nambiar, and G. I. S. Ranjani, "A classification of studies on properties of foam concrete," *Cement and Concrete Composites*, 2009
- 7- M. I. Norlia, R. C. Amat, N. L. Rahim, and S. Sallehuddin, "Performance of lightweight foamed concrete with replacement of concrete sludge aggregate as coarse aggregate," *Advanced Materials Research*, 2013
- 8- C. Bing, W. Zhen, and L. Ning, "Experimental research on properties of high-strength foamed concrete," *Journal of Materials in Civil Engineering*, 2011
- 9- M. A. O. Mydin, N. A. Rozlan, and S. Ganesan, "Experimental study on the mechanical properties of coconut fibre reinforced lightweight foamed concrete," *Journal of Materials and Environmental Science*, 2015.
- 10- K. Ramamurthy, K. K. K. Nambiar, and G. I. S. Ranjani, "A classification of studies on properties of foam concrete," *Cement and Concrete Composites*, 2009
- 11- I. T. Koudriashoff, "Manufacture of reinforced foam concrete roof slabs," *ACI Journal Proceedings*, 1949.
- 12- R. C. Valore, "Cellular concrete part 2 physical properties," *ACI Journal Proceedings*, 1954
- 13- D. M. A. Huiskes, A. Keulen, Q. L. Yu, and H. J. H. Brouwers, "Design and performance evaluation of ultra-lightweight geopolymer concrete," *Materials and Design*, 2016

- 14- Mydin, A.O.: Effective thermal conductivity of foam of different densities. In: Concrete Research Letters 2 (2011)
- 15- Gilka-Bötzow, A., Koenders, E.A.B.: Rheological behavior of the continuous phase of foams and its effect on the dispersed phase. In: Proceedings of 24. Workshop und Kolloquium Rheologische Messungen an Baustoffen (2015)
- 16- ACI Committee 523, Guide for Cast-in-Place Lowdensity Cellular Concrete, Farmington Hills, MI, USA, 2006.
- 17- L. Cox and S. Van Dijk, "Foam concrete: a different kind of mix," Concrete, 2002.
- 18- E. K. K. Nambiar and K. Ramamurthy, "Sorption characteristics of foam concrete," Cement and Concrete Research, 2007.
- 19- P. Chindaprasirt, S. Rukzon, and V. Sirivivatnanon, "Resistance to chloride penetration of blended Portland cement mortar containing palm oil fuel ash, rice husk ash and fly ash," Construction and Building Materials, 2008
- 20- M. R. Jones and A. McCarthy, Behaviour and Assessment of Foamed Concrete for Construction Applications, Thomas Telford, London, UK, 2005.
- 21- T. G. Richard, J. A. Dobogai, T. D. Gerhardt, and W. C. Young, "Cellular concrete—a potential load-bearing insulation for cryogenic applications," IEEE Transactions on Magnetics, 1975.
- 22- https://www.researchgate.net/figure/Pore-sizes-in-foam-concrete-of-various-densities_fig3_283641278
- 23- A. A. Hilal, N. H. ,om, and A. R. Dawson, "On void structure and strength of foamed concrete made without/ with additives," Construction and Building Materials, 2015
- 24- Bomberg, M. / Lstiburek, J. / Nabhan, F. Long-Term, Hygrothermal Performance of Exterior Insulation and Finish Systems (EIFS), Journal of Building Physics, Jan 1997.
- 25- Dol, K.; Haffner, M. 2010. Housing Statistics in the European Union 2010. OTB Research Institute for the Built Environment, Delft University of Technology
- 26- Dall'O', G., Galante, A., Pasetti, G. A methodology for evaluating the potential energy savings of retrofitting residential building stocks. Sustainable Cities and Society. 4-1, October 2012,
- 27- EN ISO 10211 Thermal bridges in building construction - Heat flows and surface temperatures - Detailed calculations. Part 1:2000 and Part 2:2001.
- 28- EN 13829 Thermal performance of buildings - Determination of air permeability of buildings - Fan pressurization method

- 29- Holm, A. and Künzeli, H.M, (1999), Combined effect of temperature and humidity of the deterioration process of insulation materials in ETICS, Building Physics in the Nordic Country, August, Gothenburg.
- 30- Kalamees T; Õiger K; Kõiv T. A., et al. 2009. Technical condition and service life of Estonian apartment buildings, built with prefabricated concrete elements. Tallinn University of Technology (in Estonian)
- 31- Krus, M., Hofbauer, W. and Lengsfeld, K. Microbial Growth on ETICS as a Result of the New Building Technology? Building Physics Symposium. Leuven, Belgium 2008
- 32- Nicolai, A. 2008. Modeling and Numerical Simulation of Salt Transport and Phase Transitions in Unsaturated Porous Building Materials, Dissertation, Syracuse University
- 33- Uihlein, A., Eder, P. Policy options towards an energy efficient residential building stock in the EU-27. 2010. Energy and Buildings

<https://www.arcon.pk/understanding-energy-modeling-and-building-simulation/>

<https://www.hindawi.com/journals/amse/2020/6153602/>